

Regulation of the Antiviral Innate Immune Response by Ufmylation

by

Daltry L. Snider

Department of Molecular Genetics and Microbiology
Duke University

Date: _____

Approved: _____

Stacy Horner, Supervisor

Micah Luftig

Jörn Coers

Gianna Hammer

Gustavo Silva

Dissertation submitted in partial fulfillment of
the requirements for the degree of Doctor of Philosophy in the Department of
Molecular Genetics and Microbiology in the Graduate School
of Duke University

2022

ABSTRACT

Ufmylation as a Novel Control of Antiviral Innate Immune Sensing

by

Daltry L. Snider

Department of Molecular Genetics and Microbiology
Duke University

Date: _____

Approved:

Stacy Horner, Supervisor

Micah Luftig

Jörn Coers

Gianna Hammer

Gustavo Silva

Dissertation submitted in partial fulfillment of
the requirements for the degree of Doctor of Philosophy in the Department of
Molecular Genetics and Microbiology in the Graduate School
of Duke University

2022

Copyright by
Daltry L. Snider
2022

Abstract

Cellular detection of viral infection activates an antiviral program through the induction of interferons (IFN), which ultimately limit viral replication and reduce viral spread. This induction of IFNs is initiated by proteins that sense viral RNA, such as RIG-I, and proteins that coordinate the resulting signaling, like its adaptor protein MAVS. These proteins, along with others, form a signaling pathway that is highly controlled to provide a fine balance between clearance of viral infection, while preventing prolonged or excessive IFN induction which can lead to autoimmunity. As such, the RIG-I signaling cascade is carefully regulated by multiple mechanisms, including post-translational modifications (PTMs), protein-protein interactions, and protein localization. For example, following sensing of viral RNA, RIG-I is ubiquitinated, leading to its activation and subsequent interaction with the molecular trafficking protein 14-3-3 ϵ , forming a RIG-I signaling complex. This interaction with 14-3-3 ϵ facilitates the relocalization of activated RIG-I from the cytosol to intracellular membranes where it interacts with the adaptor protein MAVS leading to the propagation of various signals that induce IFN. Importantly, while some post-translational modifications are well studied in regulation of the RIG-I signaling pathway and are known control many aspects of IFN induction, our current knowledge of the full set of regulatory mechanisms that govern the RIG-I activation cascade is incomplete.

Previously, to determine novel regulators of RIG-I signaling, we identified proteins that relocalize to the RIG-I/MAVS signaling platform at ER-mitochondrial membrane contact sites. These relocalized proteins include UFL1, the E3 ligase of the small ubiquitin-like modification called UFM1. Similar to ubiquitination, the ufmylation

process conjugates a small protein (UFM1) to lysine residues of target proteins using an E1, E2, and E3 ligase machinery system. Further, a protease specific to ufmylation can remove the modification, allowing for dynamic regulation of protein function. However, in contrast to ubiquitin, the ways in which ufmylation regulates protein function is still unclear.

While the role of well-described PTMs such as ubiquitination and phosphorylation have a well-respected role in the regulation of the RIG-I signaling pathway, little is known about how emerging ubiquitin-like modifications, such as ufmylation, regulate this antiviral signaling pathway. Indeed, how these newly discovered PTMs regulate protein function has not yet been elucidated, requiring further study. Through investigating how ufmylation may regulate RIG-I signaling, I found that UFL1 is essential for the induction of IFN following RNA virus infection using a combination of IFN reporter assays, RT-qPCR to assess transcription, and immunoblots and ELISA to investigate protein expression. This regulatory role of UFL1 relies on its ability to conjugate UFM1 onto target proteins, leading me to hypothesize that ufmylation of proteins themselves may be driving signaling regulation. Indeed, altered expression of UFM1, or any of the proteins involved in its conjugation also positively regulated IFN. Utilizing co-immunoprecipitation assays, I found that following RNA virus infection, UFL1 is recruited to the membrane targeting protein 14-3-3 ϵ . Further, I found that this complex is then recruited to activated RIG-I to promote downstream innate immune signaling utilizing a series of RIG-I activation mutants. As I hypothesized that the primary role of UFL1 in RIG-I signaling regulation was through ufmylation of an interacting protein, I assessed the ufmylation status of 14-3-3 ϵ , and I found that 14-3-3 ϵ has an increase in covalent UFM1-

conjugation when RIG-I activation is induced by viral infection. Additionally, loss of either cellular UFM1 or UFL1 expression prevents the interaction of 14-3-3 ϵ with RIG-I. The consequences of which are impaired RIG-I recruitment to MAVS sites at ER-mitochondrial membranes. Indeed, I found that loss of UFM1 abrogates the interaction of RIG-I with MAVS via co-immunoprecipitation, and MAVS activation by oligomerization using semi-denaturing detergent agarose gel electrophoresis, and thus downstream signal transduction which induces IFN. These results reveal ufmylation as an integral regulatory component of the RIG-I signaling pathway and as a novel post-translational control for IFN induction.

Having discovered a role for ufmylation in regulating the interaction of 14-3-3 ϵ with RIG-I, I hypothesized that there might be other proteins regulated by ufmylation during RIG-I signaling, as PTMs play a crucial role in the regulation of a multitude of proteins in the antiviral response pathways. Utilizing an unbiased proteomics approach, I profiled all the UFM1-interacting proteins during viral infection. These data revealed multiple proteins that display differential UFM1-interaction, including TBK1, the serine-threonine kinase that plays a key role in the induction of IFNs. Follow-up work revealed that five of the top 8 proteins identified modulate IFN induction. Further studies to identify how ufmylation influences these proteins functions, and how their ufmylation status regulates their role in RIG-I signaling is needed, but this reveals a broad role for ufmylation as an important RIG-I pathway regulatory PTM. Further, as many intracellular pathogen sensing pathways share common signaling proteins, ufmylation may also regulate these signaling processes as well. Overall, my work has revealed a previously

undiscovered node of RIG-I regulation and uncovered a new class of RIG-I regulatory proteins that become ufmylated during the antiviral response.

Dedication

To my parents-

For giving me the freedom and opportunity to succeed.

Contents

Abstract.....	iv
List of Tables.....	xiv
List of Figures	xv
Acknowledgements.....	xvi
1. Introduction	1
1.1 Intracellular RNA sensing & antiviral responses	1
1.2 RLRs sense cytosolic viral RNA and activate antiviral responses	2
1.2.1 RIG-I.....	4
1.2.2 MDA5	5
1.2.3 LGP2	6
1.3 Type I IFN response.....	7
1.3.1 Activation of the IFN response	8
1.3.2 ISGs establish the antiviral state.....	9
1.4 Regulation of RIG-I pathway signaling.....	10
1.4.1 Regulation by host proteins.....	12
1.4.2 Regulation by PTMs.....	13
1.4.3 Viral immune evasion of RIG-I signaling.....	15
1.5 Emerging roles of PTMs in cellular signaling regulation	17
1.5.1 Ubiquitination	17
1.5.1.1 Types of ubiquitin ligases and their functions	19
1.5.1.2 Ubiquitin-linkages with roles in RIG-I signaling	20
1.5.2 Ubiquitin-like modifications.....	22

1.5.2.1 SUMOylation	23
1.5.2.2 NEDDylation.....	24
1.5.2.3 FATylation	24
1.5.2.4 ISGylation.....	25
1.6 Ufmylation	25
1.6.1 The ufmylation conjugation system.....	26
1.6.2 Functional consequences of UFM1 addition	29
1.7 Summary of the work presented in this dissertation	30
2. Signaling from the RNA sensor RIG-I is regulated by ufmylation	33
2.1 Introduction	33
2.2 Results	35
2.2.1 The ufmylation E3 ligase, UFL1, promotes RIG-I signaling	35
2.2.2 The ufmylation activity of UFL1 drives RIG-I signaling regulation.....	38
2.2.3 The ufmylation machinery proteins positively regulate RIG-I signaling.....	39
2.2.4 UFM1 is required for the RIG-I-driven transcriptional response.....	42
2.3 Conclusions.....	44
2.4 Materials and Methods.....	45
2.4.1 Cell lines, viruses, and treatments.	45
2.4.2 Plasmids.....	45
2.4.3 Generation of RNA PAMP.....	46
2.4.4 Transfections.....	46
2.4.5 ELISAs.	47
2.4.6 Generation of cell lines.....	47
2.4.7 RNA analysis.....	47

2.4.8 RNA-seq.....	47
2.4.9 Immunoblotting.....	48
3.4.9 Quantification of immunoblots.....	49
3.4.10 Statistical analysis.....	49
3. Ufmylation regulates IFN induction through RIG-I membrane targeting	50
3.1 Introduction	50
3.2 Results	51
3.2.1 UFL1 is recruited to intracellular membranes and interacts with 14-3-3 ϵ and RIG-I during RNA virus infection	51
3.2.2 UFL1 interaction with RIG-I requires 14-3-3 ϵ and UFM1	54
3.2.3 Ufmylation promotes RIG-I interaction with 14-3-3 ϵ for MAVS activation	57
3.3 Conclusions.....	58
3.4 Materials and Methods.....	59
3.4.1 Cell lines, viruses, and treatments.....	59
3.4.2 Plasmids.....	60
3.4.3 Transfection.....	61
3.4.4 Generation of cell lines.....	61
3.4.5 Immunoblotting.....	61
3.4.6 Immunoprecipitation.....	62
3.4.7 Subcellular membrane fractionation.....	63
3.4.8 Semi-denaturing detergent agarose gel electrophoresis.....	63
3.4.9 Quantification of immunoblots.....	64
3.4.10 Statistical analysis.....	64
4. RIG-I signaling induces a subset of ufmylated proteins that control interferon induction	65

4.1 Introduction	65
4.2 Results	66
4.2.1 Utilizing proteomics to uncover the targets of ufmylation during RIG-I signaling	66
4.2.2. Identification of proteins that are ufmylated in a RIG-I dependent manner ...	67
4.2.3 Ufmylated proteins differentially regulate IFN induction	68
4.3 Conclusions.....	69
4.4 Methods	70
4.4.1 Cell lines, viruses, and treatments.	70
4.4.2 Plasmids.....	71
4.4.3 Transfection.	72
4.4.4 Immunoprecipitation.....	72
4.4.5 Proteomics sample preparation.	72
4.4.6 Quantitative analysis for proteomics samples.....	73
4.4.7 Statistical analysis.....	74
5. Discussion.....	75
5.1 Summary.....	75
5.2 Future directions and discussion.....	80
5.2.1 By what mechanism does UFM1 dictate RIG-I selection by 14-3-3ε?	80
5.2.2 How is ufmylation functionalized to regulate diverse biological processes? ..	83
5.2.2.1 Ufmylation regulates multiple cell stress response pathways	83
5.2.2.2 Do UFL1 co-factors direct ufmylation?.....	86
5.2.3 Does ufmylation regulate RIG-I signaling through multiple mechanisms?.....	87
5.2.4 Does ufmylation regulate other antiviral sensing pathways?	90

5.3 Broader impacts of this research	93
References.....	94
Biography.....	114

List of Tables

Table 1: Differential expression analysis from RNA-seq analysis for UFM1 KO / WT 293T cells.....	44
Table 2: Gene Set Enrichment Analysis for UFM1 KO / WT 293T cells.....	44

List of Figures

Figure 1: RLR sensing pathway.....	3
Figure 2: Diagram of the cytosolic IFN signaling pathways.	8
Figure 3: Diagram of early RIG-I signaling activation.	12
Figure 4: The ufmylation machinery system.	27
Figure 5: Graphical summary of work presented in this dissertation.	32
Figure 6: The ufmylation E3 ligase, UFL1, promotes RIG-I signaling.....	37
Figure 7: The ufmylation activity of UFL1 drives RIG-I signaling regulation.	39
Figure 8: The ufmylation machinery proteins positively regulate RIG-I signaling.	41
Figure 9: UFM1 is required for the RIG-I driven transcriptional response.	43
Figure 10: UFL1 is recruited to intracellular membranes and interacts with 14-3-3 ϵ and RIG-I during RNA virus infection.....	53
Figure 11: UFL1 interaction with RIG-I requires 14-3-3 ϵ and ufmylation.	56
Figure 12: Ufmylation promotes RIG-I interaction with 14-3-3 ϵ for MAVS activation.....	58
Figure 13: Schematic of experimental workflow for IP-LC-MS/MS to identify ufmylated proteins.	67
Figure 14: Candidate UFM1-interacting proteins.	68
Figure 15: Proteins ufmylated during RIG-I signaling regulate IFN induction.	69

Acknowledgements

My graduate school journey was made possible first and foremost by my undergraduate professors who believed in me. Thank you to Dr. Bell, who always believed that I would do something great. Thank you to Dr. Edwards who knew that I was a scientist even when I didn't. Thank you to all the other professors who educated, encouraged, and challenged me.

Thank you to my graduate advisor, Dr. Stacy Horner, for her dedication to my success. Through her, I have become an excellent scientist, writer, communicator, and community member. She has always given me the opportunity and encouragement to explore my interests outside of lab and pushed me to grow within the lab. Thank you for always encouraging us to be our authentic selves and putting up with our schemes like the lab garden, the year-round Christmas tree, pet pictures in lab meeting, and individualized Slack emojis. The training I have received in the Horner lab will no doubt contribute to my future success, and the fun I always had in lab will stay with me for years to come.

My PhD experience has been enriched beyond understanding by all the members of the Horner lab, past and present. To Nandan, Christine, Allison, and Mike, thank you for being the role models I needed when I started graduate school, and for setting the bar for success high. The lab is what it is thanks to you all. To Matt, for your friendship and support, thank you for all the advice, sanity checks, statistics tutoring, and commiseration. To Hannah, who was my sounding board, ufmylation lab partner, and friend, thank you for being the best bay mate I could ask for. Thank you to Moonhee for your determination and partnership. Matthew, thank you for your unique perspective,

creative ideas, and always being willing to brainstorm. To the entire Horner lab, past, present, and future, thank you for the lab meetings, small groups, afternoon coffee runs, happy hours, lunches, and the environment of excellence that we have created.

The MGM department has provided an excellent scientific community these past years which has fostered friendship, scientific growth and excitement, and a sense of community. The professors and trainees in this department have enriched me in ways beyond helping me to become a scientist and have made my graduate experience more rewarding than I thought possible. Thank you to my committee members: Dr. Micah Luftig, Dr. Jörn Coers, Dr. Gianna Hammer, and Dr. Gustavo Silva, for your feedback, guidance, and always helping me to see the bigger picture. To Dr. Beth Sullivan, since my first day you have been someone I looked up to. Thank you for your support, kindness, and for always listening.

My parents, Ricky and Cappy, thank you for always giving me the room I needed to grow. You encouraged me without pushing, supported me without overbearing, and always made sure that I knew I was loved. Thank you to my sister, Lily, who reminds me to be young and has kept me on my toes my whole life. I owe all my successes to you. To my best friend, Maria, thank you for the decade of friendship and joy you have shared with me, which has kept me grounded throughout the entirety of my education. Finally, thank you to my partner, Alex, for your unwavering support, companionship, comfort, and strength. Thank you for always believing in me when I didn't.

1. Introduction

1.1 *Intracellular RNA sensing & antiviral responses*

Innate immune responses are essential to provide host protection against pathogens such as viruses. Further, activation of innate immunity primes adaptive immunity in response to viral infections, and therefore acts as a major determinant of the antiviral response and viral clearance (1). Regulation of these pathways is important as aberrant or prolonged activation can lead to interferonopathies or uncontrolled viral replication (2, 3). Following RNA virus infection, the innate immune response is initiated when the virus enters the cell and pattern recognition receptors (PRRs) sense features unique to viruses (pattern associated molecular patterns, PAMPS) and then interact with a cognate signaling adaptor protein, which organizes and directs downstream signaling (4, 5). These complexes activate signaling cascades which culminate in the production of type I & III interferons (IFNs). IFNs then trigger induction of hundreds of interferon stimulated genes (ISGs) that directly and indirectly limit viral replication (6). Multiple PRRs exist to rapidly sense viral infection and activate innate immune responses (7, 8). Though they sense distinct features of RNA, viruses can be sensed by multiple simultaneously (7). The PRRs responsible for sensing viral RNA include the retinoic acid-inducible gene I (RIG-I)-like receptors (RLRs), the Toll-like receptors (TLRs) and the NOD-like receptors (NLRs), along with the double-stranded RNA (dsRNA)-activated protein kinase R (PKR) (9). These sensors exist in diverse spatial compartments of the cell allowing detection of PAMPs regardless of entry route. Although the importance of PAMP detection and innate immune activation in cells has long been appreciated, recent advances in our understanding of innate immunity have highlighted the intricacy of the

regulation of these sensors, and their nuanced ability to distinguish self-nucleic acids from those of the invading pathogen. In particular, the cytoplasmic RLRs play an essential role in detecting the presence of viral RNA, and regulation of their activation has been the primary focus of my thesis work.

1.2 RLRs sense cytosolic viral RNA and activate antiviral responses

The RLRs belong to a class of DExD/H helicases and have diverse functional features that mediate ATP binding and hydrolysis, and RNA binding and helicase activity, as well as structural features that are essential to their functions in cytosolic PAMP detection and subsequent IFN activation. The RLRs RIG-I, melanoma differentiation factor 5 (MDA5), and laboratory of genetics and physiology 2 (LGP2) share similar structures, but the features of RNA they detect remain diverse (10). Following interaction with the target RNA, these proteins induce IFN production through their interaction with mitochondrial antiviral signaling protein (MAVS), which forms higher-order oligomers acting as a large platform for the assembly and activation of other RLR pathway members (11). These proteins include tumor necrosis factor receptor-associated factor (TRAF) proteins, which are ubiquitin ligases essential for full MAVS activation. Following this, subsequent signaling is propagated through TANK-binding kinase 1 (TBK1) and I κ B-kinase- ϵ (IKK ϵ), along with the I κ B kinase complex (IKK). TBK1, once recruited and activated, mediates phosphorylation of IKK phosphorylate interferon regulatory factor 3 and 7 (IRF3/IRF7) and the inhibitory subunit of nuclear factor kappa B (NF- κ B) (I κ B α), respectively (12). The phosphorylated IRFs translocate to the nucleus where they serve as the transcription factor for type I IFNs

(IFN- α and IFN- β) and type III IFNS (IFN- λ) (Figure 1) (13). Type I and III IFN production drives autocrine and paracrine responses through their cognate receptor, which activates the JAK/STAT signaling pathway to ultimately induce the transcription of hundreds of IFN-stimulated genes (ISGs). These include many antiviral factors, which can inhibit viral replication in diverse ways (6, 14, 15).

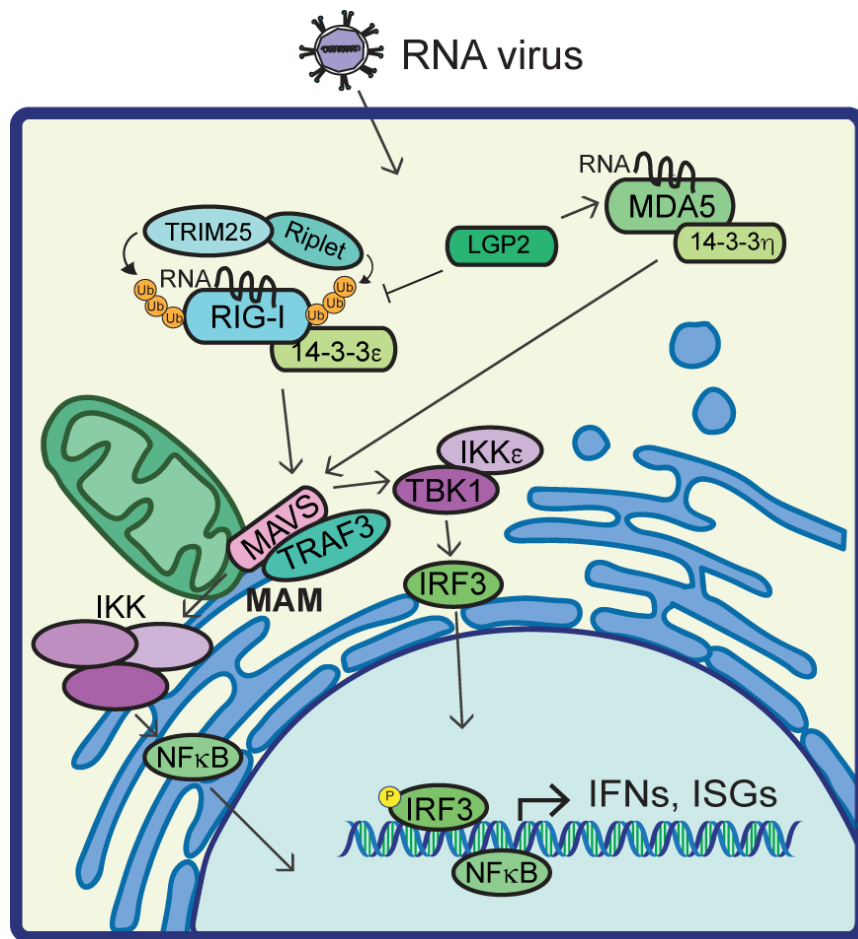


Figure 1: RLR sensing pathway.

Viral RNA PAMPs (dsRNA or 5' triphosphate dsRNA) are recognized by cytosolic receptors, such as RIG-I and MDA5. RIG-I is ubiquitinated (Ub) by the E3 ubiquitin ligases TRIM25 and Riplet. RIG-I binds to RNA via its C-terminal helicase domain and contains two caspase activation and recruitment domains. LGP2, another cytosolic receptor, can negatively or positively regulate this IFN induction. RIG-I and MDA5 can then interact with MAVS, which is localized at the mitochondrial-associated endoplasmic reticulum membrane (MAM) and form a MAVS signalosome. This then leads to

interaction with the kinases IKK, TBK1, and IKK ϵ that then phosphorylate (P) the transcription factors IRF3 and NF- κ B. This leads to their nuclear translocation and the transcriptional induction of IFNs and IFN-stimulated genes (ISGs).

1.2.1 RIG-I

RIG-I is essential for sensing a variety of RNA viruses including flaviviruses, coronaviruses, orthomyxoviruses, paramyxoviruses, and reoviruses, among others (16–18). Through its RNA binding domain, RIG-I primarily senses PAMPs comprised of short double-stranded RNA (dsRNA) containing an exposed 5'-tri- or 5'-diphosphate moiety that are recognized as non-self or foreign RNAs. Cellular mRNA contains features that prevent sensing by RIG-I, including the 7-methylguanosine cap and 2'O-methylation on the first nucleotide (19). Indeed, the crucial role of these features is underscored by the fact that many viruses either encode their own machinery to cap RNA or have evolved ways to co-opt host processes that conjugate these modifications (20). Additionally, recent work has uncovered the importance of internal RNA modifications in shielding RNA from PRR sensing, such as N-6 methyladenosine (m⁶A), which can protect host mRNA from recognition by RIG-I, and is utilized by viruses to evade RIG-I sensing (20–22). In addition to its RNA-binding domain, RIG-I contains two N-terminal caspase activation and recruitment domains (CARDs), followed by two tandem helicase domains (Hel1, Hel2) separated by an insertion domain (Hel2i), as well as a C-terminal repressor domain (RD), all of which regulate its sensing of PAMPs and subsequent IFN induction (23–25). Prior to RNA PAMP binding, monomeric RIG-I is maintained in an auto-repressed state by Hel2i interacting with the second CARD, with the RD preventing RIG-I oligomerization and CARD interaction with MAVS (24). Following RNA binding by the RD, a coordinated conformational change takes place where the CARD is released from

Hel2i allowing RIG-I to alter its conformation to a helical tetramer that allows for its interaction with MAVS, which also contains a CARD domain (25–28). The CARD-CARD interaction of RIG-I and MAVS serves to activate the MAVS signaling platform which results in the recruitment of signaling proteins that ultimately serve to induce IFNs. In addition to this elegant structural regulation of RIG-I, its activation is also regulated by multiple post-translational modifications (PTMs) that serve to promote RIG-I activity via conformational changes and facilitating intracellular translocation. PTMs also deactivate RIG-I in order to terminate signaling and prevent excessive IFN production leading to inflammation. PTMs that modulate RIG-I signaling are discussed in detail in sections 1.4-1.5 of this chapter. Our understanding of the nuances of RIG-I activation is still emerging and is of utmost importance, as these regulatory mechanisms are essential for a successful antiviral defense, but also to prevent aberrant RIG-I activation and subsequent autoimmune disorders.

1.2.2 MDA5

MDA5 has similar structural domains to RIG-I and likewise also signals downstream through MAVS, as do many of the intracellular antiviral detectors (8). However, MDA5 senses long dsRNA, which are common viral replication intermediates (29, 30). Though RIG-I and MDA5 sense viruses in a semi-redundant manner – with viruses such as flaviviruses, alphaviruses, coronaviruses, reoviruses, and paramyxoviruses often serving to dual activate the PRRs – MDA5 plays an indispensable role in detection of picornaviruses and caliciviruses (10). Similar to RIG-I, 2'-O-methylation at the 5' end of RNAs also shields from MDA5 detection (31). Importantly, MDA5 selectively recognizes the internal double stranded structure of dsRNA in a length-dependent fashion (29). The crystal structure of MDA5 bound to

dsRNA reveals that MDA5 stacks along dsRNA, forming filamentous structures, in a head-to-tail arrangement for signaling (32). Similar to RIG-I, the ATP hydrolysis activity of the helicase domains is required for MDA5 filament formation (32, 33). This highly ordered structural filament exposes the CARDS of MDA5 for interaction with the CARD motif of MAVS (32). MDA5 activation is also highly regulated by PTMs, for example, PP1 dephosphorylates MDA5 CARDS, leading to MDA5 activation (34). However, little is known about other PTMs that may regulate MDA5 activation, such as lysine (K) 63-linked ubiquitination (10). Additionally, the cell biology of associated host factors that regulate MDA5 activation is not well understood. Future studies to address these aspects of the regulation of MDA5 will be of interest.

1.2.3 LGP2

LGP2 is less well characterized than RIG-I and MDA5, but gathering evidence indicates that LGP2 acts as a negative regulator of RIG-I signaling and as a positive regulator of MDA5 signaling (35–38). LGP2 retains similar domains to the other RLRs, containing a helicase and RD region, however it lacks the N-terminal CARDS required for interaction with MAVS (8). While it has been shown that LGP2 recognizes both dsRNA and single-stranded RNA (ssRNA), with a preference for RNA with a 5'triphosphate, LGP2 requires another RLR to activate downstream signaling to MAVS as it lacks N-terminal CARDS required for this interaction. In addition, multiple conflicting functions have been attributed to LGP2, including negative regulation of RIG-I (36), as well as negative regulation of MDA5 (39), in addition to positive regulation of MDA5 (37, 39). Recently, LGP2 was found to regulate the binding of MDA5 to RNA and regulate MDA5 filament assembly for enhanced signaling activity (37). Additionally, LGP2 along with MDA5 was shown to play a role in the development of Aicardi-Goutières Syndrome

through self-RNA sensing that leads to chronic type-I IFN production (40). Therefore, it seems LGP2 may serve multiple, diverse functions in response to different viruses, and may be differentially regulated by host factors, PTMs, or both that ascribe diverse functions to LGP2. Further research will be required to appreciate the role and function of LGP2 in regulation of RNA virus sensing and downstream signaling.

1.3 Type I IFN response

While these described cytosolic PRRs recognize distinct PAMPs and activate different signaling pathways, they ultimately converge on the activation of the transcription factors like IRF3, IRF7, and NF- κ B (Figure 2, left). This suggests that, despite requiring unique surveillance proteins to recognize diverse viral pathogens, ultimately, the response to these cytosolic PAMPs is very similar. IRF3, IRF7, and NF- κ B function with the shared goal to induce cytokines, especially type I IFNs. The IFNs are essential for inducing ISGs which function in various ways that ultimately control viral replication (Figure 2, right).

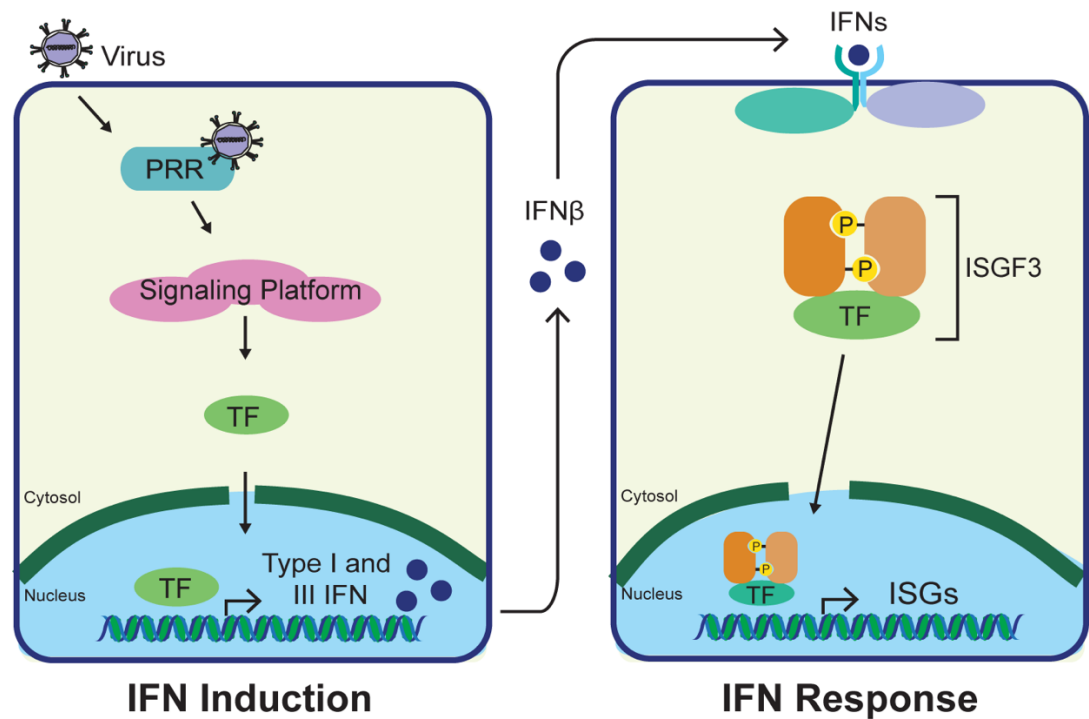


Figure 2: Diagram of the cytosolic IFN signaling pathways.

(Left) Following viral RNA sensing, PRRs are trafficked to MAVS signaling platforms which recruits signaling proteins that activate various transcription factors (TF) to transcriptionally upregulate type I & III IFNs. (Right) IFNs are released from the cell and bind to their receptor on neighboring cells, this activates the ISGF3 TF complex, which serves to induce ISGs.

1.3.1 Activation of the IFN response

Type I IFNs induce the upregulation of hundreds of ISGs in both an autocrine and paracrine fashion, and many of these genes encode antiviral effector proteins (41), essential for viral restriction (42, 43). This activation occurs as type I IFNs bind to their cognate receptor, the IFN- α/β receptor (IFNAR), composed of IFNAR1 and IFNAR2 (44–46). Then, IFNAR engagement activates the Janus family kinases JAK1 and TYK2 (47, 48), which phosphorylate the transcription factors STAT1 and STAT2 (49, 50). This allows the dimerization of STAT1 and STAT2, which, along with their co-factor, IRF9,

form the ISGF3 transcription factor complex (51, 52). Nuclear ISGF3 then binds to interferon-stimulated response elements within the promoters of ISGs to induce their transcription (Figure 2, right). The production of ISGs establishes an antiviral cellular state, in which cells are then able to restrict multiple stages of viral replication (53).

1.3.2 ISGs establish the antiviral state

Establishment of an antiviral state requires first, sensing of the pathogen by PRRs which induce IFN, and second, the IFN response which functions to upregulate ISGs, a specialized class of inducible proteins which display a wide variety of effects to protect cells and slow or abrogate viral replication (41). The total ISG population composes multiple classes of molecules with varying antiviral effects, and this diversity aids in the balance of protecting the host cells from excessive inflammation while also controlling viral replication (14). Indeed, the PRRs RIG-I and MDA5, while basally expressed, are also transcriptionally upregulated in response to IFN creating a positive feedback loop (54). However, most ISGs are minimally expressed or are absent during basal conditions (55). As there are hundreds of diverse ISGs induced during viral infection, their effects have been found to target nearly every stage of viral replication, such as ISG20, an RNA exonuclease that interferes with viral mRNA synthesis, or BST2, which blocks viral egress (6, 56, 57). Further, many ISGs impact viral replication through their host-directed functions, such as the ISG CMTR1 which catalyzes 2'-O-methylation at the 5' end of RNA, including other ISGs, and the 2'-O-methylation shields these RNAs from self-RNA sensing by specialized surveillance proteins (58–60). However, specific functions are known for only a small number of ISGs, emphasizing that we are only just beginning to uncover how ISGs function during the antiviral response.

1.4 Regulation of RIG-I pathway signaling

Aside from its autoregulation, activation of RIG-I is coordinated by a number of host factors. Proper activation of innate immune responses are essential to provide host protection against viruses and proper activation of innate immunity primes adaptive immunity in response to viral infections (1). As such, regulation of these pathways is important as aberrant activation can lead to interferonopathies or uncontrolled viral replication (2, 3). Multiple layers of regulation exist to modify the activation of many of the key innate immune signaling proteins, including RIG-I, often through relocalization, protein-protein interactions, and PTMs. Indeed, PTMs often serve as the master coordinators of this signaling cascade, their dynamic nature being essential for rapid redirection of protein function, often controlling the localization and differential protein-protein interactions. Thus, PTMs serve as a mechanism to rapidly activate and deactivate antiviral signaling. However, the full spectrum of post-translational mechanisms that regulate RIG-I signaling have not yet been elucidated and are the focus of my thesis work.

To ensure a rapid response to invading pathogens, RIG-I is expressed basally in uninfected cells. In order to maintain homeostatic conditions, multiple regulatory layers keep RIG-I bound in an inactive state, including the structural regulation described previously. In addition to its conformational inactivity, RIG-I is phosphorylated to hold it in its auto-repressed state. Following RNA binding, RIG-I is de-phosphorylated which allows for its association with ubiquitin E3 ligases Riplet and tripartite motif-containing protein 25 (TRIM25), which catalyze unanchored and K63-linked polyubiquitination in multiple domains of RIG-I (18). This ultimately allows for RIG-I to associate with its molecular chaperone, 14-3-3 ϵ , a trafficking protein that aids in the translocation of RIG-I,

along with its core regulatory host factors, to MAVS signaling sites localized at ER-mitochondrial contact sites (MAM) (Figure 1, Figure 3) (61). Interestingly, it has recently been discovered that MDA5 is relocalized from the cytosol to MAVS signaling sites by another 14-3-3 family protein, 14-3-3 η , indicating a potentially broad role for 14-3-3 proteins during antiviral sensing (62). MAVS aids in the organization of the other key RIG-I pathway members from their various cellular compartments, converging at the MAM in order to continue downstream pathway activation and eventual IFN induction (11, 63, 64). For example, TRAF ubiquitin ligases are recruited to MAVS sites where they catalyze the ubiquitination of MAVS (65, 66). TBK1 is also recruited to the MAM where once activated, it phosphorylates MAVS, which allows for IRF3 recruitment (67–69). TBK1 then phosphorylates IRF3, and activated IRF3 translocates to the nucleus where it serves as the transcription factor for type I & III IFNs (12, 13). Though it is well appreciated that these factors must be recruited to the MAM in order to propagate RIG-I signaling, little is understood about the mechanisms which control this intracellular reorganization. However, recruitment failure of any of these proteins could have detrimental impacts on IFN induction, indeed, it has been shown that loss of 14-3-3 ϵ interaction with RIG-I leads to less IFN and higher viral replication for several viruses (61, 70–72). Additionally, multiple viruses have evolved mechanisms to subvert this interaction to benefit their own replication (70–72). Thus, understanding the mechanisms that underly recruitment of these factors to the MAM will broaden our understanding of host-mediated antiviral responses and could uncover novel viral immune evasion strategies.

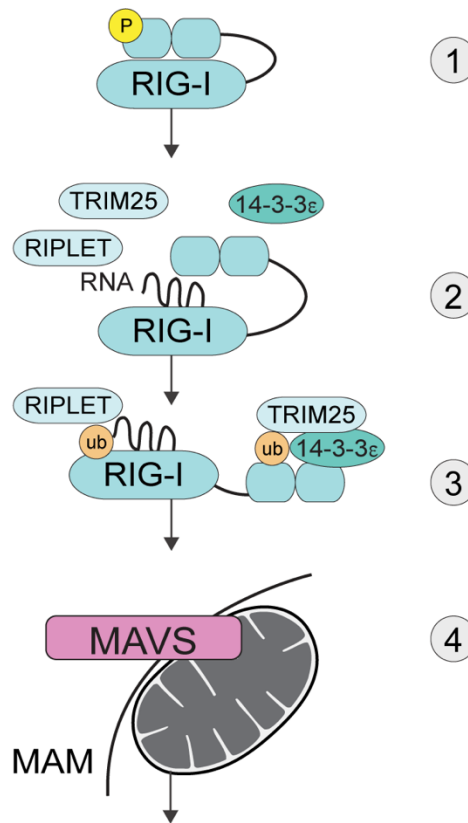


Figure 3: Diagram of early RIG-I signaling activation.

1) RIG-I is held in an auto-repressed state through its repressor domain and phosphorylated residue. 2) Following binding RNA and a slight conformational change, RIG-I loosely associates with its co-factors Riplet, TRIM25, and 14-3-3ε. 3) RIG-I is ubiquitinated by RIPLET and TRIM25, 4) and translocated to the MAM by 14-3-3ε where downstream signaling can then occur.

1.4.1 Regulation by host proteins

Host factors that modulate RIG-I function tend to regulate distinct steps of RIG-I activation such as dsRNA binding, oligomerization, localization, or they are proteins that catalyze PTMs. While RIG-I can bind RNA efficiently on its own, cofactors can aid in nucleic acid binding making it more efficient. For example, PACT interacts with the RIG-I CTD and stimulates the ATPase activity of RIG-I (73, 74). Interestingly, recent studies have suggested that both RIG-I and MDA5 might utilize a co-receptor in order to bind

their associated PAMPs. The zinc-finger protein ZCCHC3 forms a bridge between the RNA and the RLRs to enhance RNA binding (75). Following viral RNA binding, RIG-I forms a helical tetramer that aids MAVS activation by providing a template for MAVS oligomerization (27, 76). Intriguingly, the tetrameric conformation of RIG-I is stabilized through a non-covalent protein-protein interaction between RIG-I unanchored ubiquitin chains that are formed by Riplet.

As mentioned, RIG-I relocalization is highly important for IFN activation. It was previously found that 14-3-3 ϵ , a mitochondrial trafficking protein that is a member of the larger protein subclass of regulatory 14-3-3 proteins, interacts with RIG-I following RNA binding and brings RIG-I to the MAM. Classically, 14-3-3 proteins are well characterized to utilize phosphorylated residues to select their cargo, however, the only phosphorylation sites of RIG-I were found indispensable for its 14-3-3 ϵ interaction (34, 61, 70, 71, 77). Thus, this indicates that there are numerous other factors that govern RIG-I and its downstream signaling proteins that we have yet to elucidate. Indeed, previously in attempt to uncover some of these factors, we profiled the proteome of specific cell compartments to determine the factors that become relocalized to the MAM during infection (78). One factor, RAB1B, was later found to influence RIG-I signaling by acting to traffic TRAF3 to the MAM, where it can then aid in the ubiquitination of MAVS (66, 69, 79). These data indicate that we only are just uncovering the nuances of RIG-I signaling regulation.

1.4.2 Regulation by PTMs

RIG-I regulation by host factors is often through their ability to catalyze PTMs. PTMs play a highly important role at every stage of the RIG-I pathway, proving essential for their ability to quickly modulate protein function (80). As mentioned, prior to RNA

sensing, RIG-I is held in its inhibited form in part by phosphorylation of the CARD domain that is maintained by kinases PKC and CKII, and acetylation in the RD (81–84). Following viral sensing, RIG-I is dephosphorylated by PP1 and de-acetylated by HDAC6 which allows for further RIG-I activation steps (34, 83, 84).

Additionally, RIG-I is highly regulated by ubiquitin, which is discussed in detail in section 1.5. The primary types of ubiquitin which direct RIG-I function are K63-linked ubiquitin, which typically activates RIG-I signaling through altering protein-protein interactions, localization, or conformation, or through K48-linked ubiquitin, which typically deactivates RIG-I through proteasomal degradation (80). Indeed, the RD of RIG-I is subject to K63-linked polyubiquitination by the E3 ubiquitin ligase Riplet (85, 86). This promotes TRIM25 K63-linked ubiquitination of the RIG-I CARDS (87). Riplet is then able to catalyze the unanchored ubiquitin chains that non-covalently interact with RIG-I for oligomerization (27, 76). Mex-3 RNA Binding Family Member C (MEX3C) was recently identified as an additional essential E3 ubiquitin ligase that mediates K63-linked ubiquitination on RIG-I CARDS, and TRIM4 was found to enhance RIG-I signaling via K63-linked ubiquitination that is redundant with TRIM25 and Riplet, this redundancy highlighting the importance of non-degradative ubiquitination events (88, 89).

Conversely, RIG-I signaling termination is also essential in maintaining host homeostasis and prevent excessive IFN induction (90). In part, signaling termination can be achieved by disrupting the stability of key regulatory molecules such as RIG-I, MAVS, or other host co-factors. This can be mediated by K48-linked ubiquitination, which classically marks proteins for proteasomal degradation. For RIG-I, E3 ligases RNF122 and RNF125 add K48-linked ubiquitin to RIG-I, and linear ubiquitin chain assembly complex (LUBAC) destabilizes TRIM25 through ubiquitination as well terminating

downstream signaling (91–94). Further, as ubiquitination is a dynamic process, termination of RIG-I pathway protein signaling can also in part be achieved through removal of the activating K63-linked ubiquitination events in order to halt active signaling. De-ubiquitination enzymes ubiquitin specific peptidase 3 (USP3), USP21 and CYLD lysine 63 deubiquitinase (CYLD), modulate RIG-I signaling by removing K63-polyubiquitin chains (95).

The importance of these well-defined PTMs in regulating biological processes, including antiviral innate immunity, is well respected and accepted in the field. However, we are only beginning to understand how novel and emerging PTMs can regulate the functions of target proteins and how they may play a role in antiviral immune signaling. One of these emerging PTMs, ufmylation (discussed in section 1.6), has been the focus of my thesis work.

1.4.3 Viral immune evasion of RIG-I signaling

Viruses, by definition, require host cell machinery and co-factors to replicate and must evade host defenses to establish infection. Mammalian cells have evolved highly specialized defense mechanisms to detect and inhibit infection. However, this host pressure in turn stimulates rapid evolution from quickly replicating viruses from which has arisen countless viral immune evasion strategies.

Viruses display a multitude of mechanisms that aid in evading host defenses (96). These vary from being virally focused mechanisms to the viruses directly antagonizing host proteins. For example, tick-borne encephalitis virus, dengue virus (DENV), and hepatitis C virus (HCV) can shield their dsRNA in intracellular membrane vesicles, hiding it from RIG-I surveillance (97–99). Additionally, viruses can bind to, cleave, and/or promote the degradation of the signaling proteins in the RIG-I innate

immune response pathway. HCV cleaves multiple proteins involved in antiviral signaling via the actions of its NS3-NS4A protease complex, such as the signaling adaptor MAVS, preventing downstream IFN signaling. The influenza A virus protein PB1 contributes to mitochondrial fragmentation, which disrupts the MAM and MAVS signaling(100). Recently, it has been found that multiple flavivirus NS3 proteins have evolved to contain a phosphomimetic motif that mimics a binding pattern for 14-3-3 family proteins. This allows the NS3 protein to compete with RIG-I or MDA5 for binding to their molecular trafficking proteins, 14-3-3 ϵ and 14-3-3 η , respectively, stifling IFN induction (70, 71). Influenza A virus also has been shown to antagonize innate immune signaling through the 14-3-3 ϵ -RIG-I interaction, where NS1 disrupts 14-3-3 ϵ binding to RIG-I, preventing RIG-I translocation to MAVS (72).

PTMs (described in detail in Section 1.5) have emerged as key regulators of IFN induction (80). As such, they are a natural target for viral antagonism. RIG-I undergoes multiple posttranslational modifications that propagate IFN induction, and relies heavily on K63-linked polyubiquitination for multiple steps of its early activation (27, 86, 87). Thus, viruses often target the E3 ligases responsible for these ubiquitination events. The NS1 protein of influenza A virus binds directly to TRIM25 preventing its activation (101). NS1 can additionally bind to Riplet, sequestering it from RIG-I, preventing ubiquitination at the CTD (102). Severe acute respiratory syndrome (SARS)-associated coronavirus encodes a de-ubiquitination enzyme, PLP, that directly removes K63-linked ubiquitin from RIG-I once catalyzed by its co-factors (103). Both MDA5 and RIG-I are constitutively phosphorylated to maintain their inactive state and are then dephosphorylated by PP1 α and PP1 γ for activation (34). However, the measles V protein binds to PP1 α and PP1 γ to prevent dephosphorylation of MDA5, maintaining its inactivity

(104). The various ways in which viruses evade host defenses, especially as it relates to PTMs, are only just being investigated. Future work defining viral evasion of host defenses is necessary for understanding the full breadth of viral antagonization mechanisms and could be important in designing novel antivirals.

1.5 Emerging roles of PTMs in cellular signaling regulation

PTMs expand the functional proteome by modulating protein function in a multitude of ways. While small chemical modifications to proteins like phosphorylation, methylation, or acetylation have long been known to alter the function of proteins, recent work has uncovered the expansive ubiquitin and ubiquitin-like protein (UBL) families. These protein-based modifications dynamically regulate proteins by altering their structure, protein-protein interaction, modification by other PTMs, localization, and stability (105–108). This section will primarily focus on ubiquitin and ubiquitin-like modifications, especially the class of newly discovered regulatory functions of UBLs, and how they impact cellular signaling pathways including RIG-I signaling.

1.5.1 Ubiquitination

Ubiquitin was first discovered in 1977 as a protein that formed covalent lysine-linked peptide bonds on histone proteins (109). This sparked a large interest in the functional consequences of protein addition which modulates target protein function, and this led to the discovery that ubiquitination of substrates led to proteasomal degradation (110). Since then, it has been shown that ubiquitin can also be an activating regulator, not only just a degradation regulator (111). Indeed, ubiquitin-regulation of innate immunity has been a topic of immense interest during recent years where it has been

discovered it is essential in the modulation of innate immune signaling through altering protein stability, localization, or protein-protein interactions (80, 112).

Ubiquitination of proteins is catalyzed through a series of enzymes that typically perform three major steps: first, ubiquitin is activated by an E1 enzymatic conjugase, then transferred to an E2 conjugase, and finally, an E3 ligase catalyzes the transfer of the charged ubiquitin to a target substrate, either directly, or by acting as a scaffold for the E2 and target protein to interact (113–118). Ubiquitin modification is a dynamic process, as de-ubiquitinating enzymes can remove the covalent modification from targets, recycling it for further use (119, 120). Indeed, there are over a thousand molecules in the cell that regulate ubiquitination, allowing a breadth of substrate specificity and linkage types that allow ubiquitin to regulate proteins in different ways (121).

Ubiquitin itself is a seventy-six amino acid peptide, with a terminal glycine (G) residue that is covalently bound to the lysine residues of target proteins. Of the seventy-six amino acids comprising a ubiquitin molecule, seven are lysine residues (K6, K11, K27, K29, K33, K48, K63). Importantly, all of these lysine residues can themselves be ubiquitinated, which allows for the formation of polyubiquitin chains (106). Additionally, the first methionine (M) residue of ubiquitin can be conjugated to other ubiquitin molecules in a head-to-tail manner creating linear M1-linked chains (122). The linkage type is named for the amino acid number of the linked lysine, and each type has unique conjugation machinery, primarily dictated by the E2 enzymes, and elicits different functions. Furthermore, ubiquitin can be modified by other PTMs such as phosphorylation, acetylation, or even other UBLs like SUMOylation, allowing for nearly endless linkage type combinations that can modulate protein function (106). Classically,

ubiquitin was thought to only regulate proteins through direct covalent addition of the ubiquitin moiety to the lysine residue of a target protein, however, it has recently become clear that ubiquitin can also form free polyubiquitin chains that interact with a protein transiently, without direct peptide bonding to a substrate lysine and regulate protein function. Indeed, the elegant tetrameric structure required for RIG-I activation is held in stable conformation by unlinked ubiquitin chains (27, 76). Though by far the most well characterized ubiquitin types as signaling regulators are K48-linked ubiquitination events, which mark proteins for proteasomal degradation, and K63-linked ubiquitination events, which typically alter protein function through non-degradative mechanism (110), many of these newly discovered linkage types have been recently found to be regulators of antiviral signaling as well and are discussed in more detail below.

1.5.1.1 Types of ubiquitin ligases and their functions

As mentioned, ubiquitination of target proteins generally requires a three-step process. First, the E1 enzyme activates the ubiquitin molecule in an ATP-dependent manner, forming a thioester bond between a charged cysteine on the E1 and the C-terminus of ubiquitin. Then, the E1-ubiquitin complex interacts with the E2 enzyme, where ubiquitin is then transferred to a catalytically active cysteine residue of the E2. Finally, an E3 ligase facilitates the transfer of the ubiquitin molecule to a lysine residue of the target protein through an isopeptide bond with the terminal glycine of ubiquitin (95, 106, 112). Surprisingly, there are only two ubiquitin E1 ligases that have been found to exist in humans, and they typically bind non-specifically with the nearly forty different E2 ligases, which often dictate the ubiquitin linkage type. The E3 primarily confers the target substrate specificity, so it is unsurprising that nearly 700 have been identified so far, and that these are often the most well-characterized of the ligases due to their importance.

There are four major families of canonical E3 ligases: Really Interesting New Gene (RING), homologous to E6-associated protein C-terminus (HECT), U-box containing (UFD2 homology), and RING-in-between-RING E3 ligases (RBR). The mechanism for ubiquitin conjugation for each of these families is quite diverse, however, the most common type of E3 ligase is the RING E3 Ligase. These E3 ligases primarily act as a scaffold, never binding directly to the ubiquitin-moiety, but instead bringing together the ubiquitin-E2 complex, and the target protein for transfer. This is quite distinct from HECT ligases, which form an intermediate bond with the ubiquitin molecule, and then with the aid of a helper protein, F-box proteins which select substrates, the E3 can transfer the ubiquitin directly to its target. U-box ligases, or E4 ligases, work to elongate polyubiquitin chains, rather than directly catalyze ubiquitin to targets. RBR ligases act as a functional hybrid between RING E3 ligases and HECT E3 ligases, where the first RING domain acts as a canonical RING E3 ligase, and the second RING domain acts with the E2 to bring it in proximity to the substrate, where it then accepts the charged ubiquitin from the E2 and then catalyzes the transfer to the target protein (123–127). Interestingly, some newly emerging PTMs are displaying E3 ligase types that borrow different functional domains from each classical E3 ligases, or function in new ways, and as such, learning about those may uncover new mechanisms for ubiquitin addition to proteins as well.

1.5.1.2 Ubiquitin-linkages with roles in RIG-I signaling

In addition to K48-linked ubiquitin marking proteins for degradation, K11-, K29-, and K33- linked chains have also been implicated in proteasomal-dependent protein degradation, as treatment of cells with proteasome inhibitors leads to an accumulation of these types of ubiquitination events within the cell (128–130). Though K48-linked ubiquitin remains the primary ubiquitin type for protein destabilization generally, it has

been suggested that the other degradation marks are specifically utilized in certain signaling pathways such as cell cycle control (K11) (131), T-cell receptor signaling (K33) (132), or AMP-active protein kinase induction (K29, and K33) (133). However, a recent report has implicated K33-linked polyubiquitin chains regulating TBK1 during antiviral signaling, where it acts as a placeholder, effectively blocking the addition of K48-linked ubiquitination of TBK1 until signaling termination is reached (134). K29-linked ubiquitination of the influenza PB2 protein was found to be involved in promoting viral replication through a proteolytic-independent pathway (135) suggesting we are only just beginning to scratch the surface of the functional consequences of these ubiquitin linkage types.

M1-linked ubiquitin chains are catalyzed by the LUBAC complex. Intriguingly, M1-linked ubiquitination has recently emerged as a potent regulator of antiviral signaling (136–138). Through the activities of its associated E3 ligases, HOIL-1 and HOIP, it has been found to negatively regulate RIG-I signaling through the RIG-I co-factor, TRIM25 (92). TRIM25 is marked for proteasome-dependent degradation through this process. Additionally, HOIL-1 competes with TRIM25 for RIG-I binding, thereby preventing TRIM25-directed ubiquitination and RIG-I activation (92). M1-linked ubiquitin has also been shown to play a role in NF κ B activation through NEMO, an IKK complex protein (137). As such, M1-linked ubiquitin chains are becoming established as a potent signaling regulator for many antiviral pathways (139).

K63-linked ubiquitination remains one of the most potent regulators of RIG-I signaling. This is highlighted by the fact that de-ubiquitinases such as CYLD constantly surveil prior to infection, removing any K63-linked ubiquitination from key signaling regulators RIG-I, TBK1, and IKK ϵ to prevent premature activation (140). Its roles in direct

activation of RIG-I are discussed in section 1.6 of this chapter, however, its reach is much broader than RIG-I alone. TBK1 K63-linked ubiquitination triggers its relocalization from the cytosol to MAVS sites during infection, which is essential for IFN induction, although the exact mechanisms of its relocalization remain unclear (68, 141). MAVS is modified by K63-linked ubiquitin during infection, and this promotes its oligomerization and recruitment of downstream molecules (79, 142, 143). These are just few of the many reported ubiquitin-dependent regulatory events controlling RIG-I signaling, and as our detection capabilities and functional verification assays become more sophisticated, surely the nuances of K63-mediated innate immune regulation will be further uncovered.

Negative regulation of RIG-I signaling remains highly important in preventing excessive inflammation following viral infection (121). This negative regulation to terminate signaling is largely mediated through K48-linked ubiquitination which marks the signaling proteins for degradation. Both RIG-I and MAVS are both ubiquitinated by a promiscuous E3 ligase, RNF125 following antiviral signaling, which reduces IFN production (91). Interestingly, an E3 ligase called AIP4 is recruited to the MAM following infection, and then aids in the K48-ubiquitin-mediated degradation of MAVS, adding to the growing evidence of the sophistication of ubiquitin-mediated regulation of RIG-I signaling (144).

1.5.2 Ubiquitin-like modifications

Since the discovery ubiquitin in the 1970s, other protein based PTMs have emerged as regulators of protein function, with more being added constantly. These PTMs interestingly do not share much sequence homology with each other or with ubiquitin, however, their 3D structure is strikingly similar. As such, these modifications were dubbed UBLs, and all such proteins containing the canonical β -grasp fold of

ubiquitin can fall into this family (145). All of the proteins contained in this family also display glycine-to-lysine linkage of their target proteins, and are conjugated by an E1, E2, E3 ligase system (105). So far, the ubiquitin-like modifications that have ascribed functions are SUMOylation, NEDDylation, ISGylation, ATGylation/ARGylation, FATylation, and Ufmylation although there are other modifiers like FUBI/MNSF β , and Hub1 that are poorly understood and do not have an identified machinery system. In contrast to ubiquitin, these modifications have been found primarily to have non-degradative roles, and typically do not form chains, with the exception of SUMOylation (146). Also in contrast to ubiquitination, very little is known about their roles and functional consequences, however, multiple have been implicated to be novel regulators of RIG-I signaling.

1.5.2.1 SUMOylation

SUMOylation is probably the most well studied ubiquitin-like modification in regulating the antiviral response (147, 148). Recently, it has been shown that SUMOylation regulates both RIG-I and MDA5 through the addition of a SUMO moiety at multiple residues of the proteins. This is catalyzed by TRIM38 during very early infection prevents the sensors from being targeted for degradation by the addition of K48-linked ubiquitin. Further, SUMOylation can be removed during signaling termination by sentrin/SUMO-specific protease 2 (SEN2) which then allows for interaction with E3 ligases that K48-linked ubiquitin and lead to RLR degradation. Interestingly, IRF3 SUMOylation is induced by RLR signaling, however, this modification dampens the induction of IFNs through IRF3 degradation (149). This disconnect in functional outcomes of PTM by a ubiquitin-like modification is common, indicating that we have yet to understand much about the dynamics of these modifications.

1.5.2.2 NEDDylation

While NEDDylation is best described as being an essential activator of RBR E3 ligases (150), it has emerging roles in regulating antiviral responses. Interestingly, it appears as though even minute amounts of the protein modifier, NEDD8 are sufficient to produce phenotypic effects, and as such, traditional siRNA-mediated knockdown experiments are not suitable for studying NEDDylation. A novel NEDDylation inhibitor was recently discovered thus allowing for expanded investigation into the effects of NEDDylation in the antiviral response (151). In zebrafish, it was found that blocking NEDDylation led to a significant downregulation of antiviral genes following infection, and that IRF3 was modified by NEDDylation, possibly producing this affect (152). A different study identified that NEDDylation of IRF3 actually prevents the binding of IRF3 to the IFN- β promoter (151), which could be the possible mechanism conserved in zebrafish. Interestingly, NEDDylation is upregulated by influenza virus infection, and this has a pro-viral affect (153). It remains unclear if influenza virus specifically upregulates NEDDylation, or it is induced by antiviral signaling, although future work investigating how viruses co-opt non-degradative PTMs is an exciting area of study.

1.5.2.3 FATylation

FATylation is a UBL that is less well-characterized, both as a ubiquitin-like modifier and as an immune signaling regulator. Interestingly, a non-covalent interaction between the modifier, FAT10 and RIG-I has been implicated as a negative regulator of RIG-I signaling by directing RIG-I localization away from the mitochondria (154); however, it is unclear if this is through regulation with a RIG-I binding protein, or it has the ability to regulate localization itself.

1.5.2.4 ISGylation

ISG15, one of the earliest interferon-stimulated genes to be identified, has diverse roles in RIG-I signaling. Despite also being one of the first ubiquitin-like modifications discovered, its definitive roles in antiviral signaling have remained conflicted and elusive. Interestingly, ISGylation has been reported to negatively regulate RIG-I through inducing its degradation (58, 155). However, ISGylation has an overall positive effect on IFN signaling through prolonging the activation state of both IRF3 and STAT1 (156, 157). A recent report found that ISGylation of MDA5 was required for its oligomerization-dependent activation, and that ISGylation was antagonized by a SARS-CoV2 encoded protein (158). Interestingly, many viruses have co-opted ISGylation for their own benefit, where ISG15 conjugation onto a viral protein aids in their translation, or allows oligomeric platforms to form which aid in replication complex assembly (159–161). Though ISGylation of the influenza NS1 protein inhibits viral infection by preventing its oligomerization (162), demonstrating that we still have much to learn about the functions of ISGylation and how its functional roles are enacted.

1.6 Ufmylation

Ufmylation is the newest addition to the ubiquitin-like modification family, with the discovery of the protein modifier, UFM1, and its associate E1 and E2 ligases, UBA5 and UFC1, respectively, in 2004 (163). This modification is conserved in all multicellular organisms, indicating that its functions are likely necessary for survival (163). UFM1, an 85 amino acid protein must be processed prior to conjugation, removing the terminal two amino acids serine and cysteine to produce a mature UFM1, now with a terminal glycine (163). Two proteases were found to be active for ufmylation, UFSP1 and UFSP2. These proteases were originally thought to process UFM1 for conjugation and also remove

UFM1 from target proteins making ufmylation a dynamic process (164), but it was later found that only UFSP2 is active in humans (165). Interestingly, knockout of UFSP2 in human cells by us and others (166, 167) reveals no defect in UFM1 conjugation, as higher order UFM1-conjugates are observed via immunoblot. Indeed, deletion of UFSP2 leads to accumulation of these higher molecular weight species and less free UFM1, indicating that UFSP2 primarily works to remove UFM1 from substrates for recycling. This suggests we do not yet understand the full dynamics of how ufmylation is conjugated, as the first processing enzyme has remained a mystery. However, recently, a group identified a previously un-annotated long isoform of UFSP1 that appears to be the first UFM1 processing enzyme, and further studies investigating this will be invaluable to understanding the regulation of ufmylation (168). As for the other machinery, the E3 ligase, UFL1, was later identified and characterized in 2010 (169). While UFM1 contains six lysine residues (K3, K7, K19, K34, K41, and K69), to date, only one protein has been found to be polyufmylated through a K69 linkage (165, 170) revealing that most likely the vast majority of ufmylation events are due to mono-ufmylation.

1.6.1 The ufmylation conjugation system

UFM1 is conjugated onto target proteins through the actions of an E1, E2, and E3 ligase system, similar to ubiquitin and other ubiquitin-like proteins (Figure 4) (171, 172). Further, it can be recycled from its target proteins by a UFM1 specific protease. It differs from ubiquitination in that only one of each type of enzyme is currently known. Additionally, UFM1 is thought largely to regulate proteins through a non-degradative manner. Interestingly, how proteins are selected for ufmylation, and how ufmylation broadly regulates protein function remains elusive.

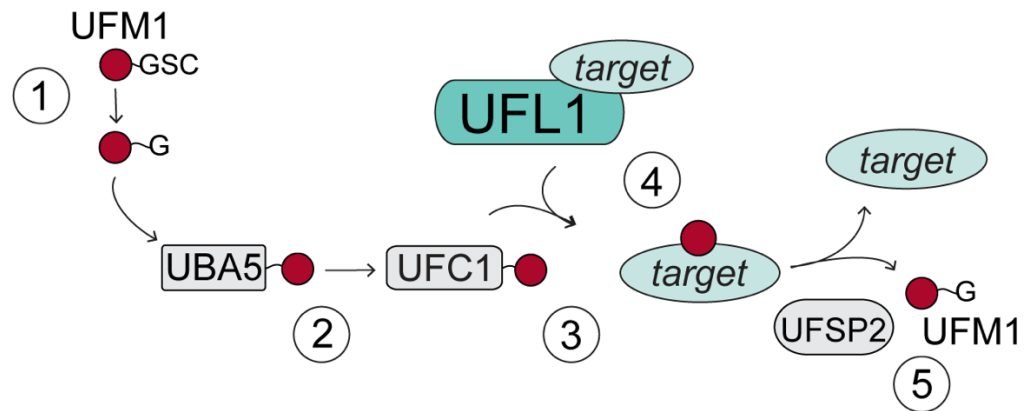


Figure 4: The ufmylation machinery system.

1) Pro-UFM1 is processed to remove the terminal two amino acids, forming UFM1. 2) UFM1 is conjugated onto the E1 ligase, UBA5, through a high-energy thioester bond. 3) UFM1 is then transferred to the E2, UFC1, forming another thioester bond. 4) UFL1 facilitates the transfer of UFM1 from the E2 onto a target protein through a covalent glycine-lysine linkage. 5) UFM1 specific protease UFSP2 can cleave UFM1 from the target protein to recycle UFM1.

Typically, substrate specificity for ubiquitin is dictated by the E3 ligase or E3 ligase-associated proteins. It is unknown if the same is true for ufmylation, as we are still learning about the dynamics of conjugation. Indeed, UFL1, the E3 ligase for ufmylation, does not fit the ascribed model of any of the four main E3 ligase families. It does not contain any of the typical annotated domains such as a RING, PRY-SPRY, or HECT (95, 169, 170). Though these canonical domains are absent in the UFL1 structure, we can make inferences on how it works based off of other characteristics. For instance, UFL1 lacks a catalytic cysteine, which would be required for UFL1 to directly transfer UFM1 to a target protein if it worked similarly to a HECT or RBR type E3 ligases (95, 123, 145, 170), suggesting it might act more like a RING or scaffold type E3 ligase, bringing together the target protein and the E2-UFM1 complex. Indeed, a new manuscript has confirmed that UFL1 acts primarily as a scaffold, and may require co-factors for the

ufmylation of certain proteins (165, 170). Early studies to determine the functional properties of the 794 amino acid UFL1 generated a series of truncation mutants to identify function domains (169). In this work, constructs were generated in which various portions of the C-terminus were deleted, 1-212, 1-452, 1-654, or where the N-terminus was deleted, 213-794, and 453-794. These truncations were analyzed based on two criteria: ability to bind to the E2 ligase, UFC1, and the ability to transfer UFM1 to a target substrate. The target substrate utilized was a UFL1/UFM1 interacting protein identified in this study, UFBP1. Interestingly, they found that the N-terminal domain containing amino acids 1-212 was the minimal region for E3 ligase activity, which has since been confirmed by us and others (167, 169, 170).

While the ufmylation pathway does appear to be intimately linked with the endoplasmic reticulum (ER) in function, the localization of the ufmylation machinery has remained elusive. While a number of reports find that UBA5 is primarily localized to the cytoplasm, one study found that a small portion of the UBA5 population can be relocalized to the ER with the aid of certain trafficking proteins (173–175). To date, no studies have focused on UFC1 localization, however, the understanding the subcellular localization of the ufmylation machinery could be important in understanding its roles in diverse pathways. The localization of UFL1 has caused much debate in the field. While some report that UFL1 is localized to the ER (169, 176–179), we and others have found that UFL1 remains cytoplasmic until a stressor is encountered, such as viral infection or DNA damage, which triggers UFL1 relocalization to cellular sites, such as the ER-mitochondrial membrane, or the nucleus, respectively (78, 167, 180, 181). It is clear however, that UFL1 localization is most likely regulated by other co-factors, and this might be different based on the signaling pathway activated (167, 178, 180, 181).

The role of UFBP1 in regulating ufmylation is also debated highly. It was first identified as a high-confidence UFL1-interacting protein and utilized in the initial characterization of UFL1 as the ufmylation E3 ligase as a highly ufmylated protein (169). However, since then it has been shown while UFBP1 does appear to form some type of lysine dependent conjugation, this is not dependent on UFL1 indicating that it is either not ufmylated, or there are other mechanisms for ufmylation we have yet to discover (178). It has been postulated that UFBP1 may play a more important role in the ufmylation pathway, as it does appear to be required for the formation of polyufmylated chains on one protein, ASC1 (165). Further, *in vitro* studies suggest that UFL1 is actually inactive on its own, and requires UFBP1 for UFM1 transfer to target proteins (170), however, studies in human cells will be required to determine if there are other factors that aid UFL1 function.

1.6.2 Functional consequences of UFM1 addition

Ufmylation is emerging as a post-translational modification that regulates diverse biological processes, including DNA repair, ER homeostasis, and even the replication of hepatitis A virus (166, 176, 178, 180–184). In these cases, UFL1, along with the other members of the ufmylation cascade, induce ufmylation of a target protein important for regulating these processes. It is unclear what signals induce ufmylation of target proteins, or why it is involved in regulating these diverse processes, but a pattern is emerging in which ufmylation of a target typically regulates its function by altering protein-protein interactions.

Both MRE11 and histone H4 are ufmylated by UFL1 in the nucleus in response to DNA damage resulting in activation the key DNA repair kinase ATM (180, 181). UFL1 also acts at the ER, where it plays a role in ER protein quality control, through ufmylation

of specific proteins, including ribosomal protein RPL26, to induce lysosomal degradation of stalled peptides and/or promote ER-phagy to prevent activation of the unfolded protein response (176, 178, 182, 184, 185). Hepatitis A virus translation, which occurs in association with the ER, also requires ufmylation of RPL26 (166). Therefore, ufmylation can regulate several aspects of translation. Ufmylation appears to play an important role in many cellular stress response pathways, and further work discovering the mechanisms of this regulation will be of great importance.

1.7 Summary of the work presented in this dissertation

Despite the work accomplished up to this point attempting to understand how innate immune signaling is regulated, our knowledge of the mechanisms controlling the intricately moving parts of RIG-I activation and immune signaling have yet to be elucidated. This has broad impacts on the outcome of viral infection, as viruses constantly evolve to subvert host defenses. Through my work, I have discovered a role for ufmylation in regulating the formation of the RIG-I relocalization complex. This complex formation consists of several host factors, including 14-3-3 ϵ , the molecular trafficking protein that relocalizes RIG-I to MAVS signaling sites. My work has uncovered a novel mechanism by which 14-3-3 ϵ selects RIG-I as cargo, allowing for MAVS interaction, and the induction of IFNs. Further, I have found that the ufmylation machinery all positively regulate the antiviral response, indicating that this could be a broadly utilized mechanism during RIG-I signaling (Figure 5). Indeed, I have found that there are many host proteins which become UFM1-conjugated in during viral infection in a RIG-I dependent manner, and a subset of those regulate IFN induction. In Chapter 2, I will discuss our work revealing the mechanisms by which the ufmylation machinery

regulates the expression of IFN and how UFM1 contributes to the antiviral response during RNA virus infection. In Chapter 3, I will discuss our discovery of the role of ufmylation in regulating early RIG-I activation through its effects on the 14-3-3 ϵ -RIG-I interaction and subsequent MAVS activation. In Chapter 4, I will discuss the class of proteins we have found to become ufmylated during viral infection. Taken together, this work reveals novel molecular regulators of RIG-I signaling, which has broad impacts on IFN induction and the antiviral response. These findings build on our understanding of how PTMs regulates viral infection and uncover a novel PTM pathway that is involved in antiviral responses.

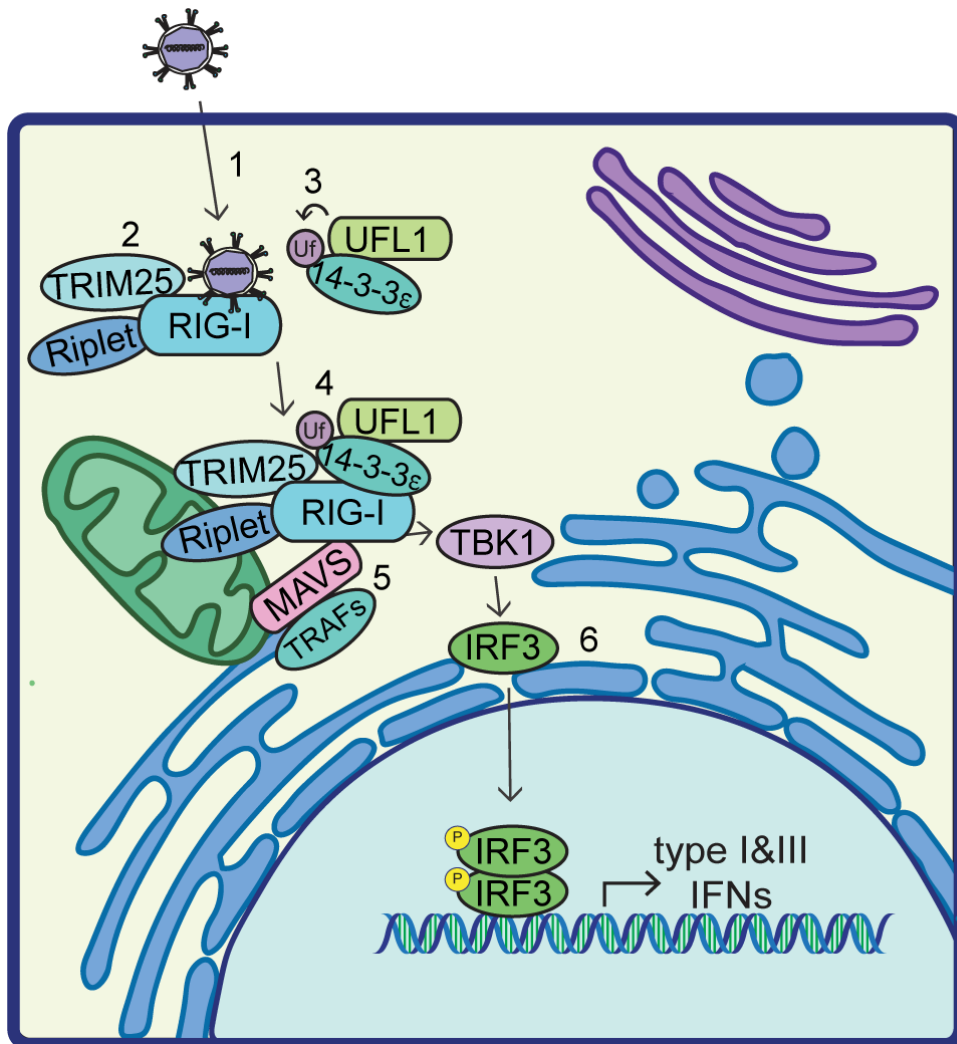


Figure 5: Graphical summary of work presented in this dissertation.

1) An RNA virus enters the cell and is sensed by RIG-I. 2) Viral infection triggers RIG-I ubiquitination (Ub) by TRIM25 and Riplet, and 3) ufmylation (Uf) of 14-3-3ε. 4) The RIG-I relocalization complex, including UFL1, is translocated to the MAM for interaction with MAVS in an ufmylation-dependent manner. 5) MAVS recruits TRAF3 and TBK1, which phosphorylates IRF3. 6) IRF3 translocates to the nucleus where it transcriptionally induces type I & III IFNs.

2. Signaling from the RNA sensor RIG-I is regulated by ufmylation

This chapter was adapted from a manuscript entitled “Signaling from the RNA sensor RIG-I is regulated by ufmylation” available in the Proceedings of the National Academy of Sciences (PNAS) (167). The authors are Daltry L. Snider, Moonhee Park, Kristen A. Murphy, Dia C. Beachboard, and Stacy M. Horner. Author contributions are as follows: D.L.S., D.C.B., and S.M.H. designed research; D.L.S., M.P., and S.M.H. performed research; D.L.S. and D.C.B. contributed new reagents/analytic tools; D.L.S., M.P., K.A.M., D.C.B., and S.M.H. analyzed data; and D.L.S. and S.M.H. wrote the manuscript with contributions from K.A.M. and D.C.B.

2.1 Introduction

Detection of RNA virus infection is initiated by cellular sensors such as RIG-I. RIG-I is a pattern recognition receptor that detects unique features of viral RNA that are generally absent in cellular RNA, referred to as pathogen-associated molecular patterns (PAMPs) (186). Sensing of viral RNA PAMPs triggers RIG-I activation and induces a downstream signaling cascade that ultimately results in transcriptional induction of type I and type III interferons (IFN) and the antiviral response (5, 18). The RIG-I signaling cascade is carefully regulated by multiple mechanisms, including post-translational modifications that influence specific protein-protein interactions that can result in changes in protein localization to mediated signaling (18, 80). For example, following sensing of RNA PAMPs, RIG-I undergoes K63-linked polyubiquitination in order to transition to its fully active conformation, which promotes its interaction with the molecular trafficking protein 14-3-3 ϵ (61, 85, 87, 187). 14-3-3 ϵ facilitates the recruitment

of activated RIG-I from the cytosol to intracellular membranes where it interacts with MAVS (61, 70, 71), which assembles other RIG-I pathway members to transduce the signals that induce IFN (61, 64). Importantly, many RNA viruses, including influenza A virus and some flaviviruses (dengue virus, Zika virus, and West Nile virus), prevent the interaction of RIG-I with 14-3-3 ϵ to limit IFN induction and evade the antiviral response (70–72).

In addition to RIG-I, a number of signaling proteins must be recruited to MAVS in order to propagate downstream IFN induction. Previously, we identified proteins that move to MAVS signaling sites at mitochondrial-associated endoplasmic reticulum (ER) membranes (MAM) during RNA virus infection (63, 78). These proteins likely aid in spatial organization of RIG-I pathway proteins during viral infection and include the GTPase RAB1B, which plays a role in recruiting TRAF3 to MAVS (188). In addition to RAB1B, we identified other proteins recruited to the MAM upon RIG-I signaling activation, one of which was UFL1 (referred to in our previous publication as KIAA0776) (78). UFL1 is an E3 ligase for UFM1, which is a ubiquitin-like modification of 85 amino acids. The process of ufmylation conjugates UFM1 covalently to lysine residues of target proteins through a process called ufmylation, which is similar to ubiquitination in that it also uses an E1, E2, and E3 ligase conjugation system (UBA5, UFC1, and UFL1; see Figure 4). UFM1 is removed by the UFSP2 protease (163, 164, 169, 171, 189). The consequence of UFM1 addition to proteins is not fully understood, but the literature supports the idea that it can promote protein-protein interactions to regulate a number of biological processes (165, 166, 176, 178, 180, 181, 183, 190–193). Here, I uncover a role for ufmylation in regulating RIG-I activation. I found that the cellular proteins that catalyze ufmylation all promote RIG-I-mediated induction of IFN including the E3 ligase

UFL1 and the protein-tag itself, UFM1. Further, I found that this signaling regulation is dependent on the ufmylation activity of UFL1. Indeed, through broadly profiling the virally induced transcriptome, I found that UFM1 was required for the induction of the antiviral response. Thus, ufmylation can regulate RIG-I activation and downstream signaling of the intracellular innate immune system.

2.2 Results

2.2.1 The ufmylation E3 ligase, UFL1, promotes RIG-I signaling

Having found that the E3 ligase of ufmylation UFL1 is recruited to MAVS signaling sites at the MAM in response to RIG-I signaling (78), I wanted to determine if UFL1 regulates RIG-I signaling. To test this, I measured induction of the IFN- β promoter following UFL1 overexpression using an IFN- β promoter luciferase reporter assay (194) and found that UFL1 increased activation of the IFN- β promoter, similar to that of RIG-I expression, in a dose-dependent fashion in response to infection with Sendai virus (SenV) (Figure 6A). SenV is a murine paramyxovirus that specifically activates RIG-I (195). In support of UFL1 enhancing RIG-I signaling specifically, exogenous expression of UFL1 also increased IFN- β promoter activity in response to transfection of 293T cells with a known RIG-I immunostimulatory RNA from hepatitis C virus (PAMP; Figure 6B) (196). However, UFL1 overexpression in 293T cells did not lead to increased induction of IFN-stimulated genes (ISG), such as *ISG56* or *ISG15*, in response to exogenous IFN- β treatment, which bypasses RIG-I signaling and IFN induction, indicating that UFL1 primarily regulates IFN induction and not the IFN response (Figure 6C). Next, I depleted UFL1 by siRNA in two different cell types and measured SenV-induced activation of the RIG-I pathway. Depletion of UFL1 in primary neonatal human dermal fibroblasts

(NHDFs) reduced the SenV-mediated induction of both *IFNB1* and *IFNL1* transcripts, as measured by RT-qPCR (Figure 6D), as well as production of IFN- β protein, as measured by an enzyme-linked immunosorbent assay (ELISA) (Figure 6E). Depletion of UFL1 in 293T cells resulted in decreased phosphorylation of IRF3, a transcription factor for both type I and III IFNs, while exogenous expression of an siRNA-resistant UFL1 restored SenV-mediated IRF3 phosphorylation (Figure 6F). Together, these data indicate that UFL1 positively regulates RIG-I signaling.

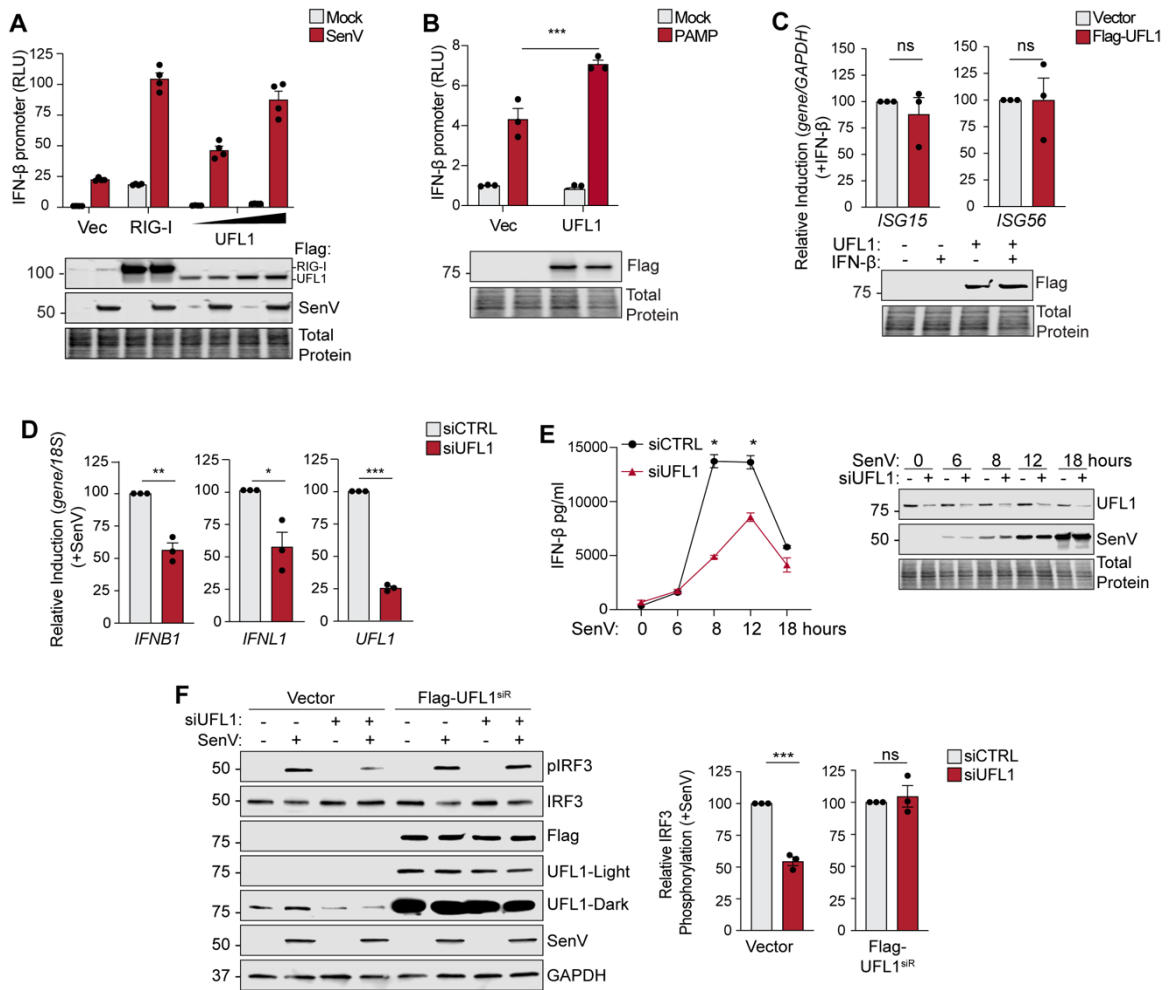


Figure 6: The ufmylation E3 ligase, UFL1, promotes RIG-I signaling.

A) IFN- β -promoter reporter luciferase expression (rel. to CMV-Renilla) from 293T cells expressing vector, Flag-UFL1, or Flag-RIG-I, followed by mock or SenV infection (18 h). B) IFN- β -promoter reporter luciferase expression (rel. to CMV-Renilla) from 293T cells transfected with vector (Vec) or Flag-UFL1, followed by mock or HCV PAMP RNA transfection (24 h). C) RT-qPCR analysis (rel. to GAPDH) of RNA extracted from 293T cells transfected vector or Flag-UFL1 that were treated with IFN- β (18 h). D) RT-qPCR analysis (rel. to 18S) of RNA extracted from primary neonatal human dermal fibroblasts (NHDFs) transfected with either siCTRL or siUFL1 followed by mock or SenV infection (8 h). E) ELISA for IFN- β of supernatants harvested from NHDFs transfected with siCTRL or siUFL1 and infected with SenV for the indicated times. F) Immunoblot analysis of p-IRF3 following siRNA transfection along with expression of vector or Flag-UFL1 siR, which has point mutations in the siRNA seed sequence. Quantification of p-IRF3/Tubulin is shown on the right. For A) mean \pm SD, $n=3$ technical replicates and representative of $n=3$ independent experiments. For all others, mean \pm SEM, $n=3$ biological replicates. * $p \leq 0.05$, ** $p \leq 0.01$, and *** $p \leq 0.001$ determined by two-way

ANOVA followed by Šidák's multiple comparisons test (B), Student's t-test (C-D, F), one-way ANOVA followed by Šidák's multiple comparisons test (E).

2.2.2 The ufmylation activity of UFL1 drives RIG-I signaling regulation

To define the domains of UFL1 that regulate RIG-I signaling, I expressed a series of previously described UFL1 truncation mutants and measured SenV-mediated activation of the IFN- β promoter in a luciferase reporter assay (169). The ability of UFL1 to transfer UFM1 to a target protein has been suggested to require the first 212 amino acids of the protein, as this domain interacts with the E2 conjugase for ufmylation, UFC1 (169). The wild-type (WT) UFL1 (aa 1-794), as well as the C-terminal deleted mutants of UFL1, aa 1-212 and aa 1-452, which all have reported ufmylation activity (169), stimulated SenV-mediated induction of the IFN- β promoter (Figure 7A). Interestingly, the N-terminal deleted mutant of UFL1 aa 213-794, which does not have reported ufmylation activity, also induced signaling, while the N-terminal deleted UFL1 mutant aa 453-794 did not (Figure 7A). To measure UFL1 conjugation activity in my hands, I quantified the formation of higher molecular weight UFM1-conjugates by immunoblotting. The 10 kDa UFM1 protein is known to be conjugated to a number of proteins, including the highly abundant RPL26 (176, 183). Indeed, my analysis of the higher molecular weight UFM1-conjugates induced by these UFL1 constructs revealed differential abundance of these UFM1-conjugates. Specifically, UFL1 WT, aa 1-212, aa 1-452, and aa 213-794 of UFL1 all retain full ufmylation activity, while aa 453-794 of UFL1 does not (Figure 7B). Thus, taken together, this reveals that the ufmylation activity of UFL1 is required to promote RIG-I signaling that results in the induction of IFN.

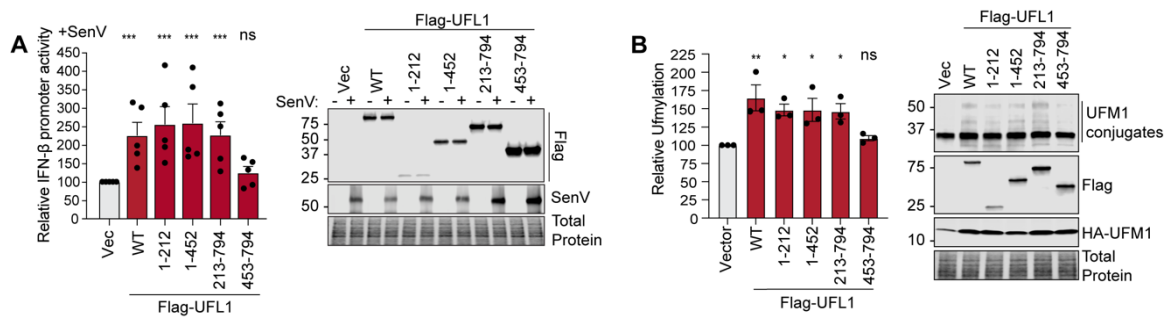


Figure 7: The ufmylation activity of UFL1 drives RIG-I signaling regulation.

A) Relative IFN- β -promoter reporter luciferase expression (rel. to CMV-Renilla) from 293T cells expressing indicated constructs followed by mock or SenV infection (12-18 h), with results graphed as relative SenV fold change for each. B) Quantification of immunoblots from 293T cells expressing HA-UFM1, and either vector or indicated Flag-UFL1 represented as the ratio of UFM1 conjugates (approximately 25-50 kDa) to total protein expression in each lane with vector set to 100. Graph indicates the mean \pm SEM for $n=3$ biological replicates. * $p \leq 0.05$ and ** $p \leq 0.01$ as determined by one-way ANOVA followed by Dunnett's multiple comparisons test.

2.2.3 The ufmylation machinery proteins positively regulate RIG-I signaling

As I determined that the ufmylation activity of UFL1 is important for its role in RIG-I signaling, I hypothesized that UFM1 and the proteins required for UFM1 conjugation would also be required to promote this signaling. Similar to my results with UFL1, overexpression of UFM1 increased SenV-mediated activation of the IFN- β promoter, resembling the magnitude of induction seen with RIG-I, in a dose-dependent fashion (Figure 8A). Conversely, the activation of the IFN- β promoter in response to SenV was significantly abrogated in 293T cells in which UFM1 was deleted by CRISPR/Cas9, as compared to WT 293T cells (Figure 8B). Importantly, this signaling was restored upon exogenous expression of UFM1 (Figure 8B). The absence of UFM1 expression also prevented the induction of IFN- β protein in response to SenV infection, as measured by ELISA (Figure 8C). The process of ufmylation has 5 steps (Figure 8D).

First, UFM1 is processed to expose the terminal glycine residue. Then, this mature UFM1 is added to the target protein by the actions of UBA5, which acts as an E1 conjugase for UFM1; UFC1, the E2 conjugase; and UFL1, the E3 ligase (171). Finally, the UFSP2 protease removes UFM1, which enables recycling of mature UFM1 (164). I found that exogenous expression of each of the proteins involved in UFM1 conjugation, including the UFSP2 protease, positively regulated SenV-mediated induction of the IFN- β promoter (Figure 8E). Conversely, the induction of *IFNB1* by SenV was abrogated in 293T cells in which UFSP2 was deleted by CRISPR/Cas9, similar to that seen upon UFM1 KO. Interestingly, I observed an increase in UFM1-retention by an ufmylated protein and a decrease in free UFM1 in the UFSP2 KO cells via anti-UFM1 immunoblot, suggesting UFSP2 may serve to primarily to increase the pool of available mature UFM1 for conjugation (Figure 8F). These results reveal that the proteins which catalyze ufmylation and the UFM1 modification itself promote RIG-I signaling.

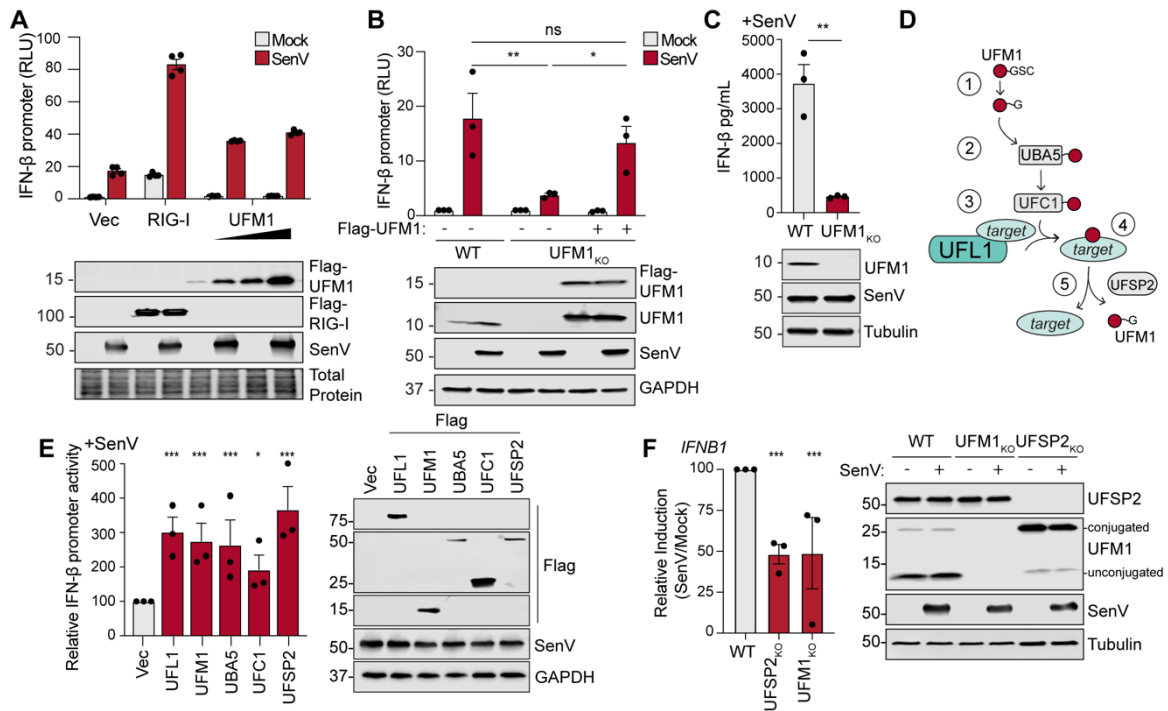


Figure 8: The ufmylation machinery proteins positively regulate RIG-I signaling.

A) IFN- β -promoter reporter luciferase expression (rel. to CMV-Renilla) from 293T cells expressing vector, Flag-UFM1, or Flag-RIG-I followed by mock or SenV infection (18 h) or in B) WT or CRISPR/CAS9 UFM1 KO 293T cells transfected with vector (Vec) or Flag-UFM1 (for KO), followed by mock or SenV infection (18 h). C) ELISA for IFN- β of supernatants harvested from WT or CRISPR/CAS9 UFM1 KO 293T cells that were SenV infected (18 h). D) Diagram of UFM1 conjugation. E) Relative IFN- β -promoter reporter luciferase expression (rel. to CMV-Renilla) from 293T cells expressing indicated constructs followed by mock or SenV infection (18 h), with results graphed as relative SenV fold change for each. F) RT-qPCR analysis (rel. to GAPDH) of RNA extracted from 293T WT, UFM1 KO or UFSP2 KO with either mock or SenV infection (18 h). For A) mean \pm SD, $n=3$ technical replicates and representative of $n=3$ independent experiments. For all others, mean \pm SEM, $n=3$ biological replicates. * $p \leq 0.05$, ** $p \leq 0.01$, and *** $p \leq 0.001$ determined by two-way ANOVA followed by Tukey's multiple comparisons test (A-B), Student's t-test (C), or one-way ANOVA followed by Dunnett's multiple comparisons test (E, F).

2.2.4 UFM1 is required for the RIG-I-driven transcriptional response

After establishing that ufmylation promotes RIG-I activation, and in turn IFN expression, I next broadly measured the impact of ufmylation upon the transcriptional response to RIG-I signaling. Using RNA-sequencing, I analyzed gene expression in either WT or UFM1 KO 293T cells, following mock or SenV infection (Table 1.1; Table 1.2). Gene set enrichment analysis (Table 2.1; Table 2.2) of the transcripts significantly reduced (adjusted $P < 0.01$) by UFM1 KO in the absence of viral infection revealed previously described pathways regulated by ufmylation such as cytosolic ribosomes, ribosome assembly, and hematopoiesis (Figure 9A; Table 2.1) (176, 182, 183, 192). Following viral infection, the top 10 gene categories negatively impacted by UFM1 KO, with a darker red color indicating more downregulation, were all related to the antiviral response, such as response to type I IFN and defense against virus (Figure 9B; Table 2.2). Indeed, of the top 50 most downregulated pathways impacted by UFM1 KO during infection, the majority were related to innate immune signaling or viral replication (Table 2.2), while upregulated gene categories were more diverse (Table 2.3; Table 2.4). Of the genes differentially expressed during UFM1 KO in response to SenV (adjusted $P < 0.01$), the majority are downregulated (Figure 9C). Indeed, these downregulated genes included *IFNB1* and *IFNL1*, as well as other known ISGs (in red) (197) (Figure 9C; Figure 9D). These data are consistent with a model in which ufmylation-mediated regulation of IFN induction has broad consequences on genes induced by the IFN response.

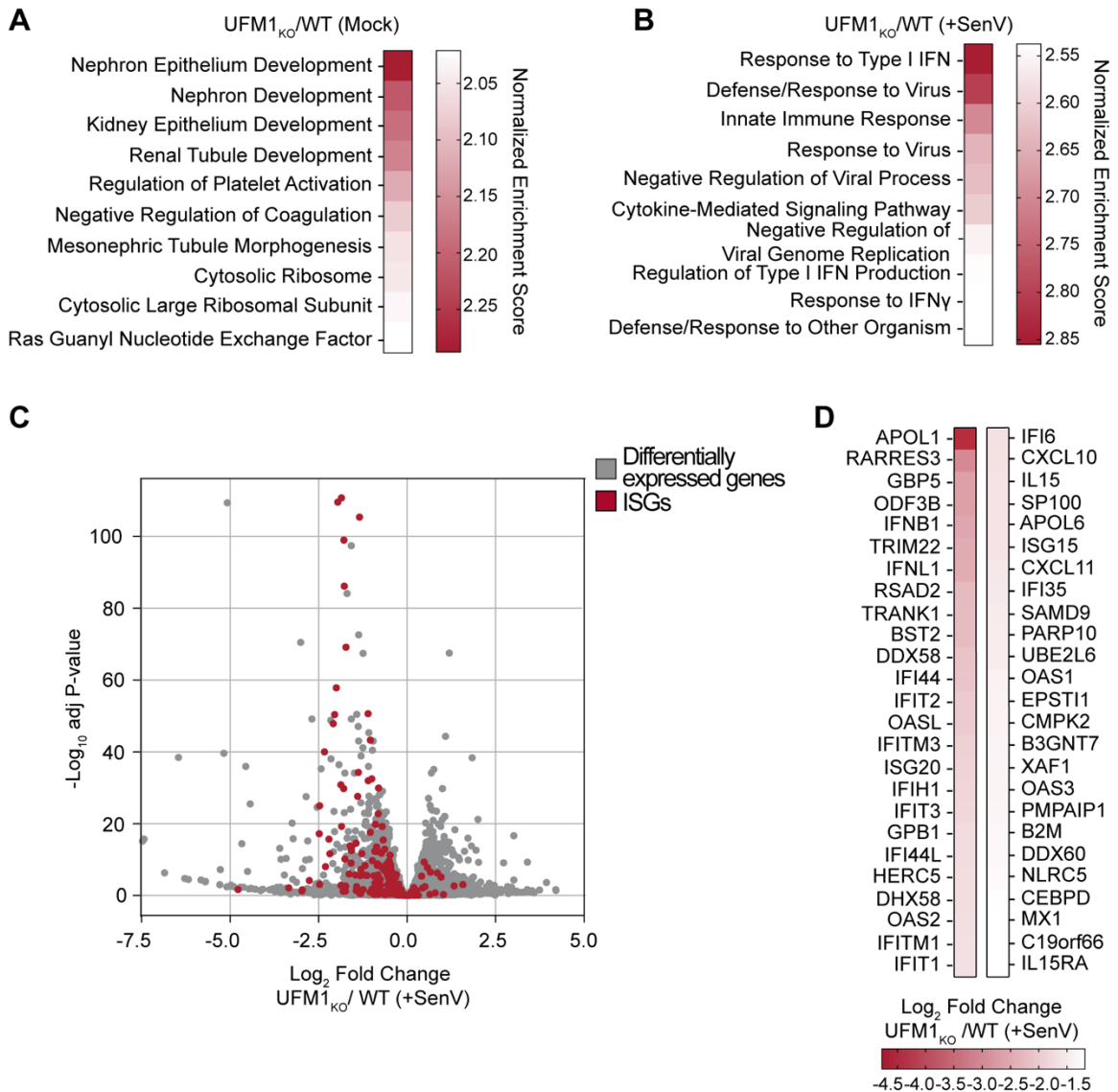


Figure 9: UFM1 is required for the RIG-I driven transcriptional response.

RNA-seq analysis of WT versus UFM1 KO 293T cells showing the gene set enrichment analysis (top 10 categories) of negatively regulated differentially expressed genes represented by normalized enrichment score to identify gene ontology terms and pathways associated with altered gene expression for each of the comparisons performed in A) mock or B) SenV-infected (18 hours) 293T cells represented by normalized enrichment score (UFM1 KO / WT). C) Volcano plot of differentially expressed genes (adj $P < 0.01$) shown in grey, with ISGs shown in red, in SenV-infected 293T cells (UFM1 KO / WT). D) Heatmap of the effect of UFM1 KO on the fold change of the 50 most induced IFN and ISGs (UFM1 KO / WT) following SenV infection (adj $P < 0.01$).

Table 1: Differential expression analysis from RNA-seq analysis for UFM1 KO / WT 293T cells.

Table 1.1: UFM1 KO / WT Mock
Table 1.2: UFM1 KO / WT SenV (18 h)
Due to size, this table has not been included in this document. It can be downloaded from this link: Dataset 1

Table 2: Gene Set Enrichment Analysis for UFM1 KO / WT 293T cells.

Table 2.1: UFM1 KO / WT Mock- negative direction
Table 2.2: UFM1 KO / WT SenV (18 h)- negative direction
Table 2.3: Table S2.3 UFM1 KO / WT Mock- positive direction
Table 2.4: UFM1 KO / WT SenV (18 h)- negative direction
Due to size, this table has not been included in this document. It can be downloaded from this link: Dataset 2

2.3 Conclusions

Regulation of RIG-I activation and downstream signaling is essential for proper induction and termination of IFN. Indeed, PTMs play a crucial role in this regulation, guiding nearly every step of the antiviral response, both in activation and deactivation of signaling, contributing to the delicate balance required for exact execution of IFN production. Here, I show that both UFL1 and the process of ufmylation promote RIG-I pathway signaling that leads to IFN induction, uncovering an important step in the activation of the RIG-I pathway. Further, I found that the ufmylation activity of UFL1 is required for this signaling regulation, providing evidence for a new type of PTM in regulating RIG-I signaling.

2.4 Materials and Methods

2.4.1 Cell lines, viruses, and treatments.

Neonatal human dermal fibroblast (NHDF) cells and embryonic kidney 293T cells were grown in Dulbecco's modification of Eagle's medium (DMEM; Mediatech) supplemented with 10% fetal bovine serum (Thermo Fisher Scientific), 1X minimum essential medium non-essential amino acids (Thermo Fisher Scientific), and 25 mM HEPES (Thermo Fisher Scientific) (cDMEM). 293T (CRL-3216) were obtained from American Type Culture Collection (ATCC), NHDF cells (CC-2509) were obtained from Lonza. All cell lines were verified as mycoplasma free by the LookOut Mycoplasma PCR detection kit (Sigma). SenV Cantell strain was obtained from Charles River Laboratories and used at 200 hemagglutination units/mL (HAU). SenV infections were performed in serum-free media (30 minutes to 1 hour), after which complete media was replenished. IFN- β (PBL Assay Science) was added to cells at a concentration of 50 units/mL in cDMEM for 18 hours.

2.4.2 Plasmids.

The following plasmids have been previously described: pEF-TAK-Flag, pEF-BOS-Flag-RIG-I (62), pIFN- β -luc (64), pCMV-Renilla (Promega), pX459 (Addgene #62988). pLJM1_Flag-UFM1 was a gift from Drs. Craig McCormick and John Rohde at Dalhousie University. The following plasmids were generated by insertion of PCR-amplified fragments into the NotI-to-PmeI digested pEF-TAK-Flag using InFusion cloning (Clontech): pEF-TAK-Flag-UFL1 (GenBank: BC036379; GeneID: 23376), pEF-TAK-Flag-UBA5 (NM_024818.6), pEF-TAK-Flag-UFC1 (NM_016406.4), pEF-TAK-Flag-UFSP2 (NM_018359.5), pEF-TAK-Flag-UFL1 1-212, pEF-TAK-Flag-UFL1 1-452, pEF-TAK-Flag-UFL1 213-794, and pEF-TAK-Flag-UFL1 453-794. pEF-TAK-Flag-UFL1siR

was generated using site-directed mutagenesis. To generate the CRISPR guide RNA plasmids px459-UFM1-E2, px459-UFM1-B, and px459-UFSP2 sgRNA oligonucleotides were annealed and inserted into the BbsI-digested pX459 (30, 66). The plasmid sequences were verified by DNA sequencing.

2.4.3 Generation of RNA PAMP.

Annealed oligonucleotides containing the sequence of the HCV 5'ppp poly-U/UC region (34) were in vitro transcribed using the MEGAscript T7 transcription kit (Ambion) followed by ethanol precipitation, with the resulting RNA resuspended at 1 $\mu\text{g}/\mu\text{L}$.

2.4.4 Transfections.

DNA transfections were performed using FuGENE6 (Promega) or TransIT-LT1 (Mirus Bio). RNA PAMP transfections were done using the TransIT-mRNA Transfection kit (Mirus Bio). The siRNA transfections were done using Lipofectamine RNAiMax (Invitrogen). siRNAs directed against UFL1 (Qiagen-SI04371318), or non-targeting AllStars negative control siRNA (Qiagen-1027280) were transfected into 293T cells (25 pmol of siRNA; final concentration of 0.0125 μM) or NHDF cells (250 pmol of siRNA; final concentration of 0.25 μM). Media was changed 4-24 hours post-transfection, and cells were incubated for 36-48 h post-transfection prior to each experimental treatment. IFN- β -promoter luciferase assays were performed as previously described at 18-24 hours post treatment and normalized to the Renilla luciferase transfection control (33).

2.4.5 ELISAs.

IFN- β ELISAs were performed using Human IFN-beta DuoSet (R&D Systems) with supernatants collected from cultured cells.

2.4.6 Generation of cell lines.

UFM1 and UFSP2 KO 293T cells were generated by CRISPR/Cas9, using two guides targeting exon 2 and 3 (UFM1) or a single guide targeting exon 6 (UFSP2), similar to others, as we have done previously. Single cell clones were validated via anti-UFM1 or anti-UFSP2 immunoblot and genomic sequencing, with one clone used here (15, 30).

2.4.7 RNA analysis.

Total cellular RNA was extracted using the RNeasy Plus mini kit (Qiagen). RNA was then reverse transcribed using the iScript cDNA synthesis kit (BioRad), as per the manufacturer's instructions. The resulting cDNA was diluted 1:3 in ddH₂O. RT-qPCR was performed in triplicate using the Power SYBR Green PCR master mix (ThermoFisher) and QuantStudio 6 Flex RT-PCR system.

2.4.8 RNA-seq.

WT and UFM1 KO 293T cells were mock or SenV-infected (18 h) and harvested in biological duplicate, followed by total RNA extraction via TRIzol reagent (ThermoFisher Scientific). Sequencing libraries were prepared using the KAPA Stranded mRNA-Seq Kit (Roche) and sequenced on an Illumina Novaseq 6000 with 50 bp paired-end

reads (>20 million reads per sample) in an S1 flow cell by the Duke University Center for Genomic and Computational Biology.

RNA-seq data was processed using the TrimGalore toolkit (67) which employs Cutadapt (68) to trim low-quality bases and Illumina sequencing adapters from the 3' end of the reads. Only reads that were 20nt or longer after trimming were kept for further analysis. Reads were mapped to the GRCh38v93 version of the human genome and transcriptome (69) using the STAR RNA-seq alignment tool (70). Reads were kept for subsequent analysis if they mapped to a single genomic location. Gene counts were compiled using the HTSeq tool (71). Only genes that had at least 10 reads in any given library were used in subsequent analysis. Normalization and differential expression analysis was carried out using the DESeq2 (72) Bioconductor (73) package with the R statistical programming environment. The false discovery rate was calculated to control for multiple hypothesis testing. Gene set enrichment analysis (74) was performed to identify gene ontology terms and pathways associated with altered gene expression for each of the comparisons performed. All RNA-seq data are deposited in the GEO database under GSE186287.

2.4.9 Immunoblotting.

Cells were lysed in a modified radioimmunoprecipitation assay (RIPA) buffer (10 mM Tris [pH 7.5], 150 mM NaCl, 0.5% sodium deoxycholate, and 1% Triton X-100) supplemented with protease inhibitor cocktail (Sigma) and Halt Phosphatase Inhibitor (Thermo-Fisher), and post-nuclear lysates were isolated by centrifugation. Quantified protein (between 5 -15 µg) was resolved by SDS/PAGE, transferred to nitrocellulose or polyvinylidene difluoride (PVDF) membranes in a 25 mM Tris-192 mM glycine-0.01% SDS buffer. Membranes were stained with Revert 700 total protein stain (LI-COR

Biosciences) and then blocked in 3% BSA in Tris-buffered saline containing 0.01% Tween-20 (TBS-T). After washing with PBS-T or TBS-T (for phosphoproteins) buffer, following incubation with primary antibodies, membranes were incubated with species-specific horseradish peroxidase-conjugated antibodies (Jackson ImmunoResearch, 1:5000) or fluorescent secondaries (LI-COR Biosciences), followed by treatment of the membrane with Clarity Western ECL substrate (BioRad) and imaging on a LICOR Odyssey FC. The following antibodies were used for immunoblotting: R-anti-SenV (MBL, 1:1000), M-anti-Tubulin (Sigma, 1:1000), R-anti-GAPDH (Cell Signaling Technology, 1:1000), R-anti-p-IRF3 (Cell Signaling Technology, 1:1000), R-anti-IRF3 (Cell Signaling Technology, 1:1000), R-anti-UFL1 (Novus Biologicals, 1:1000), R-anti-UFM1 (Abcam, 1:1000), M-anti-Flag M2 (Sigma, 1:1000), anti-Flag-HRP (Sigma, 1:1000-1:5000), R-anti-Flag (Sigma, 1:1000).

3.4.9 Quantification of immunoblots.

Immunoblots imaged using the LICOR Odyssey FC were quantified by ImageStudio software, and raw values were normalized to relevant controls for each antibody.

3.4.10 Statistical analysis.

Student's unpaired t-test, one-way ANOVA, or two-way ANOVA were implemented for statistical analysis of the data followed by appropriate post-hoc test (as indicated) using GraphPad Prism software. Graphed values are presented as mean \pm SD or SEM (n = 3 or as indicated); *p \leq 0.05, **p \leq 0.01, and ***p \leq 0.001.

3. Ufmylation regulates IFN induction through RIG-I membrane targeting

This chapter was adapted from a manuscript entitled “Signaling from the RNA sensor RIG-I is regulated by ufmylation” available as a preprint (167). The authors are Daltry L. Snider, Moonhee Park, Kristen A. Murphy, Dia C. Beachboard, and Stacy M. Horner. Author contributions are as follows: D.L.S., D.C.B., and S.M.H. designed research; D.L.S., M.P., and S.M.H. performed research; D.L.S. and D.C.B. contributed new reagents/analytic tools; D.L.S., M.P., K.A.M., D.C.B., and S.M.H. analyzed data; and D.L.S. and S.M.H. wrote the manuscript with contributions from K.A.M. and D.C.B.

3.1 Introduction

Following the binding of RIG-I to non-self RNA, it interacts with several host proteins to facilitate its activation, localization to the MAM, and interaction with MAVS. These proteins include the E3 ligases for lysine (K63-linked ubiquitin Riplet and TRIM25 (27, 85, 87), as well as the molecular trafficking protein 14-3-3 ϵ . In particular, 14-3-3 ϵ is required for RIG-I recruitment from the cytosol to MAVS signaling sites at intracellular membranes (61, 63, 85, 87); however, the mechanism underlying how 14-3-3 ϵ selects RIG-I as cargo has yet to be elucidated. Having uncovered that ufmylation promotes RIG-I signaling, I found that following RNA virus infection UFL1 interacts with both RIG-I and the molecular trafficking protein 14-3-3 ϵ , and that 14-3-3 ϵ undergoes ufmylation. Further, similar to RIG-I, UFL1 is recruited to intracellular membranes following RNA virus infection. Importantly, loss of ufmylation prevents the interaction of 14-3-3 ϵ with RIG-I, which results in decreased MAVS activation and IFN induction in response to RNA virus infection.

3.2 Results

3.2.1 UFL1 is recruited to intracellular membranes and interacts with 14-3-3 ϵ and RIG-I during RNA virus infection

Using a subcellular membrane fractionation assay (198), I confirmed that UFL1 increases its association with intracellular membranes in response to SenV, similar to RIG-I (Figure 10A; compare fraction #1, which has Cox-I and no GAPDH, with fractions #6-8, which are enriched for the cytosolic protein GAPDH) (61, 72). This finding is consistent with our previous report that UFL1 is recruited to the MAM in response to either SenV or hepatitis C virus replication (78), suggesting that UFL1 recruitment occurs prior to MAVS activation, as MAVS is cleaved by the HCV NS3-NS4A protease (199–202). As the recruitment of RIG-I to intracellular membranes is known to require 14-3-3 ϵ , and, as both UFL1 and UFM1 have been shown to interact with 14-3-3 ϵ (169), I hypothesized that UFL1 may interact with 14-3-3 ϵ to promote the IFN induction that we had observed in response to RNA virus infection. Thus, I first determined if the interaction of UFL1 with 14-3-3 ϵ is increased in response to RIG-I activation by SenV by performing co-immunoprecipitation. I found that Myc-14-3-3 ϵ did co-immunoprecipitate with Flag-UFL1, as reported previously (169), and that this interaction was increased by SenV infection (Figure 10B). Interestingly, the interaction of UFL1 with RIG-I also increased following SenV, both upon over-expression and at the level of the endogenous proteins (Figure 10C; Figure 10D). As RIG-I undergoes a series of modifications to become fully active (Figure 3) (80, 186), I next used a panel of RIG-I mutants to define which stage of RIG-I activation promotes interaction with UFL1. These mutations prevent the distinct steps of RIG-I activation such as RIG-I binding to RNA (K888/907A),

interacting with TRIM25 (T55I), or ubiquitination by Riplet and TRIM25 (K172/788R) (86, 87, 203). The interaction of UFL1 with RIG-I was significantly impaired by each of these mutations, suggesting that UFL1 regulates RIG-I function after it binds RNA and becomes ubiquitinated (Figure 10E). As this is the same step of activation at which 14-3-3 ϵ binds to RIG-I to promote its translocation to intracellular membranes (61), I next tested the ability of UFL1 to promote RIG-I signaling in conjunction with the RIG-I regulatory factors Riplet and 14-3-3 ϵ (61, 85). I found that co-expression of equal amounts of UFL1 with either Riplet or 14-3-3 ϵ increased SenV-mediated activation of the IFN- β promoter above that seen by the individual proteins (Figure 10F). Intriguingly, the expression of UFL1 appears to be stabilized or enhanced in the presence of Riplet and 14-3-3 ϵ . These data together suggest that RNA virus infection increases the interaction of 14-3-3 ϵ with UFL1, which then interacts with activated, K63-ubiquitinated RIG-I to promote downstream signaling.

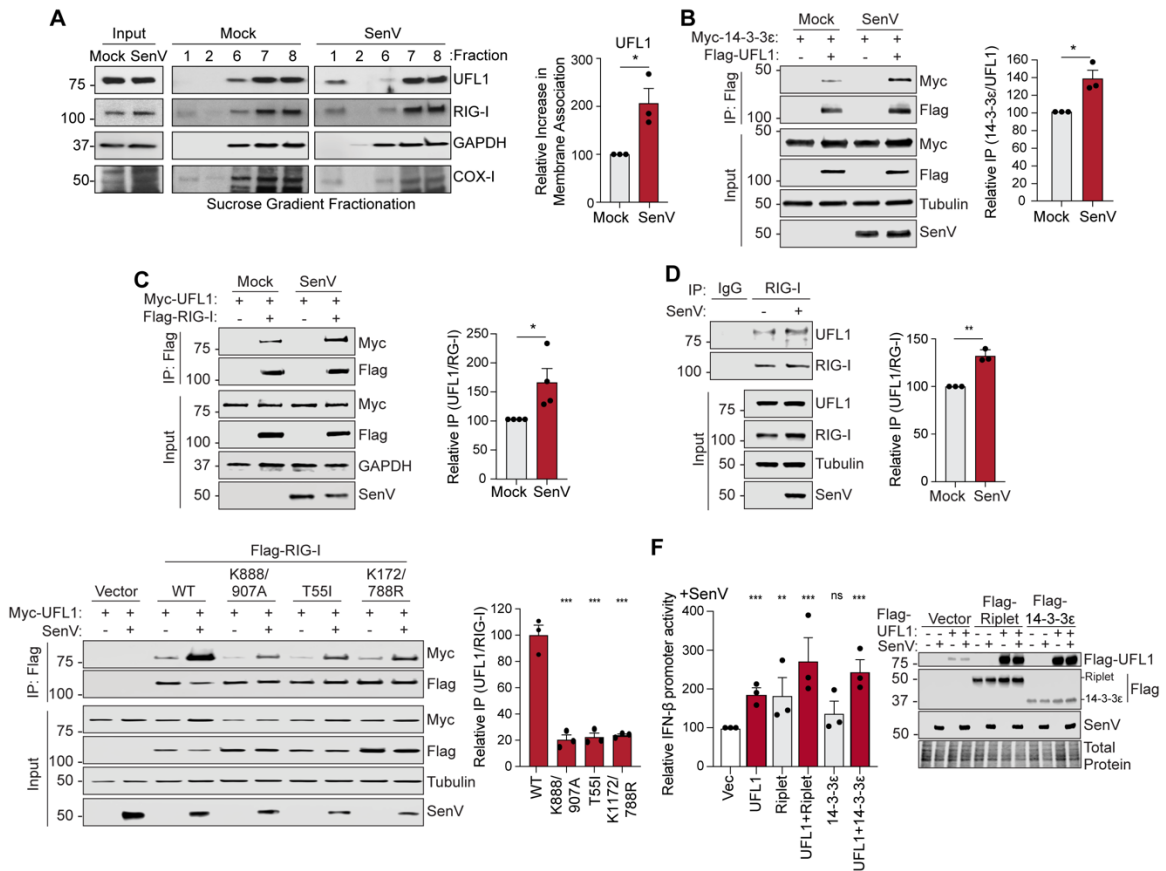


Figure 10: UFL1 is recruited to intracellular membranes and interacts with 14-3-3ε and RIG-I during RNA virus infection.

A) Immunoblot analysis of inputs and subcellular membrane flotation of 293T cell extracts that were mock or SenV-infected (4 h) followed by sucrose gradient fractionation, with fraction numbers indicated from the top of the gradient (1) to bottom (8). Fractionation controls, GAPDH for cytosol and Cox-I for membranes, are indicated and reveal that the membranes are localized to fraction #1. Relative quantification of the ratio of UFL1 to a membrane marker (Cox-I) in fraction 1 normalized to total protein levels in inputs are shown on the right. B) Immunoblot analysis of anti-Flag immunoprecipitated extracts and inputs from 293T cells expressing Myc-14-3-3ε and Flag-UFL1 that were mock- or SenV-infected (4 h), with relative quantification on right. C) Immunoblot analysis of anti-Flag immunoprecipitated extracts and inputs from 293T cells expressing Myc-UFL1 and Flag-RIG-I that were mock- or SenV-infected (4 h), with relative quantification with IP values normalized to inputs values on right. D) Immunoblot analysis of anti-RIG-I immunoprecipitated (or anti-IgG) extracts and inputs from 293T cells that were mock- or SenV-infected (4 h), with relative quantification with IP values normalized to inputs values on right. E) Immunoblot analysis of anti-Flag immunoprecipitated extracts and inputs from 293T cells expressing Myc-UFL1 and Flag-RIG-I constructs that were mock- or SenV-infected (4 h), with results quantified as relative fold change (SenV to Mock) for each. F) Relative IFN-β-promoter reporter

luciferase expression (rel. to *CMV-Renilla*) from 293T cells expressing indicated constructs followed by mock or SenV infection (18 h), with results graphed as relative SenV fold change for each. The graphs are represented as the mean \pm SEM, $n=3$ (A-B, D-F) or $n=4$ (C) biological replicates and $*p \leq 0.05$, $**p \leq 0.01$, and $***p \leq 0.001$ determined by Student's t-test (A-D) or one-way ANOVA followed by Dunnett's multiple comparisons test (E-F).

3.2.2 UFL1 interaction with RIG-I requires 14-3-3 ϵ and UFM1

Having determined that UFL1 interacts with both activated RIG-I and 14-3-3 ϵ following RNA virus infection, I next defined the dynamics of this complex formation by testing two distinct models. In the first model, UFL1 would interact first with activated RIG-I, induce its ufmylation, and then the UFL1-RIG-I complex would interact with 14-3-3 ϵ . In this model, depletion of 14-3-3 ϵ or loss of UFM1 would not be expected to change the interaction of UFL1 with RIG-I. In the second model, UFL1 would interact first with 14-3-3 ϵ and induces its ufmylation, or that of another associated protein, and then the UFL1-14-3-3 ϵ complex would interact with activated RIG-I. In this second model, depletion of 14-3-3 ϵ would be expected to prevent UFL1 interaction with RIG-I, and loss of ufmylation would limit UFL1 interaction with RIG-I but would not affect UFL1 interaction with 14-3-3 ϵ . To elucidate these possibilities, first, I used co-immunoprecipitation to measure the interaction of exogenously expressed Flag-UFL1 and HA-RIG-I in SenV-infected 293T lysates that had been depleted of 14-3-3 ϵ or CTRL by siRNA. This revealed that formation of the SenV-activated RIG-I-UFL1 complex requires 14-3-3 ϵ (Figure 11A). Next, I tested if ufmylation was required for formation of the SenV-activated RIG-I-UFL1 complex by measuring this interaction in WT or UFM1 KO 293T cells. I found that UFM1 was required for SenV-activated RIG-I-UFL1 complex (Figure 11B). The results of these two experiments reveal that both 14-3-3 ϵ and UFM1

are required for UFL1 to interact with RIG-I, supporting the second model of complex formation in which UFL1 interacts first with 14-3-3 ϵ and catalyzes its ufmylation, and then this complex associates with RIG-I. In support of this, I found that UFM1 was not required for UFL1 to interact with 14-3-3 ϵ (Figure 11C). To test if 14-3-3 ϵ is UFM1-conjugated, I performed an immunoprecipitation of Flag-14-3-3 ϵ from cell extracts that were mock or SenV-infected and expressed either HA-UFM1-WT or HA-UFM1DC3, which lacks the terminal 3 amino acids required conjugation to target proteins (163). Importantly, these extracts were boiled prior to immunoprecipitation to remove non-covalent interactions. Following immunoprecipitation of Flag-14-3-3 ϵ , immunoblotting with an anti-HA antibody revealed a slower migrating form of 14-3-3 ϵ approximately 15 kDa heavier (HA+UFM1) than the predicted molecular weight of 14-3-3 ϵ (37 kDa) (Figure 11D), suggestive of covalent UFM1 modification. Additionally, the proportion of 14-3-3 ϵ , conjugated by UFM1 increases following SenV infection. Together, these data indicate that ufmylation promotes the interaction of UFL1 with 14-3-3 ϵ and activated RIG-I and that UFM1 has increased conjugation to 14-3-3 ϵ following RIG-I activation.

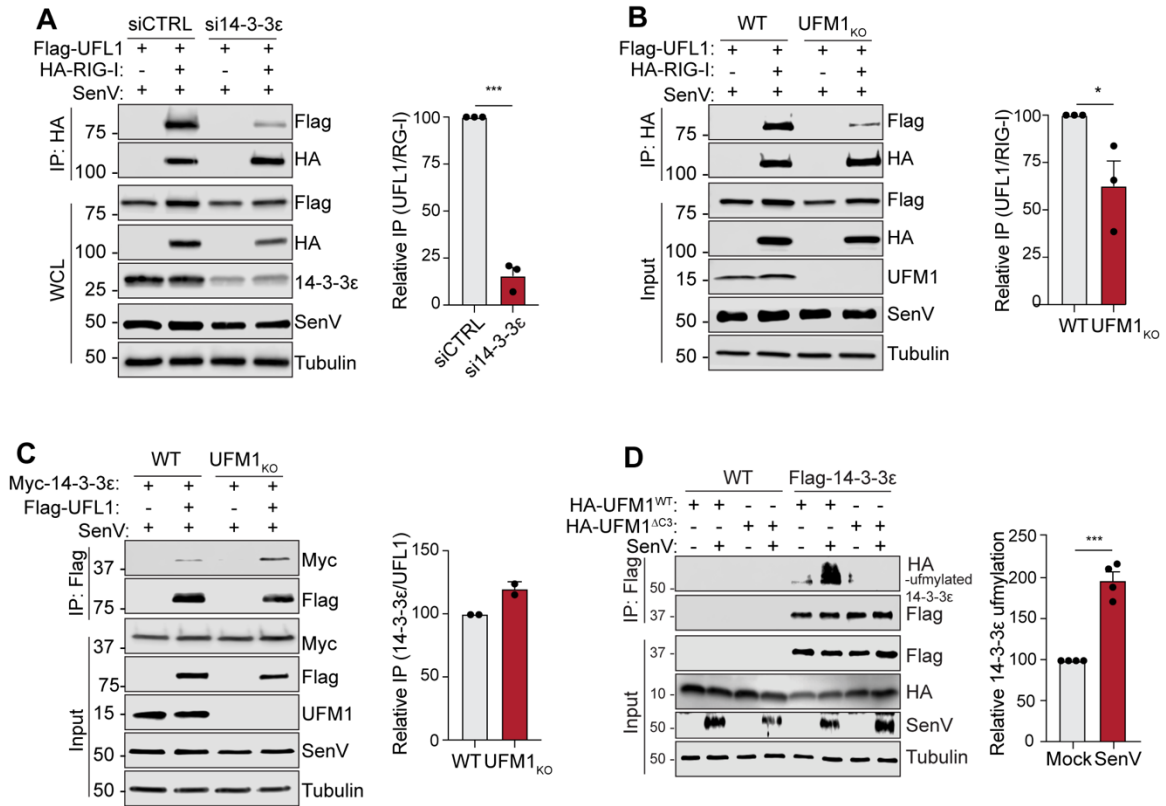


Figure 11: UFL1 interaction with RIG-I requires 14-3-3ε and ufmylation.

A) Immunoblot analysis of anti-HA immunoprecipitated extracts and inputs from 293T cells transfected with siCTRL or si14-3-3ε followed by SenV infection (4h). B) Immunoblot of anti-HA immunoprecipitated extracts and inputs from 293T WT or UFM1 KO cells transfected with HA-RIG-I and Flag-UFL1. C) Immunoblot of anti-Flag immunoprecipitated extracts and inputs from 293T WT or UFM1 KO cells transfected with Flag-UFL1 and Myc-14-3-3ε. D) Immunoblot of anti-flag immunoprecipitated extracts and inputs from either 293T-WT or 293T-Flag-14-3-3ε cells transfected with either HA-UFM1-WT or HA-UFM1^{ΔC3}. In (A-D), SenV infection was for 4 hours, and for all, relative quantification of the interacting protein vs. IP protein is shown to the right as a graph, indicating the mean \pm SEM (A, B, D), $n=3$ (A, B) or $n=4$ (D) biological replicates. For (C) values shown are SD of IP values adjusted for input expression, with $n=2$ biological replicates. * $p \leq 0.05$, ** $p \leq 0.01$, and *** $p \leq 0.001$ determined by Student's t-test.

3.2.3 Ufmylation promotes RIG-I interaction with 14-3-3 ϵ for MAVS activation

As I found that that UFL1 requires 14-3-3 ϵ to interact with activated RIG-I, I next tested if UFL1 is required for the interaction of 14-3-3 ϵ with RIG-I, which is essential for activated RIG-I to translocate from the cytosol to intracellular membranes for interaction with MAVS (61). I performed a co-immunoprecipitation of Flag-RIG-I and Myc-14-3-3 ϵ from 293T cells and found that this SenV-mediated interaction was significantly decreased upon UFL1 depletion (Figure 12A). In addition, loss of UFM1 expression also decreased the SenV-induced interaction of RIG-I with 14-3-3 ϵ (Figure 12B). Importantly, I also found that UFM1 is required for the SenV-induced interaction of RIG-I with MAVS (Figure 12C) and MAVS higher-order oligomerization, which is a hallmark of MAVS activation (11, 204) (Figure 12D). In summary, these data reveal that UFL1 and UFM1 are required for the RIG-I interaction with 14-3-3 ϵ , for interaction with MAVS, and for MAVS activation by oligomerization.

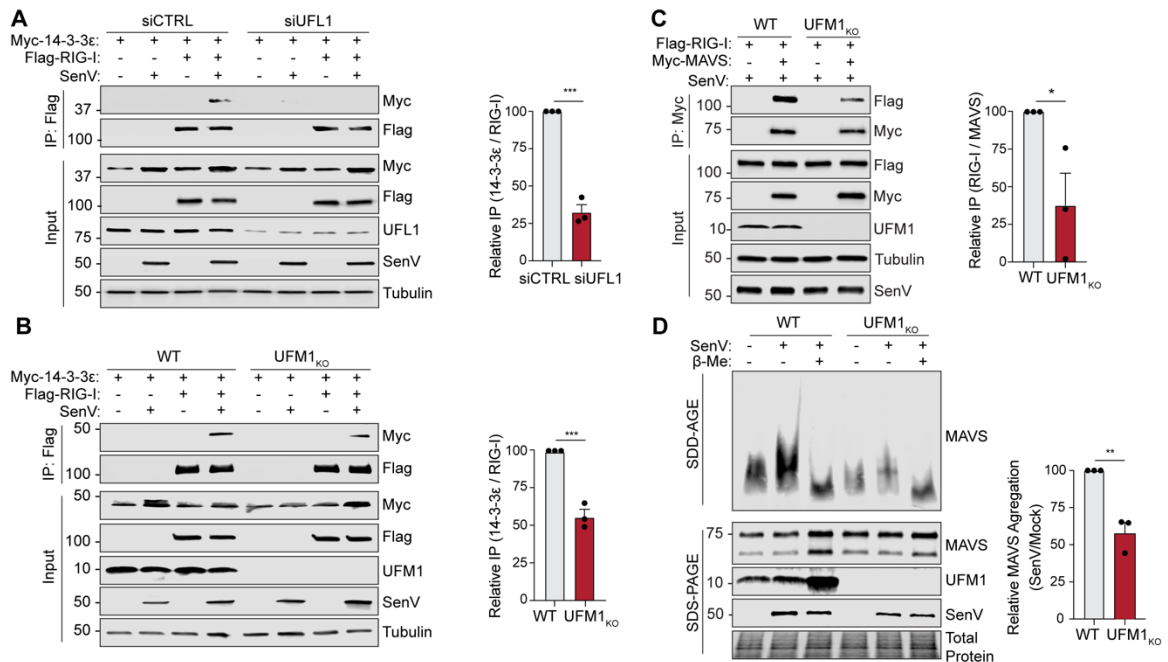


Figure 12: Ufmylation promotes RIG-I interaction with 14-3-3ε for MAVS activation.

A) Immunoblot of anti-Flag immunoprecipitated extracts and inputs from 293T cells transfected with siCTRL or siUFL1 and indicated constructs. B) Immunoblot of anti-Flag immunoprecipitated extracts and inputs from 293T WT or UFM1 KO cells. C) Immunoblot of anti-Myc immunoprecipitated extracts from 293T WT or UFM1 KO cells. D) 293T WT or UFM1 KO were mock or SenV-infected (12 h) followed by immunoblotting. Immunoblot shows endogenous MAVS in input samples and MAVS aggregation from P5 fractions, in the presence or absence of denaturing reagent (β -mercaptoethanol). SenV infection was for 4 h (A-C) or 12 h (D). In (A-C), relative quantification of indicated protein in the IP is shown on the right; in (D) SDD-AGE MAVS values are normalized to corresponding SDS-PAGE values. Graphs show the mean \pm SEM for $n=3$ biological replicates. * $p \leq 0.05$, ** $p \leq 0.01$, and *** $p \leq 0.001$ determined by Student's t-test.

3.3 Conclusions

RIG-I activation begins upon RNA binding. Then, RIG-I undergoes ATP hydrolysis, and interaction with K63-linked polyubiquitin chains, both covalently and non-covalently (5, 44, 47), which promotes formation of a RIG-I tetramer (48). This polyubiquitinated, activated RIG-I oligomer then interacts with the membrane trafficking

protein 14-3-3 ϵ for translocation to MAVS at ER-mitochondrial contact sites (7). We found that UFL1 is recruited to 14-3-3 ϵ following RNA virus infection and that ufmylation facilitates the interaction between 14-3-3 ϵ and activated RIG-I. Importantly, this results in increased interaction of RIG-I with MAVS and MAVS oligomerization, ultimately promoting the downstream signal transduction which produces IFN. These findings uncover a previously unknown mechanism for 14-3-3 ϵ selection of RIG-I, an added layer of understanding of the factors that govern RIG-I activation and membrane recruitment, and additional knowledge about the targets of ufmylation, a PTM that we are only just beginning to understand.

3.4 Materials and Methods

3.4.1 Cell lines, viruses, and treatments.

Neonatal human dermal fibroblast (NHDF) cells and embryonic kidney 293T cells were grown in Dulbecco's modification of Eagle's medium (DMEM; Mediatech) supplemented with 10% fetal bovine serum (Thermo Fisher Scientific), 1X minimum essential medium non-essential amino acids (Thermo Fisher Scientific), and 25 mM HEPES (Thermo Fisher Scientific) (cDMEM). 293T (CRL-3216) were obtained from American Type Culture Collection (ATCC), NHDF cells (CC-2509) were obtained from Lonza. All cell lines were verified as mycoplasma free by the LookOut Mycoplasma PCR detection kit (Sigma). SenV Cantell strain was obtained from Charles River Laboratories and used at 200 hemagglutination units/mL (HAU). SenV infections were performed in serum-free media (30 minutes to 1 hour), after which complete media was replenished.

IFN- β (PBL Assay Science) was added to cells at a concentration of 50 units/mL in cDMEM for 18 hours.

3.4.2 Plasmids.

The following plasmids have been previously described: pEF-TAK-Flag, pEF-BOS-Flag-RIG-I (36), pEF-TAK-Flag-Riplet (205) pIFN- β -luc (206), pCMV-Renilla (Promega), pX459 (Addgene #62988), psPAX2 (Addgene #12260), and pMD2.G (Addgene #12259), pEF-BOS-Flag-RIG-I T55I (24), pEF-TAK-Myc-MAVS (194). pEF-TAK-Flag-UFL1 (GenBank: BC036379; GeneID: 23376) was generated by insertion of PCR-amplified fragments into the NotI-to-PmeI digested pEF-TAK-Flag using InFusion cloning (Clontech). Both pEF-TAK-Myc-14-3-3e and pEF-TAK-Myc-UFL1 were generated by insertion of PCR-amplified fragments into the AgeI-NotI digested pEF-TAK-Myc (pEF-TAK-Myc-MAVS) by InFusion. The pEF-TAK-HA vector was generated by PCR to replace Flag with HA, and pEF-TAK-HA-RIG-I, and pEF-TAK-HA-UFM1 were generated by insertion of a PCR-amplified fragment into the NotI-AgeI digested pEF-TAK-HA vector. pLEX-Flag-14-3-3e was generated by ligation of a PCR-amplified Flag-14-3-3e into the BamHI-to-XhoI digested pLEX using InFusion cloning. The following plasmids were generated by site-directed mutagenesis: pEF-TAK-Flag-UFL1^{siR}, pEF-TAK-HA-UFM1 Δ C3, pEF-BOS-Flag-RIG-I K888/907A, and pEF-BOS-Flag-RIG-I K172/788R. To generate the CRISPR guide RNA plasmids px459-UFM1-E2 and px459-UFM1-B sgRNA oligonucleotides were annealed and inserted into the BbsI-digested pX459 (166, 207). The plasmid sequences were verified by DNA sequencing.

3.4.3 Transfection.

DNA transfections were performed using FuGENE6 (Promega) or TransIT-LT1 (Mirus Bio). RNA PAMP transfections were done using the TransIT-mRNA Transfection kit (Mirus Bio). The siRNA transfections were done using Lipofectamine RNAiMax (Invitrogen). siRNAs directed against 14-3-3 ϵ (Dharmacon-L-017302-02-0005), UFL1 (Qiagen-SI04371318) or non-targeting AllStars negative control siRNA (Qiagen-1027280) were transfected into 293T cells (25 pmol of siRNA; final concentration of 0.0125 μ M). Media was changed 4-24 hours post-transfection, and cells were incubated for 36-48 h post-transfection prior to each experimental treatment. IFN- β -promoter luciferase assays were performed as previously described at 18-24 hours post treatment and normalized to the *Renilla* luciferase transfection control (195).

3.4.4 Generation of cell lines.

UFM1 KO 293T cells were generated by CRISPR/Cas9, using two guides targeting exon 2 and 3 (UFM1) similar to others, as we have done previously. Single cell clones were validated via anti-UFM1 immunoblot and genomic sequencing, with one clone used here (166, 188). 293T cell pools overexpressing Flag-14-3-3 ϵ were generated by lentiviral transduction, as previously (197).

3.4.5 Immunoblotting.

Cells were lysed in a modified radioimmunoprecipitation assay (RIPA) buffer (10 mM Tris [pH 7.5], 150 mM NaCl, 0.5% sodium deoxycholate, and 1% Triton X-100) supplemented with protease inhibitor cocktail (Sigma) and Halt Phosphatase Inhibitor (Thermo-Fisher), and post-nuclear lysates were isolated by centrifugation. Quantified protein (between 5 -15 μ g) was resolved by SDS/PAGE, transferred to nitrocellulose or

polyvinylidene difluoride (PVDF) membranes in a 25 mM Tris-192 mM glycine-0.01% SDS buffer. Membranes were stained with Revert 700 total protein stain (LI-COR Biosciences) and then blocked in 3% BSA in Tris-buffered saline containing 0.01% Tween-20 (TBS-T). After washing with PBS-T or TBS-T (for phosphoproteins) buffer, following incubation with primary antibodies, membranes were incubated with species-specific horseradish peroxidase-conjugated antibodies (Jackson ImmunoResearch, 1:5000) or fluorescent secondaries (LI-COR Biosciences), followed by treatment of the membrane with Clarity Western ECL substrate (BioRad) and imaging on a LICOR Odyssey FC. The following antibodies were used for immunoblotting: R-anti-SenV (MBL, 1:1000), M-anti-Tubulin (Sigma, 1:1000), R-anti-GAPDH (Cell Signaling Technology, 1:1000), R-anti-UFL1 (Novus Biologicals, 1:1000), R-anti-UFM1 (Abcam, 1:1000), anti-RIG-I (M-AdipoGen, R-Abcam, 1:1000), R-anti-14-3-3 ϵ (Cell Signaling Technology, 1:1000), M-anti-Flag M2 (Sigma, 1:1000), anti-Flag-HRP (Sigma, 1:1000-1:5000), R-anti-Flag (Sigma, 1:1000), anti-HA (M- and R-Sigma, 1:1000), and anti-Myc (M-Santa Cruz or R-Cell Signaling Technology, 1:1000).

3.4.6 Immunoprecipitation.

Cells were lysed in RIPA buffer with or without 10% glycerol. Quantified protein (between 100-500 μ g) was incubated with protein-specific, isotype control antibody (R-Cell Signaling Technology or M-Thermo Fisher), or anti-Flag M2 magnetic beads (Sigma), in lysis buffer either at room temperature for 2 h or at 4°C overnight with head over tail rotation. The lysate/antibody mixture was then incubated with Protein G Dynabeads (Invitrogen) for 1 h. Beads were washed 3X in PBS or RIPA buffer and eluted in 2X Laemmli Buffer (BioRad) with or without 5% 2-Mercaptoethanol at 95°C for 5 min. Proteins were resolved by SDS/PAGE and immunoblotting, as above. For

ufmylation immunoprecipitations, cells were lysed with NP-40 buffer (50 mM Tris [pH 8], 150 mM NaCl, 0.5% sodium deoxycholate, and 1% NP-40) supplemented with 10% glycerol, protease and phosphatase inhibitors, as above, and N-ethylmaleimide (Sigma-Aldrich). Post-nuclear lysates were boiled at 95°C for 5 min and incubated with anti-Flag M2 magnetic beads, as above.

3.4.7 Subcellular membrane fractionation.

Membrane fractionation was performed as previously described (61, 72, 198, 208). Cells were lysed in hypotonic buffer (10 mM Tris-HCL (pH 7.5), 10 mM KCl, and 5 mM MgCl₂ supplemented with protease inhibitor cocktail) for 10 minutes on ice followed by 20 passages through a 20-gauge needle. Nuclei and unbroken cells were removed by centrifugation at 1000xg for 5 min at 4°C. The resulting supernatants were mixed thoroughly with 72% sucrose and overlaid with 55% sucrose, followed by 10% sucrose, all in low-salt buffer (2 nM EDTA, 20 nM HEPES (pH 8.0), 150 mM NaCl, 0.1% SDS, 1% Triton X-100). The gradients were subjected to centrifugation at 38,000 RPM in a Beckman SW41 Ti Rotor for 14 h at 4°C. 1 mL fractions were collected using a BioComp piston gradient fractionator and resulting fractions were divided in half and mixed with 2 parts 100% methanol and precipitated overnight at -80°C. Protein pellets were collected by centrifugation and resuspended in 2X Laemmli buffer and heated for 5 min at 95°C for immunoblot analysis. 10% pre-fractionated cells from each condition were collected as the input.

3.4.8 Semi-denaturing detergent agarose gel electrophoresis.

SDD-AGE was performed as described (11, 204). Briefly, crude mitochondria (P5 fraction) were isolated from an equal number of WT or UFM1 KO 293T cells that were

mock or SenV infected (12 h), resuspended in hypotonic buffer (10 mM Tris, pH 7.5, 10 mM KCl, 1.5 mM MgCl₂, and 0.5 mM EDTA). Resulting samples were split and 2X SDD-AGE sample buffer (0.5X TBE, 10% glycerol, 2% SDS, 0.2 mM Bromophenol Blue) buffer with or without 5% 2-Mercaptoethanol was added, and samples were loaded onto a vertical 1.5% agarose gel. Electrophoresis was performed with a constant voltage of 70 V at 4 °C in SDD-AGE running buffer (1X TBE and 0.1% SDS). Gels were transferred onto a nitrocellulose membrane overnight on ice at 25 V. Membranes were fixed in 0.25% glutaraldehyde in PBS and immunoblotting was performed as usual. 15% of the SDD-AGE samples were reserved for input.

3.4.9 Quantification of immunoblots.

Immunoblots imaged using the LICOR Odyssey FC were quantified by ImageStudio software, and raw values were normalized to relevant controls for each antibody. Relative membrane association of UFL1 was quantified as the ratio of UFL1 to Cox-1 in fraction 1 normalized to total protein levels of UFL1 in the input and displayed as the percentage of UFL1 membrane association normalized to mock values.

3.4.10 Statistical analysis.

Student's unpaired t-test, one-way ANOVA, or two-way ANOVA were implemented for statistical analysis of the data followed by appropriate post-hoc test (as indicated) using GraphPad Prism software. Graphed values are presented as mean \pm SD or SEM (n = 3 or as indicated); *p \leq 0.05, **p \leq 0.01, and ***p \leq 0.001.

4. RIG-I signaling induces a subset of ufmylated proteins that control interferon induction

The data in chapter is currently unpublished. The people who generated this data are Daltry L. Snider, Michelle Kim, and Stacy M. Horner. Author contributions are as follows: D.L.S. and S.M.H. designed research; D.L.S performed research and contributed new reagents/analytic tools; M.K. generated constructs from top hits and performed secondary validation. D.L.S., M.K., and S.M.H. analyzed data.

4.1 Introduction

Antiviral signaling induces many host-driven changes in order to quickly regulate protein function to control viral replication rapidly. Indeed, in part this is orchestrated by altering PTMs of many proteins in the RIG-I pathway in response to viral infection, including dephosphorylation, ubiquitination, and acetylation. These and other newly discovered ubiquitin-like modifications can serve to release their target protein from auto-repression, induce changes in protein-protein interactions, or alter their localization for a rapid response to infection without needing to translate new proteins, which is a costly expense that takes time that is not available during viral infection. Further, during termination of signaling, many proteins are marked for degradation in order to prevent excessive inflammation (80, 209).

As my data indicates a clear role for ufmylation in regulating RIG-I signaling, I hypothesized that this was because of modification of proteins by UFM1 during viral infection. Therefore, I identified the host of proteins that become ufmylated in response to RIG-I signaling using an unbiased approach. Through proteomics studies, I identified fourteen candidate proteins that are ufmylated following RIG-I-dependent antiviral

signaling. Of these top ten candidates, nine had no known role in antiviral innate immunity. Through follow-up studies, I determined that four candidates positively regulated IFN induction, and one negatively regulated IFN induction. These results suggest that ufmylation may regulate RIG-I signaling broadly through previously unknown host proteins in addition to its role in RIG-I membrane recruitment by 14-3-3 ϵ .

4.2 Results

4.2.1 Utilizing proteomics to uncover the targets of ufmylation during RIG-I signaling

To identify the targets of ufmylation during RIG-I signaling, I performed quantitative liquid chromatography-tandem mass spectrometry (LC-MS/MS) in collaboration with the Duke Proteomics Core Facility using overexpression of a Flag-UFM1 construct in either Huh7 WT or RIG-I KO cells (210) that were mock or SenV infected, in biological triplicate. Following anti-Flag-immunoprecipitation (IP), proteins which undergo virus-dependent ufmylation would be more enriched in the SenV condition than in mock. Candidate IFN regulatory proteins would be those that are enriched ≥ 2 fold in the WT SenV vs. WT mock conditions but displayed no interaction with UFM1 in the RIG-I KO cells, indicating a RIG-I dependent ufmylation event (Figure 13).

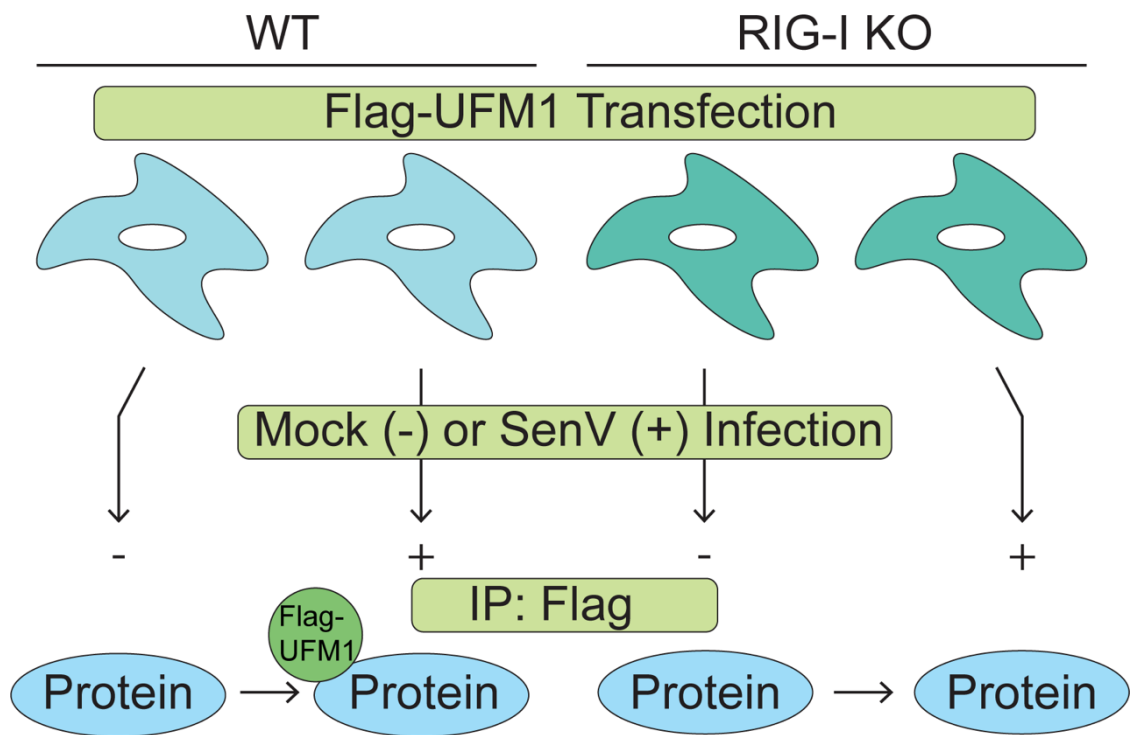


Figure 13: Schematic of experimental workflow for IP-LC-MS/MS to identify ufmylated proteins.

Either WT or RIG-I KO Huh7 cells were transfected with either vector (not shown), or Flag-UFM1, followed by mock or SenV infection (18 h). Following anti-Flag immunoprecipitation, samples were analyzed for protein composition by LC-MS/MS.

4.2.2. Identification of proteins that are ufmylated in a RIG-I dependent manner

After initial filtering to remove proteins that were not enriched above a vector control, I identified fourteen candidate proteins that that displayed ≥ 2 fold enrichment in the WT SenV over WT mock conditions (top 10 candidates shown in Figure 14A). Importantly, these candidates were not ufmylated in cells lacking RIG-I, indicating they are ufmylated in a RIG-I signaling dependent manner. As validation of this technique, I found that all known components of the ufmylation machinery system were identified as

UFM1-interactors using this method (Figure 14B). Surprisingly, the protein that was most ufmylated during infection was the known RIG-I signaling regulator TBK1 (Figure 14A), which is the serine-threonine kinase responsible for phosphorylation of MAVS and IRF3 (12, 67). Of the other nine proteins found to be ufmylated, none had previously described roles in the innate immune response to viral infection.

Protein Identity	WT UFM+/ KO UFM+
TBK1	9.4
GNAI3	5.3
KLHL22	3.6
UBE2J2	3.4
FMR1	2.9
BAG3	2.6
PSMB8	2.5
INTS3	2.1
GRIPAP1	2.0
HIF1AN	2.0

Protein Identity	WT UFM+/ WT V+
UBA5	2.2
UFC1	29.8
UFL1	1.1
UFM1	39.6

Figure 14: Candidate UFM1-interacting proteins.

A) Candidate proteins identified using quantitative IP-LC-MS/MS listed in order of fold change magnitude. Fold change was calculated using the average of 3 biological replicates for each condition, and “hits” were defined as proteins that had a fold change of >2 when comparing WT+ to WT- (not shown), and when comparing WT+ to KO+. B) UFM1 interacting proteins using quantitative IP-LC-MS/MS with respective fold change for the indicated conditions.

4.2.3 Ufmylated proteins differentially regulate IFN induction

To investigate if these potentially ufmylated proteins could regulate IFN induction, we expressed a selection of our top hits in 293T cells and measured the SenV-induced

IFN- β levels using a reporter assay (194). Of the eight candidates tested, four promoted RIG-I-directed IFN induction, GRIPAP1 (Figure 15A), FMR1, GNAI3, and BAG3 (Figure 15B). Interestingly, one candidate, INTS3, negatively regulated IFN induction (Figure 15A). Together, this data suggests that proteins which contain virally induced ufmylation in a RIG-I dependent manner can modulate IFN signaling. Further work validating their ufmylation status will be required to understand the full scope of the functional outcomes of ufmylation on these host proteins during RIG-I signaling.

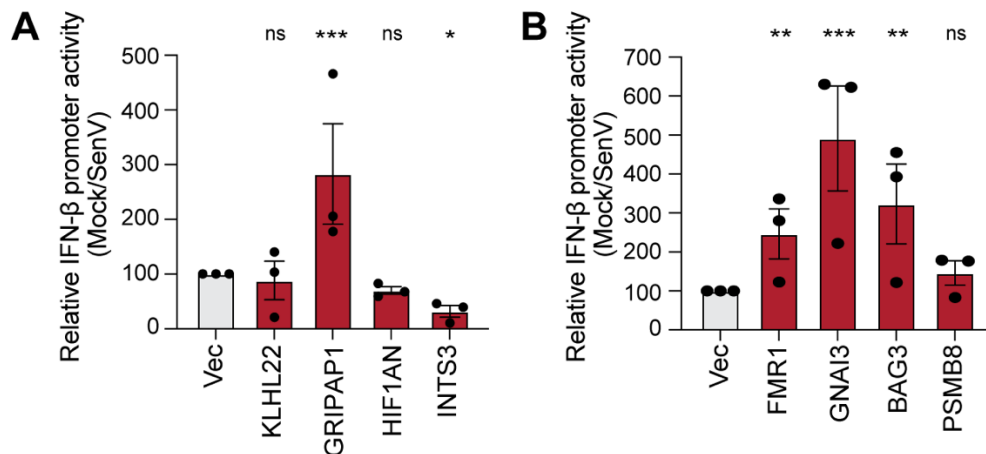


Figure 15: Proteins ufmylated during RIG-I signaling regulate IFN induction.

A-B) Relative IFN- β -promoter reporter luciferase expression (rel. to CMV-*Renilla*) from 293T cells expressing indicated constructs followed by mock or SenV infection (18 h), with results graphed as relative SenV fold change for each. The graphs are represented as the mean \pm SEM, n=3 biological replicates and * $p \leq 0.05$, ** $p \leq 0.01$, and *** $p \leq 0.001$ determined one-way ANOVA followed by Dunnett's multiple comparisons test.

4.3 Conclusions

Though it is not yet known how ufmylation of these candidates modulates their function, many of these candidates have previously described roles which may give us clues into how they may be modulating RIG-I signaling. For example, GRIPAP1 is a known regulator of GRIP1, which has roles in promoting IRF3-dependent gene

expression (211–213). FRM1 is well characterized as an RNA-binding protein and has recently been revealed to have roles in DNA virus infection. Interestingly, the RNA modification m⁶A seems to play a role in FMR1 RNA binding, which is highly important in regulating the host response to viral infection (21, 197, 214–217). GNAI3 regulates intracellular vesicle trafficking (218, 219), which is highly important in the rapid relocalization of proteins during innate immune signaling (61, 62, 66). Interestingly, BAG3 has been shown to regulate DNA viruses in both a positive and negative manner through interactions with their viral proteins utilizing a specific binding motif (220–223). INTS3 which displayed negative IFN- β regulation, is known as a key member of the DNA damage repair machinery (224–226). In all of these cases, it is possible that ufmylation of these proteins during RIG-I signaling may alter their interacting proteins to aid in the induction of IFNs.

Overall, these candidates provide evidence for a widespread regulation of RIG-I signaling by ufmylation of host proteins. Future work on these candidates to assess their ufmylation status, how that impacts IFN induction, and the underlying mechanisms of this UFM1-dependent regulation will be important in understanding not only how PTMs regulate host responses during infection but will provide further evidence into how ufmylation regulates its targets.

4.4 Methods

4.4.1 Cell lines, viruses, and treatments.

Human hepatoma Huh7 cells embryonic kidney 293T cells were grown in Dulbecco's modification of Eagle's medium (DMEM; Mediatech) supplemented with 10% fetal bovine serum (Thermo Fisher Scientific), 1X minimum essential medium non-essential amino acids (Thermo Fisher Scientific), and 25 mM HEPES (Thermo Fisher

Scientific) (cDMEM). 293T (CRL-3216) were obtained from American Type Culture Collection (ATCC), NHDF cells (CC-2509) were obtained from Lonza. Huh7 cells used in this study were a gift of Dr. Michael Gale, and their identity was verified by using the GenePrint STR kit (Promega) (DNA Analysis Facility, Duke University, Durham, NC, USA). All cell lines were verified as mycoplasma free by the LookOut Mycoplasma PCR detection kit (Sigma). SenV Cantell strain was obtained from Charles River Laboratories and used at 200 hemagglutination units/mL (HAU). SenV infections were performed in serum-free media (30 minutes to 1 hour), after which complete media was replenished. IFN- β (PBL Assay Science) was added to cells at a concentration of 50 units/mL in cDMEM for 18 hours.

4.4.2 Plasmids.

The following plasmids have been previously described: pEF-TAK-Flag, pIFN- β -luc (64), pCMV-Renilla (Promega), pX459 (Addgene #62988). pLJM1_Flag-UFM1 was a gift from Drs. Craig McCormick and John Rohde at Dalhousie University. The pEF-TAK-HA vector was generated by PCR to replace Flag with HA. The following plasmids were generated by insertion of PCR-amplified fragments into the NotI-to-PmeI digested pEF-TAK-HA using InFusion cloning (Clontech): pEF-TAK-HA-FMR1 (NM_032775.4), pEF-TAK-HA-GRIPAP1 (NM_020137.5), pEF-TAK-HA-HIF1AN (Addgene #21399), pEF-TAK-HA-INTS3 (NM_023015.5), pEF-TAK-HA-FMR1 (Addgene #48690), pEF-TAK-HA-GNAI3 (NM_006496.4), pEF-TAK-HA-BAG3 (Addgene #98182), and pEF-TAK-HA-PSMB8 (NM_004159.5). The plasmid sequences were verified by DNA sequencing.

4.4.3 Transfection.

DNA transfections were performed using FuGENE6 (Promega) or TransIT-LT1 (Mirus Bio). IFN- β -promoter luciferase assays were performed as previously described at 18-24 hours post treatment and normalized to the *Renilla* luciferase transfection control (195).

4.4.4 Immunoprecipitation.

For immunoprecipitations, cells were lysed with NP-40 buffer (50 mM Tris [pH 8], 150 mM NaCl, 0.5% sodium deoxycholate, and 1% NP-40) supplemented with 10% glycerol, protease and phosphatase inhibitors. Post-nuclear lysates were incubated with anti-Flag M2 magnetic beads (Sigma), in lysis buffer 4°C overnight with head over tail rotation. Beads were washed 3X in PBS and eluted in 2X Laemmli Buffer (BioRad) at 95°C for 5 min.

4.4.5 Proteomics sample preparation.

Samples were reduced with 10 mM dithiothreitol for 30 min at 80C and alkylated with 20 mM iodoacetamide for 30 min at room temperature. Next, they were supplemented with a final concentration of 1.2% phosphoric acid and 256 μ L of S-Trap (Protifi) binding buffer (90% MeOH/100mM TEAB). Proteins were trapped on the S-Trap, digested using 20 ng/ μ l sequencing grade trypsin (Promega) for 1 hr at 47C, and eluted using 50 mM TEAB, followed by 0.2% FA, and lastly using 50% ACN/0.2% FA. All samples were then lyophilized to dryness and resuspended in 20 μ L 1%TFA/2% acetonitrile containing 25 fmol/ μ L yeast alcohol dehydrogenase (ADH_YEAST). From each sample, 3 μ L was removed to create a QC Pool sample which was run periodically throughout the acquisition period.

4.4.6 Quantitative analysis for proteomics samples.

Quantitative LC/MS/MS was performed on 3 μ L of each sample, using a nanoAcquity UPLC system (Waters Corp) coupled to a Thermo Orbitrap Fusion Lumos high resolution accurate mass tandem mass spectrometer (Thermo) via a nanoelectrospray ionization source. Briefly, the sample was first trapped on a Symmetry C18 20 mm \times 180 μ m trapping column (5 μ L/min at 99.9/0.1 v/v water/acetonitrile), after which the analytical separation was performed using a 1.8 μ m Acquity HSS T3 C18 75 μ m \times 250 mm column (Waters Corp.) with a 90-min linear gradient of 5 to 30% acetonitrile with 0.1% formic acid at a flow rate of 400 nanoliters/minute (nL/min) with a column temperature of 55C. Data collection on the Fusion Lumos mass spectrometer was performed in a data-dependent acquisition (DDA) mode of acquisition with a $r=120,000$ (@ m/z 200) full MS scan from m/z 375 – 1500 with a target AGC value of $2e5$ ions. MS/MS scans were acquired at Rapid scan rate (Ion Trap) with an AGC target of $5e3$ ions and a max injection time of 100 ms. The total cycle time for MS and MS/MS scans was 3 sec. A 20s dynamic exclusion was employed to increase depth of coverage. The total analysis cycle time for each sample injection was approximately 2 hours. Following 22 total UPLC-MS/MS analyses (excluding conditioning runs but including 4 replicate QC injections; Table 1), data was imported into Proteome Discoverer 2.2 (Thermo Scientific), and analyses were aligned based on the accurate mass and retention time of detected ions (“features”) using Minora Feature Detector algorithm in Proteome Discoverer. Relative peptide abundance was calculated based on area-under-the-curve (AUC) of the selected ion chromatograms of the aligned features across all runs. The MS/MS data was searched against the SwissProt H. sapiens database (downloaded in Nov 2017) with additional proteins, including yeast ADH1,

bovine serum albumin, as well as an equal number of reversed sequence “decoys” false discovery rate determination. Mascot Distiller and Mascot Server (v 2.5, Matrix Sciences) were utilized to produce fragment ion spectra and to perform the database searches. Database search parameters included fixed modification on Cys (carbamidomethyl) and variable modifications on Meth (oxidation) and Asn and Gln (deamidation). Peptide Validator and Protein FDR Validator nodes in Proteome Discoverer were used to annotate the data at a maximum 1% protein false discovery rate.

4.4.7 Statistical analysis.

Student’s unpaired t-test, one-way ANOVA, or two-way ANOVA were implemented for statistical analysis of the data followed by appropriate post-hoc test (as indicated) using GraphPad Prism software. Graphed values are presented as mean \pm SD or SEM (n = 3 or as indicated); *p \leq 0.05, **p \leq 0.01, and ***p \leq 0.001.

5. Discussion

5.1 Summary

My dissertation research has centered around investigating a role for the PTM ufmylation in regulation of the signaling pathways that establish antiviral innate immunity. When I began my work, little was known about what proteins are selected for ufmylation, how modification impacts protein function, and its roles in cellular biology, especially with regards to regulation of immune signaling. PTMs play a vital role in the regulation of many cellular signaling pathways and are unique in their ability to rapidly modify protein function. Therefore, elucidating the role of novel PTMs, like ufmylation, in antiviral signaling is essential for our overall understanding of the host response to viral infection. By modulating the expression of the ufmylation E3 ligase UFL1 in diverse cell types and activating RIG-I through either viral infection or a direct RNA PAMP, I found that it is a positive regulator IFN- β as measured by IFN reporter assays, ELISA, or RT-qPCR, and IFN- λ by RT-qPCR. Further, loss of UFL1 led to significantly less phosphorylation of the IFN- β transcription factor, IRF3, while restoration of UFL1 protein expression rescued IRF3 phosphorylation. Interestingly, UFL1 had no impact on the IFN response, as bypassing IFN induction through direct treatment with purified IFN- β protein lead to no difference in ISG induction between a vector control or a plasmid expressing UFL1. Further, using an IFN- β reporter assay, I determined that UFL1s ability to regulate IFN is dependent on its ufmylation activity. Indeed, by measuring the relative amounts of UFM1-conjugates produced by expressing a series of UFL1 truncations, I found that the regions of UFL1 which positively regulate IFN, are those that produce increased UFM1-conjugates. As proteins are ufmylated using a multi-enzyme conjugation system, I next

investigated whether the other components of the ufmylation machinery could regulate IFN induction as well. Indeed, I found that UFM1 exogenous over-expression and CRISPR-mediated deletion positively impacted IFN- β induction using reporter assays and ELISA. All other components of the ufmylation machinery including the E1 and E2 conjugases, as well as the UFM1-specific protease, all promoted IFN induction. Together, these data indicate that ufmylation positively regulate IFN induction that is driven by RIG-I activation.

As I determined ufmylation to be a potent regulator of IFN- β induction, I next broadly measured the impact of ufmylation on the transcriptional response to RIG-I signaling. IFN induction ultimately results in ISG expression, which in part helps determine the outcome of an infection. Using RNA-sequencing, I analyzed gene expression in either WT or UFM1 KO 293T cells, following mock or SenV infection. Following viral infection, I found that the top 10 gene ontology categories negatively impacted by UFM1 KO, were all related to the antiviral response, such as “Response to type I IFN” and “Defense against virus”. Of the genes differentially expressed during UFM1 KO in response to viral infection, I found that the majority of genes were involved in the antiviral response including *IFNB1* and *IFNL1*, as well as other known ISGs, which were all significantly downregulated. These data are consistent with a model in which ufmylation-mediated regulation of IFN induction has broad consequences on genes induced by the IFN response.

Our initial studies identifying UFL1 as a potential RIG-I regulatory factor indicated that UFL1 was recruited to the MAM following viral infection. Indeed, I confirmed this using a membrane fractionation technique which isolates intracellular membranes from the cytosol. I found that UFL1 was significantly enriched in the membrane-containing

fraction following infection, as well as RIG-I which others have found as well. Interestingly, our initial studies found that UFL1 is likely recruited to the MAM early in infection, prior to MAVS activation (78). As both RIG-I and UFL1 relocate to the MAM early in infection, I hypothesized that a similar mechanism might drive this localization change. Indeed, using co-immunoprecipitation, I found that UFL1 forms a virally induced complex with the RIG-I trafficking protein, 14-3-3 ϵ , which is known to facilitate RIG-I relocation to MAVS. Further, using both exogenous and endogenous expression, I found that UFL1 and RIG-I form a virally induced complex. As RIG-I activation requires a series of coordinated steps, I next utilized point mutants that block RNA binding, interaction with the E3 ligase TRIM25, or ubiquitination mediated by both TRIM25 and RIPLET, to test which stage of RIG-I activation is required for its interaction with UFL1. Surprisingly, I found that full RIG-I activation was required for its interaction with UFL1, the same RIG-I activation steps required for its 14-3-3 ϵ interaction. To understand if UFL1 may be regulating early RIG-I activation, I expressed equal amounts of UFL1 alone, or co-expressed with Riplet and found that UFL1 increased virally mediated activation of the IFN- β promoter above that seen by the individual proteins. Together, these data suggest that RNA virus infection increases the interaction of 14-3-3 ϵ with UFL1, which then interacts with activated, K63-ubiquitinated RIG-I to promote downstream signaling.

My data suggested that one of two models was responsible for the ufmylation-mediated regulation of RIG-I. Either UFL1 interacts first with activated RIG-I, induces its ufmylation, and then the UFL1-RIG-I complex interacts with 14-3-3 ϵ . As such, depletion of 14-3-3 ϵ or loss of UFM1 would not be expected to change the interaction of UFL1 with RIG-I. In the second model, UFL1 interacts first with 14-3-3 ϵ and induces its ufmylation,

or that of another associated protein, and then the UFL1-14-3-3 ϵ complex interacts with activated RIG-I. In this second model, depletion of 14-3-3 ϵ would be expected to prevent UFL1 interaction with RIG-I, and loss of ufmylation would limit UFL1 interaction with RIG-I but would not affect UFL1 interaction with 14-3-3 ϵ . Indeed, knockdown of 14-3-3 ϵ significantly decreased the RIG-I-UFL1 interaction. Next, I tested if ufmylation was required for formation of the virally induced RIG-I-UFL1 complex by measuring this interaction in WT or UFM1 KO 293T cells and I found that UFM1 was required for the virally activated RIG-I-UFL1 complex. These results indicate that both 14-3-3 ϵ and UFM1 are required for UFL1 to interact with RIG-I, supporting the second model of complex formation in which UFL1 interacts first with 14-3-3 ϵ and catalyzes its ufmylation, and this complex associates with RIG-I. In support of this, I found that UFM1 was not required for UFL1 to interact with 14-3-3 ϵ , indicating that 14-3-3 ϵ may be regulated by ufmylation, not RIG-I.

To test if 14-3-3 ϵ is UFM1-conjugated, I performed an immunoprecipitation of Flag-14-3-3 ϵ from cell extracts that were mock or virus-infected and exogenously expressed either UFM1-WT or UFM1 Δ C3, which lacks the terminal 3 amino acids required conjugation to target protein. Prior to immunoprecipitation, lysates were boiled to remove non-covalent interactions. Following immunoprecipitation 14-3-3 ϵ , I observed a slower migrating form of 14-3-3 ϵ approximately 15 kDa heavier (the mass of UFM1) than the predicted molecular mass of 14-3-3 ϵ (37 kDa), suggestive of covalent UFM1 modification. Additionally, the proportion of 14-3-3 ϵ , conjugated by UFM1 increases following viral infection. Together, these data indicate that ufmylation promotes the

interaction of UFL1 with 14-3-3 ϵ and activated RIG-I and that UFM1 has increased conjugation to 14-3-3 ϵ following RIG-I activation.

As I found that that UFL1 requires 14-3-3 ϵ to interact with activated RIG-I, I next tested if ufmylation is required for the interaction of 14-3-3 ϵ with RIG-I, which is essential for activated RIG-I to translocate from the cytosol to intracellular membranes for interaction with MAVS. Indeed, my data indicate that both UFL1 and UFM1 are required for the RIG-I-14-3-3 ϵ interaction. Importantly, I also found that UFM1 is required for the virus-induced interaction of RIG-I with MAVS and MAVS higher-order oligomerization, which is a hallmark of MAVS activation. In summary, these data reveal that UFL1 and UFM1 are required for the RIG-I interaction with 14-3-3 ϵ , for interaction with MAVS, and for MAVS activation by oligomerization.

As PTM of host proteins that regulate the antiviral response are often diverse and multi-faceted, I next wanted to know if there were other proteins that became ufmylated during RIG-I signaling. Indeed, I discovered fourteen high-confidence proteins that displayed an increase in ufmylation following virus infection in a RIG-I dependent manner. Surprisingly, our top candidate was TBK1, the serine/threonine protein kinase responsible for phosphorylation of IRF3, the type I IFN transcription factor. The other proteins were diverse in function and have few described roles in antiviral immunity. I found that five of the top eight candidates (excluding TBK1 as it has previously known roles in IFN induction) had the ability to regulate an IFN- β reporter, with four displaying positive regulation and one displaying negative regulation. Overall, this work has identified a class of proteins that are ufmylated in response to RIG-I signaling and found that some proteins which have virally induced ufmylation can regulate the induction of IFNs.

Through my research, I have uncovered a novel control of RIG-I signaling. I found that ufmylation orchestrates the selection of RIG-I by 14-3-3 ϵ , which was a previously unknown mechanism. Further, I found that the ufmylation machinery are all positive regulators of antiviral innate immunity. Indeed, I have uncovered many proteins which are ufmylated in response to RIG-I signaling and understanding how their ufmylation contributes to their regulation of RIG-I signaling will be an exciting investigation of ufmylation-mediated control of antiviral immunity. This research adds valuable layers to our understanding of the functions of ufmylation and its related machinery in immunity and at the virus-host interface. However, many important questions remain regarding this research and these research fields. I will discuss future directions that will enhance our understanding of the phenomena described in this dissertation, as well as our overall understanding of ufmylation and its functions in immunity and infection.

5.2 Future directions and discussion

5.2.1 By what mechanism does UFM1 dictate RIG-I selection by 14-3-3 ϵ ?

How 14-3-3 ϵ ufmylation impacts its ability to select substrates is still unclear. I found that UFL1 and UFM1 both are required for 14-3-3 ϵ selection of RIG-I. Further, I identified that 14-3-3 ϵ is ufmylated, likely by mono-ufmylation at one lysine residue. However, it is not yet clear if the ufmylated residue is responsible for the 14-3-3 ϵ -RIG-I interaction. 14-3-3 ϵ contains eighteen lysine residues. Of those, two are highly conserved among 14-3-3 family proteins and function as part of the canonical phosphorylated residue binding pocket that typically dictates 14-3-3 selection of

substrates, K49 and K120 (227). Though this pocket typically recognizes substrates, it is possible that one of these residues is ufmylated which allows 14-3-3 ϵ to interact with RIG-I. Indeed, though the function of ufmylation on target proteins has been studied relatively little, it does appear that it primarily serves to alter protein-protein interactions (165, 180, 181, 184). The ufmylated lysine residue of 14-3-3 ϵ could be identified utilizing approaches that have been pioneered for ubiquitination (228), and have been recently co-opted for studying ufmylation (106, 168, 176). Following enrichment, the target protein is trypsin digested to generate peptides where the terminal two amino acids of UFM1 (V-G) remain conjugated to any modified lysine, and ufmylated lysine residues can be identified using LC-MS/MS. The digestion results in a unique shift in the known mass-to-charge ratio of the peptides (+156.09 Da) for identification of ufmylated residues (168, 176). This technique could be utilized to find which lysine of 14-3-3 ϵ is conjugated to UFM1. Then, the identified lysine could be mutated to arginine (R) which cannot become UFM1-conjugated, and this 14-3-3 ϵ -KR could be used to study the direct effects of 14-3-3 ϵ -UFM1 conjugation on RIG-I signaling.

Additionally, while my data reveal an increase in the proportion of 14-3-3 ϵ that is ufmylated following SenV infection, it is not yet clear what signals induce ufmylation of 14-3-3 ϵ . My work suggests that UFL1 and UFM1 are required for 14-3-3 ϵ interaction with RIG-I, which indicates that the signal for 14-3-3 ϵ ufmylation is most likely very rapid following infection. It is likely that the signal is RIG-I dependent, as SenV is specifically sensed by RIG-I (7), however, to test if this is RIG-I dependent or SenV dependent, the ufmylation assay could be performed in WT or RIG-I KO cells. It is possible that RIG-I signaling induces some type of activation of UFL1 which then allows it to ufmylation 14-

3-3 ϵ . Indeed UFL1 is phosphorylated in response to DNA damage, which is required for its ufmylation ability in this context (180). The known mechanisms of UFL1 activation are discussed below, however it is possible that UFL1 may be activated during RIG-I signaling through a previously unknown mechanism. Indeed, my results suggest that UFL1, RIG-I, and 14-3-3 ϵ interact at low levels prior to infection. Therefore, it is possible that UFL1 is modified by ubiquitin or some other PTM following RIG-I RNA binding, similar to RIG-I itself. This could be determined by profiling UFL1 for PTMs such as ubiquitin or phosphorylation using co-immunoprecipitation. If UFL1 is modified by these, a likely candidate would be those kinases and ubiquitin ligases that are already known to modulate RIG-I activation (80). It is also possible that a helper protein allows 14-3-3 ϵ to become ufmylated, and indeed, the activity of UFL1 has been hypothesized to rely on other accessory proteins, which is discussed below (165, 170). As this could be a previously unidentified protein, and as such, a proteomics-based approach could be utilized to uncover novel interactors with UFL1 during early viral infection. This work will be essential in determining how ufmylation of 14-3-3 ϵ is controlled and provide new insights into the ways in which ufmylation selects target proteins.

Since the discovery that RIG-I was trafficked to the MAM by 14-3-3 ϵ (61), the mechanisms by which 14-3-3 ϵ selects RIG-I has remained a mystery. Indeed, as mentioned, 14-3-3 family proteins are well-characterized to bind to phosphorylated residues on targets through one of two motifs: R[SFYW]XpSXP or RX[SYFWTQAD]Xp(S/T)X[PLM], however, RIG-I contains neither (61, 77, 229). My work supports the work of others demonstrating that 14-3-3 ϵ interacts with UFM1 and other members of the ufmylation pathway, and it reveals that viral infection increases the proportion of ufmylated 14-3-3 ϵ (169). It is likely that 14-3-3 ϵ is mono-ufmylated as the

apparent molecular weight of 14-3-3 ϵ increased by one ufmylation group. As we do not yet know if the ufmylation site of 14-3-3 ϵ is primarily driving its interaction with RIG-I, it could also be that a yet to be identified 14-3-3 ϵ regulatory factor is ufmylated, and this mediates the selection of RIG-I, which could be identified using an unbiased proteomics approach identifying virus-induced 14-3-3 ϵ interacting proteins in either WT or UFM1 KO cells. In either case, it is clear that ufmylation mediates the 14-3-3 ϵ -RIG-I interaction. However, a number of 14-3-3 family proteins are post-translationally modified by phosphorylation, acetylation, and oxidation to regulate their functions (230). Therefore, it is possible that post-translational modification of 14-3-3 ϵ by ufmylation could define how cargo proteins, including RIG-I, are selected. Indeed, this mechanism could be shared with other RNA virus sensing pathways, such as the RIG-I-like-receptor MDA5, which also interacts with another 14-3-3 protein, 14-3-3 η , by an unknown mechanism (62). Thus, ufmylation may broadly influence how 14-3-3 proteins or other host proteins interact with each other to regulate the intracellular innate immune response, and this work could uncover a new mechanism that governs 14-3-3 family proteins.

5.2.2 How is ufmylation functionalized to regulate diverse biological processes?

5.2.2.1 Ufmylation regulates multiple cell stress response pathways

Ufmylation is emerging as a post-translational modification that regulates diverse biological processes, including DNA repair, ER homeostasis, the translation of hepatitis A virus, macrophage activation, and through my work, RIG-I signaling (166, 167, 176, 178, 180–184, 193). Though ubiquitin is well understood to have roles in diverse processes as well, this is typically dictated by the ubiquitin linkage type (95, 106); however, ufmylation largely produces mono-ufmylation events. Typically, UFL1, along

with the other members of the ufmylation cascade, induce ufmylation of a target protein important for regulating these processes, but how UFL1 and the ufmylation pathway are activated in response to these stressors is unclear. Studying how ufmylation regulates diverse biological process may uncover some patterns in its regulatory mechanisms.

In its regulation of the DNA damage response, UFL1 was found to be recruited to double-stranded breaks in DNA (231, 232). Further, it was found to induce the ufmylation of MRE11, an essential component of the larger MRN complex, essential for downstream signal transduction and ultimate DNA repair. Importantly, this study was one of the first to suggest that ufmylation may have an impact on protein-protein interactions, as they found mutation of the ufmylated MRE11 residue led to diminished formation of the MRN complex, and disrupted ATM phosphorylation, a kinase in the DNA damage pathway (181). Prior to this, the mechanism for ATM activation was unknown. Additionally, another group found that following this recruitment of UFL1, it was phosphorylated by activated ATM which led to ufmylation of histone H4 in the nucleus. This ufmylation event serves to recruit further DNA repair machinery (180). To date, no other studies have uncovered phosphorylation-dependent ufmylation, which may suggest this is one way UFL1 is activated for the DAN damage response specifically, or we have yet to uncover other PTMs which regulate ufmylation.

Ufmylation has also been implicated in regulating cancer progression. ASC1, which is a transcriptional coactivator of ER α , is ufmylated. ER α is associated with enhanced transcription of many cancer progression genes, and is highly dysregulated in breast cancer. Interestingly, it was found that ASC1 was modified by K69-linked polyufmylated chains, the only example of this phenomenon to date, which was found to require UFBP1. This ufmylation of ASC1 allowed for increased interaction between

ASC1 and ER α , promoting tumor formation. Conversely, ufmylation was found to have a protective effect against tumor formation through ufmylation of the tumor suppressor p53 (233). It was found that UFL1 competes with an E3 ubiquitin ligase to prevent K48-ubiquitin-mediated degradation of P53, which would promote tumor formation. Interestingly, this study found that UFL1 was downregulated in renal cell carcinomas, which correlated with lower p53 expression, suggesting that the ufmylation process may be targeted by certain types of cancer (172).

UFL1 can also act at the ER, where it plays a role in ER protein quality control. Indeed, one of the earliest studies identifying ufmylation found that many ribosomal proteins were ufmylated, although no function was determined (182). Future work has uncovered that ufmylation of specific proteins, including ribosomal protein RPL26, induces lysosomal degradation of stalled peptides and/or the ER and prevents the unfolded protein response (176, 178, 184, 185). Hepatitis A virus translation, which occurs in association with the ER, also requires ufmylation of RPL26 (166). Therefore, ufmylation can regulate several aspects of translation. It is possible that ufmylation regulates translation of certain mRNAs important for RIG-I signaling and subsequent IFN induction. However, I identified a role for ufmylation in regulating the interaction of RIG-I with 14-3-3 ϵ , one of the earliest known steps of RIG-I signaling, strongly supporting a mechanism in which following RIG-I activation, ufmylation is controlling this specific protein-protein interaction.

How ufmylation can be involved in such diverse pathways has yet to be uncovered. It is possible that PTM of UFL1 or the other machinery itself by non-UFM1 modifications may be important, such as phosphorylation of UFL1 being required for its roles in the DNA damage response (180). Indeed, other PTM machinery have been

shown to be regulated by modifications they do not themselves conjugate (234, 235). Further work uncovering how regulation of ufmylation occurs will be vital to our understanding of this process.

5.2.2.2 Do UFL1 co-factors direct ufmylation?

The mechanisms underlying how cytoplasmic UFL1 is recruited to its protein targets that reside in different subcellular compartments are not fully known. For example, we found that RIG-I activation induces UFL1 translocation to intracellular membranes, and while we know that UFL1 is recruited to the MAM during infection, the mechanism by which UFL1 becomes membrane-associated remains unknown (78). UFBP1 may facilitate UFL1 targeting to the MAM, as UFBP1 is localized to mitochondrial-ER contact sites (169, 236) and in some cases it is required for UFL1 recruitment to membranes (176, 178). Thus, both UFBP1 and mitochondrial-ER contact sites could function as a regulatory hub that aids in the recruitment of UFL1 and RIG-I pathway signaling proteins. Indeed, a new study has suggested that UFBP1 may be required for ufmylation of some targets, which supports the data of others (165, 170). This leads to the possibility that UFL1 may act with a helper protein, such as UFBP1 or other unidentified proteins, to induce ufmylation of substrates. Perhaps viral infection could induce the PTM of helper proteins which then allow for interaction with RIG-I. In support of this, two higher molecular weight species of UFBP1 can be observed via immunoblot. The formation of these is dependent on lysine residues in UFBP1 and was originally thought to be ufmylation (169), however this has been disproven (178). Though these lysine residues, which appear to be conjugated to a PTM, were found to be indispensable for the progression of ER-phagy, its possible they regulate the ufmylation machinery recruitment in response to other signals, such as viral infection. As UFL1

contains no functional domains common to other E3 ligases that might allow one to predict how its targets are selected (106, 145, 169), defining the signals and features that control UFL1 localization, as well as the target proteins ufmylated in response to RIG-I activation, will undoubtedly reveal clues into how the process of ufmylation is activated and how specific targets are selected.

5.2.3 Does ufmylation regulate RIG-I signaling through multiple mechanisms?

The mechanisms by which the process of UFM1 addition regulates interactions between proteins or alters other aspects of protein function are largely unknown. Indeed, I found that in both overexpression and KO of UFSP2, the protease that removes UFM1 from proteins (164), promoted virally-mediated IFN induction, suggesting that we do not yet have a full grasp on the ufmylation process. It is possible that the dynamic process of ufmylation or the enhanced formation of mature UFM1 following deconjugation from targets promote RIG-I signaling independent of deconjugation activity. It is not yet clear the dynamics of protein de-ufmylation by UFSP2, whether some proteins are more likely to become targeted by UFSP2, or if other factors may control UFSP2 activity such as transcriptional upregulation, localization, or PTMs. In the UFSP2 KO cells, I observed increased amounts of a specific higher molecular weight UFM1-conjugates by immunoblot, suggesting that UFSP2 is important for the generation of free UFM1 for conjugation. Indeed, in support of this idea, others have shown that UFSP2 in myeloid cells is required for influenza virus resistance in mice (193). It is also possible that UFSP2 acts on other members of the RIG-I pathway to alter their function. Interestingly, RAB1B, a GTPase that we found is recruited to the MAM and important for RIG-I signaling (78, 188) is ufmylated (237, 238), which reveals that ufmylation likely regulates

a number of RIG-I pathway signaling proteins. Through my work, I was able to uncover that this is indeed the case, as I found that a subset of proteins are ufmylated during RIG-I signaling, including TBK1, a crucial activator of IFNs (12, 69, 141, 239). Further validation revealed that a number of these likely ufmylated proteins are novel regulators of IFN- β induction. In this section, I discuss the known roles of these candidates in viral infection, and possible mechanisms for their signaling regulation.

GRIPAP1, or GRIP-associated protein-1, (also known as GRASP-1), is a guanine nucleotide exchange factor that is important in regulating AMPA signaling in neurons (213, 240–242). Little is known about its roles in other cell types, however, it is a clear regulator of its binding partner, GRIP1 (241). Interestingly, multiple studies have implicated GRIP1 as a regulator of IRF3 (212, 243), either in response to TLR3 signaling or lipopolysaccharide (LPS) treatment. Further, it has been shown that GRIP1 can utilize PTMS to interact with binding partners (211). Therefore, it is possible that GRIPAP1 ufmylation may regulate IFN through the GRIP1-IRF3 interaction.

FMR1, or fragile X mental retardation protein (FMRP), has been well studied as the causative agent for fragile X syndrome, with loss of protein expression causing cognitive defects (244). Importantly, as this is due to a mutation in the *FMR1* gene, this disease is inherited and affects nearly 1 in 4,000 males and 1 in 8,000 females (245). Normally, FMR1 has functional roles as an RNA binding protein, and facilitates the export of RNAs from the nucleus to the cytoplasm (214, 246–249). Interestingly, FMR1 has also been reported to regulate RNA stability through interacting with RNAs that contain the modification m⁶A (216, 250), which is known to regulate viral infection and the innate immune response to infection, in addition to shielding self-RNAs from RIG-I sensing (20, 197, 251–254). FMR1 has been reported to regulate hepatitis B virus (a

DNA virus) infection by promoting nuclear export in an m⁶A dependent manner (217). Indeed, ufmylation has been shown previously to be a highly prevalent modification of RNA binding proteins (182), so it could be that UFM1-conjugation regulates the RNA binding ability of FMR1 leading to differential outcomes during infection.

GNAI3 has been reported to function in intracellular vesicle trafficking (218, 219). Indeed, it has been shown that through its interaction with co-factors, is required for efficient hepatitis B virus replication through increasing endosomal trafficking during infection, increasing progeny formation (218). Other known vesicle trafficking proteins are highly important in regulating intracellular innate immunity, and as previously discussed, we are still uncovering the trafficking proteins responsible for the multitude of relocalization events that are required for an efficient immune response (61, 62, 188). GNAI3 could be involved in the innate immune response through its trafficking functions, and the proteins it selects for trafficking could be due to UFM1, as I found for 14-3-3ε.

BAG3 is perhaps the most well-defined candidate in regulating viral infection. BAG3, of Bcl-2 associated athanogene 3, is a member of the BAG family of chaperone proteins that have been shown to regulate diverse cellular processes such as apoptosis, tumorigenesis, neuronal differentiation, stress responses, and the cell cycle (223). BAG3 has been found to primarily bind proteins containing a specific PPxY motif, which is found in many viral proteins encoded by DNA viruses that interact with BAG3 (220–222, 255–257). Interestingly, the mechanisms by which BAG3 regulates viral proteins are diverse, displaying both positive and negative regulation which may be virus dependent. Though much work has been done studying the impact of BAG3 on viral proteins, little work has investigated its role as a host innate immunity factor. Surprisingly, however, a study done in an orange-spotted grouper model for nervous necrosis virus, a devastating

RNA virus that has plagued marine aquaculture (258) found that BAG3 expression promoted viral replication through upregulating autophagy pathways which downregulated IRFs (259). Contrary to their study, my data indicates that BAG3 promotes IFN induction. Though potentially, in humans, its ufmylation in response viral infection repurpose its function to play a positive role on IRF activation.

INTS3 is a key member of the DNA damage repair machinery (224–226). Surprisingly, it was recently found that RIG-I was recruited to double-strand DNA breaks and actually suppresses repair (260). The ufmylation machinery is also recruited to sites of DNA damage, so it is possible that INTS3 is ufmylated as part of the UFM1-regulated DNA damage machinery (180, 181, 232). Interestingly, RIG-I can be recruited to sites of DNA damage (260). As my data has shown that ufmylation can regulate RIG-I interaction with binding partners (167), it therefore may be possible that INTS3 aids in RIG-I recruitment to sites of DNA damage effectively sequestering it from the viral RNA sensing pathways, as RNA viruses are well-established to promote DNA damage (261).

Overall, the exploration into the functional mechanisms of these proteins in their regulation of innate immune signaling, and how ufmylation mediates that, will provide novel insights into how ufmylation regulates protein function. Additionally, continuation of this work will uncover a new set of host-derived regulatory factors that govern RIG-I signaling, adding a layer of complexity to our understanding of this process.

5.2.4 Does ufmylation regulate other antiviral sensing pathways?

My thesis work identifying a role for ufmylation in RIG-I signaling, along with the current body of literature suggesting that ufmylation may regulate diverse stress response pathways, raises the possibility that ufmylation may be involved in regulation of other host antiviral pathways.

As previously discussed, it could be likely that ufmylation regulates MDA5 through a similar mechanism as it regulates RIG-I. Though MDA5 contains a 14-3-3 binding motif, phosphorylation of this residue actually prevented 14-3-3 η interaction with MDA5, suggesting that they interact through a novel mechanism (62). Further work characterizing the role of ufmylation in other antiviral signaling pathways will be highly important. Indeed, SARS-CoV-2, the virus that causes COVID-19, is sensed by MDA5 (262). Additionally, the SARS-CoV-2 papain-like protease which serves to cleave viral polyproteins, is also involved in evasion of immune signaling (263). The papain-like protease of SARS-CoV2 is predicted to target multiple ufmylation machinery proteins, which could indicate that this is a strategy employed by this virus to evade host immunity through MDA5 signaling (264). Further, a different study utilizing a proximity-based labeling assay identified interactions between multiple SARS-CoV2 proteins and the ufmylation machinery (265). Together, these could suggest that ufmylation is somehow activated during MDA5 signaling. Aside from potential 14-3-3 regulation by ufmylation, my data profiling the proteins that become ufmylated during RIG-I signaling revealed that TBK1 is ufmylated. Importantly, TBK1 is a key kinase that multiple cellular pathogen sensing pathways converge on, including RNA sensing by RIG-I, MDA5, TLR3/7, and DNA virus sensing by cGAS/STING (12, 67, 96, 239, 266, 267). It is possible that ufmylation may regulate its function more broadly than RIG-I signaling alone and could be a regulatory mechanism in many pathogen sensing pathways.

Ufmylation was first suggested to have a role in pathogen defense through playing a negative role in NF κ B induction in endothelial cells (268). It was determined that depletion of UFM1 increased NF κ B induction following LPS treatment, although the consequences of this on bacterial growth and the mechanisms by which UFM1 regulates

this pathway was not explored. Further work revealed that following either IFN- γ or LPS treatment in macrophages, the ufmylation pathway played a negative role in macrophage activation by maintaining ER homeostasis (193). Paradoxically, KO of the ufmylation machinery in mice led to increased mortality from influenza virus, which is consistent with my work, suggesting that a careful balance of macrophage activation is required for the antiviral response, and ufmylation plays a role in maintaining this balance. It is unclear however, how ufmylation-dependent regulation can act both in a positive and negative manner. As such, it will be important to understand how ufmylation is involved in multiple pathways, and what features functionalize it differently based on which signals are activated.

In the evolutionary arms race between viral pathogenesis and host defenses, viruses often evolve ways to subvert host immunity by antagonizing factors that promote immune signaling (4, 96, 269). It is therefore possible that there are viruses which are sensed by RIG-I that antagonize ufmylation. Importantly, many viruses target 14-3-3 proteins, as this is a crucial step in RIG-I and MDA5 activation. Viruses such as dengue virus, Zika virus, influenza, and even herpes simplex virus all antagonize 14-3-3 proteins to promote their own replication. This has been shown to happen through a phosphomimetic motif on a viral protein which allows them to bind with 14-3-3 proteins preferentially, sequestering 14-3-3 from its cargo, preventing their relocalization, although there are slight differences in this mechanism between viruses (70–72, 270). As such, it could be possible that viruses antagonize ufmylation as well, to prevent 14-3-3 ϵ (or other 14-3-3 proteins which may be regulated by ufmylation) from trafficking RIG-I or other RLRs to intracellular membranes for IFN induction. The exploration of the complex network of interactions between host and viral proteins, and novel viral immune

evasion mechanisms, will be invaluable to our understanding of the host-pathogen interface.

5.3 Broader impacts of this research

Overall, the results presented in this dissertation are important discoveries for our understanding of antiviral innate immunity, RIG-I sensing regulation, post-translational protein regulation, and provide new insights into the roles of ufmylation during cellular stress. Our knowledge of how antiviral signaling is regulated by post-translational modifications remains poorly understood and these results suggest that studying novel post-translational modifications broadens our understanding of RIG-I activation and the IFN response, with potential implications for auto-inflammatory conditions. Additionally, discovering a novel role for ufmylation as a regulator of the RNA-sensor RIG-I may be an important revelation for understanding its roles in broader human health, especially as ufmylation is linked to a number of human diseases. There are many important new questions associated with my findings, and I look forward to seeing the progress of this field in the future.

References

1. A. Iwasaki, R. Medzhitov, Control of adaptive immunity by the innate immune system. *Nat. Immunol.* **16**, 343–353 (2015).
2. Y. J. Crow, Type I interferonopathies: mendelian type I interferon up-regulation. *Curr. Opin. Immunol.* **32**, 7–12 (2015).
3. O. Takeuchi, S. Akira, Innate immunity to virus infection. *Immunol. Rev.* **227**, 75–86 (2009).
4. D. C. Beachboard, S. M. Horner, Innate immune evasion strategies of DNA and RNA viruses. *Curr. Opin. Microbiol.* **32**, 113–119 (2016).
5. M. J. McFadden, N. S. Gokhale, S. M. Horner, Protect this house: cytosolic sensing of viruses. *Current Opinion in Virology* **22**, 36–43 (2017).
6. J. W. Schoggins, C. M. Rice, Interferon-stimulated genes and their antiviral effector functions. *Curr Opin Virol* **1**, 519–525 (2011).
7. Y.-M. Loo, *et al.*, Distinct RIG-I and MDA5 Signaling by RNA Viruses in Innate Immunity. *Journal of Virology* **82**, 335–345 (2008).
8. Y.-M. Loo, M. Gale, Immune Signaling by RIG-I-like Receptors. *Immunity* **34**, 680–692 (2011).
9. G. Liu, M. U. Gack, Distinct and Orchestrated Functions of RNA Sensors in Innate Immunity. *Immunity* **53**, 26–42 (2020).
10. M. U. Gack, Mechanisms of RIG-I-like receptor activation and manipulation by viral pathogens. *J Virol* **88**, 5213–5216 (2014).
11. F. Hou, *et al.*, MAVS Forms Functional Prion-like Aggregates to Activate and Propagate Antiviral Innate Immune Response. *Cell* **146**, 448–461 (2011).
12. K. A. Fitzgerald, *et al.*, IKKepsilon and TBK1 are essential components of the IRF3 signaling pathway. *Nat. Immunol.* **4**, 491–496 (2003).
13. R. Lin, C. Heylbroeck, P. M. Pitha, J. Hiscott, Virus-Dependent Phosphorylation of the IRF-3 Transcription Factor Regulates Nuclear Translocation, Transactivation Potential, and Proteasome-Mediated Degradation. *Mol Cell Biol* **18**, 2986–2996 (1998).
14. J. W. Schoggins, *et al.*, A diverse range of gene products are effectors of the type I interferon antiviral response. *Nature* **472**, 481–485 (2011).

15. P. Metz, *et al.*, Identification of type I and type II interferon-induced effectors controlling hepatitis C virus replication. *Hepatology* **56**, 2082–2093 (2012).
16. S. Jensen, A. R. Thomsen, Sensing of RNA viruses: a review of innate immune receptors involved in recognizing RNA virus invasion. *J Virol* **86**, 2900–2910 (2012).
17. A. M. Kell, M. Gale, RIG-I in RNA virus recognition. *Virology* **479–480**, 110–121 (2015).
18. J. Rehwinkel, M. U. Gack, RIG-I-like receptors: their regulation and roles in RNA sensing. *Nature Reviews Immunology*, 1–15 (2020).
19. S. C. Devarkar, *et al.*, Structural basis for m7G recognition and 2'-O-methyl discrimination in capped RNAs by the innate immune receptor RIG-I. *PNAS* **113**, 596–601 (2016).
20. M. G. Thompson, M. T. Sacco, S. M. Horner, How RNA modifications regulate the antiviral response. *Immunol Rev* **304**, 169–180 (2021).
21. N. S. Gokhale, J. R. Smith, R. D. Van Gelder, R. Savan, RNA regulatory mechanisms that control antiviral innate immunity. *Immunological Reviews* **304**, 77–96 (2021).
22. M. T. Sacco, S. M. Horner, Flipping the script: viral capitalization of RNA modifications. *Brief Funct Genomics* **20**, 86–93 (2021).
23. M. Yoneyama, *et al.*, The RNA helicase RIG-I has an essential function in double-stranded RNA-induced innate antiviral responses. *Nature Immunology* **5**, 730–737 (2004).
24. T. Saito, *et al.*, Regulation of innate antiviral defenses through a shared repressor domain in RIG-I and LGP2. *PNAS* **104**, 582–587 (2007).
25. F. Jiang, *et al.*, Structural basis of RNA recognition and activation by innate immune receptor RIG-I. *Nature* **479**, 423–427 (2011).
26. E. Kowalinski, *et al.*, Structural Basis for the Activation of Innate Immune Pattern-Recognition Receptor RIG-I by Viral RNA. *Cell* **147**, 423–435 (2011).
27. A. Peisley, B. Wu, H. Xu, Z. J. Chen, S. Hur, Structural basis for ubiquitin-mediated antiviral signal activation by RIG-I. *Nature* **509**, 110–114 (2014).
28. R. B. Seth, L. Sun, C.-K. Ea, Z. J. Chen, Identification and Characterization of MAVS, a Mitochondrial Antiviral Signaling Protein that Activates NF- κ B and IRF3. *Cell* **122**, 669–682 (2005).

29. H. Kato, *et al.*, Length-dependent recognition of double-stranded ribonucleic acids by retinoic acid-inducible gene-I and melanoma differentiation-associated gene 5. *J Exp Med* **205**, 1601–1610 (2008).
30. D. Kang, *et al.*, mda-5: An interferon-inducible putative RNA helicase with double-stranded RNA-dependent ATPase activity and melanoma growth-suppressive properties. *Proc Natl Acad Sci U S A* **99**, 637–642 (2002).
31. R. Züst, *et al.*, Ribose 2'-O-methylation provides a molecular signature for the distinction of self and non-self mRNA dependent on the RNA sensor Mda5. *Nat Immunol* **12**, 137–143 (2011).
32. B. Wu, *et al.*, Structural basis for dsRNA recognition, filament formation, and antiviral signal activation by MDA5. *Cell* **152**, 276–289 (2013).
33. K. R. Rodriguez, C. M. Horvath, Paramyxovirus V Protein Interaction with the Antiviral Sensor LGP2 Disrupts MDA5 Signaling Enhancement but Is Not Relevant to LGP2-Mediated RLR Signaling Inhibition. *J Virol* **88**, 8180–8188 (2014).
34. E. Wies, *et al.*, Dephosphorylation of the RNA Sensors RIG-I and MDA5 by the Phosphatase PP1 Is Essential for Innate Immune Signaling. *Immunity* **38**, 437–449 (2013).
35. S. Rothenfusser, *et al.*, The RNA helicase Lgp2 inhibits TLR-independent sensing of viral replication by retinoic acid-inducible gene-I. *J Immunol* **175**, 5260–5268 (2005).
36. M. Yoneyama, *et al.*, Shared and Unique Functions of the DExD/H-Box Helicases RIG-I, MDA5, and LGP2 in Antiviral Innate Immunity. *The Journal of Immunology* **175**, 2851–2858 (2005).
37. A. M. Bruns, G. P. Leser, R. A. Lamb, C. M. Horvath, The innate immune sensor LGP2 activates antiviral signaling by regulating MDA5-RNA interaction and filament assembly. *Mol Cell* **55**, 771–781 (2014).
38. E. Uchikawa, *et al.*, Structural Analysis of dsRNA Binding to Anti-viral Pattern Recognition Receptors LGP2 and MDA5. *Mol Cell* **62**, 586–602 (2016).
39. T. Venkataraman, *et al.*, Loss of DExD/H Box RNA Helicase LGP2 Manifests Disparate Antiviral Responses. *The Journal of Immunology* **178**, 6444–6455 (2007).
40. J. E. Stok, *et al.*, RNA sensing via the RIG-I-like receptor LGP2 is essential for the induction of a type I IFN response in ADAR1 deficiency. *EMBO J*, e109760 (2022).

41. J. W. Schoggins, Interferon-Stimulated Genes: What Do They All Do? *Annual Review of Virology* **6**, 567–584 (2019).
42. P. Bastard, *et al.*, Herpes simplex encephalitis in a patient with a distinctive form of inherited IFNAR1 deficiency. *J Clin Invest* **131**, 139980 (2021).
43. P. Bastard, *et al.*, Autoantibodies against type I IFNs in patients with life-threatening COVID-19. *Science* **370**, eabd4585 (2020).
44. G. Uzé, G. Lutfalla, I. Gresser, Genetic transfer of a functional human interferon alpha receptor into mouse cells: cloning and expression of its cDNA. *Cell* **60**, 225–234 (1990).
45. D. Novick, B. Cohen, M. Rubinstein, The human interferon alpha/beta receptor: characterization and molecular cloning. *Cell* **77**, 391–400 (1994).
46. B. Cohen, D. Novick, S. Barak, M. Rubinstein, Ligand-induced association of the type I interferon receptor components. *Mol Cell Biol* **15**, 4208–4214 (1995).
47. L. Velazquez, M. Fellous, G. R. Stark, S. Pellegrini, A protein tyrosine kinase in the interferon alpha/beta signaling pathway. *Cell* **70**, 313–322 (1992).
48. M. Müller, *et al.*, The protein tyrosine kinase JAK1 complements defects in interferon- α/β and - γ signal transduction. *Nature* **366**, 129–135 (1993).
49. T. Improta, *et al.*, Transcription factor ISGF-3 formation requires phosphorylated Stat91 protein, but Stat113 protein is phosphorylated independently of Stat91 protein. *Proc Natl Acad Sci U S A* **91**, 4776–4780 (1994).
50. S. Leung, S. A. Qureshi, I. M. Kerr, J. E. Darnell, G. R. Stark, Role of STAT2 in the alpha interferon signaling pathway. *Mol Cell Biol* **15**, 1312–1317 (1995).
51. X. Y. Fu, C. Schindler, T. Improta, R. Aebersold, J. E. Darnell, The proteins of ISGF-3, the interferon alpha-induced transcriptional activator, define a gene family involved in signal transduction. *Proc Natl Acad Sci U S A* **89**, 7840–7843 (1992).
52. S. A. Veals, *et al.*, Subunit of an alpha-interferon-responsive transcription factor is related to interferon regulatory factor and Myb families of DNA-binding proteins. *Mol Cell Biol* **12**, 3315–3324 (1992).
53. W. M. Schneider, M. D. Chevillotte, C. M. Rice, Interferon-stimulated genes: a complex web of host defenses. *Annu Rev Immunol* **32**, 513–545 (2014).
54. H. Kato, *et al.*, Differential roles of MDA5 and RIG-I helicases in the recognition of RNA viruses. *Nature* **441**, 101–105 (2006).
55. S. Mostafavi, *et al.*, Parsing the Interferon Transcriptional Network and Its Disease Associations. *Cell* **164**, 564–578 (2016).

56. L. Espert, *et al.*, ISG20, a new interferon-induced RNase specific for single-stranded RNA, defines an alternative antiviral pathway against RNA genomic viruses. *J Biol Chem* **278**, 16151–16158 (2003).
57. J. M. Weidner, *et al.*, Interferon-induced cell membrane proteins, IFITM3 and tetherin, inhibit vesicular stomatitis virus infection via distinct mechanisms. *J Virol* **84**, 12646–12657 (2010).
58. T. Haline-Vaz, T. C. L. Silva, N. I. T. Zanchin, The human interferon-regulated ISG95 protein interacts with RNA polymerase II and shows methyltransferase activity. *Biochem. Biophys. Res. Commun.* **372**, 719–724 (2008).
59. M. S. Diamond, IFIT1: A dual sensor and effector molecule that detects non-2'-O methylated viral RNA and inhibits its translation. *Cytokine Growth Factor Rev* **25**, 543–550 (2014).
60. G. D. Williams, N. S. Gokhale, D. L. Snider, S. M. Horner, The mRNA Cap 2'-O-Methyltransferase CMTR1 Regulates the Expression of Certain Interferon-Stimulated Genes. *mSphere* **5** (2020).
61. H. M. Liu, *et al.*, The Mitochondrial Targeting Chaperone 14-3-3 ϵ Regulates a RIG-I Translocon that Mediates Membrane Association and Innate Antiviral Immunity. *Cell Host & Microbe* **11**, 528–537 (2012).
62. J.-P. Lin, Y.-K. Fan, H. M. Liu, The 14-3-3 η chaperone protein promotes antiviral innate immunity via facilitating MDA5 oligomerization and intracellular redistribution. *PLoS Pathog.* **15**, e1007582 (2019).
63. S. M. Horner, H. M. Liu, H. S. Park, J. Briley, M. Gale, Mitochondrial-associated endoplasmic reticulum membranes (MAM) form innate immune synapses and are targeted by hepatitis C virus. *Proc Natl Acad Sci U S A* **108**, 14590–14595 (2011).
64. C. Vazquez, S. M. Horner, MAVS Coordination of Antiviral Innate Immunity. *J Virol* **89**, 6974–6977 (2015).
65. Y.-M. Loo, M. Gale, Immune signaling by RIG-I-like receptors. *Immunity* **34**, 680–692 (2011).
66. D. C. Beachboard, *et al.*, The small GTPase RAB1B promotes antiviral innate immunity by interacting with TNF receptor–associated factor 3 (TRAF3). *J. Biol. Chem.* **294**, 14231–14240 (2019).
67. S. Liu, *et al.*, Phosphorylation of innate immune adaptor proteins MAVS, STING, and TRIF induces IRF3 activation. *Science* **347**, aaa2630 (2015).
68. M. Pourcelot, *et al.*, The Golgi apparatus acts as a platform for TBK1 activation after viral RNA sensing. *BMC Biology* **14**, 69 (2016).

69. R. Fang, *et al.*, MAVS activates TBK1 and IKK ϵ through TRAFs in NEMO dependent and independent manner. *PLoS Pathog* **13** (2017).
70. Y. K. Chan, M. U. Gack, A phosphomimetic-based mechanism of dengue virus to antagonize innate immunity. *Nature Immunology* **17**, 523–530 (2016).
71. W. Riedl, *et al.*, Zika Virus NS3 Mimics a Cellular 14-3-3-Binding Motif to Antagonize RIG-I- and MDA5-Mediated Innate Immunity. *Cell Host & Microbe* **26**, 493-503.e6 (2019).
72. E.-H. Tam, *et al.*, Role of the chaperone protein 14-3-3 ϵ in the regulation of influenza A virus-activated beta interferon. *J Virol*, JVI0023121 (2021).
73. K.-H. Kok, *et al.*, The double-stranded RNA-binding protein PACT functions as a cellular activator of RIG-I to facilitate innate antiviral response. *Cell Host Microbe* **9**, 299–309 (2011).
74. P. Luthra, *et al.*, Mutual antagonism between the Ebola virus VP35 protein and the RIG-I activator PACT determines infection outcome. *Cell Host Microbe* **14**, 74–84 (2013).
75. H. Lian, *et al.*, The Zinc-Finger Protein ZCCHC3 Binds RNA and Facilitates Viral RNA Sensing and Activation of the RIG-I-like Receptors. *Immunity* **49**, 438-448.e5 (2018).
76. X. Jiang, *et al.*, Ubiquitin-induced oligomerization of the RNA sensors RIG-I and MDA5 activates antiviral innate immune response. *Immunity* **36**, 959–973 (2012).
77. A. J. Muslin, J. W. Tanner, P. M. Allen, A. S. Shaw, Interaction of 14-3-3 with Signaling Proteins Is Mediated by the Recognition of Phosphoserine. *Cell* **84**, 889–897 (1996).
78. S. M. Horner, C. Wilkins, S. Badil, J. Iskarpatyoti, M. G. Jr, Proteomic Analysis of Mitochondrial-Associated ER Membranes (MAM) during RNA Virus Infection Reveals Dynamic Changes in Protein and Organelle Trafficking. *PLOS ONE* **10**, e0117963 (2015).
79. S. Liu, *et al.*, MAVS recruits multiple ubiquitin E3 ligases to activate antiviral signaling cascades. *eLife* **2**, e00785 (2013).
80. C. Chiang, M. U. Gack, Post-translational Control of Intracellular Pathogen Sensing Pathways. *Trends in Immunology* **38**, 39–52 (2017).
81. Z. Sun, H. Ren, Y. Liu, J. L. Teeling, J. Gu, Phosphorylation of RIG-I by casein kinase II inhibits its antiviral response. *J Virol* **85**, 1036–1047 (2011).

82. N. P. Maharaj, E. Wies, A. Stoll, M. U. Gack, Conventional Protein Kinase C- α (PKC- α) and PKC- β Negatively Regulate RIG-I Antiviral Signal Transduction. *J Virol* **86**, 1358–1371 (2012).
83. S. J. Choi, *et al.*, HDAC6 regulates cellular viral RNA sensing by deacetylation of RIG-I. *EMBO J.* **35**, 429–442 (2016).
84. H. M. Liu, *et al.*, Regulation of Retinoic Acid Inducible Gene-I (RIG-I) Activation by the Histone Deacetylase 6. *EBioMedicine* **9**, 195–206 (2016).
85. H. Oshiumi, M. Matsumoto, S. Hatakeyama, T. Seya, Riplet/RNF135, a RING finger protein, ubiquitinates RIG-I to promote interferon-beta induction during the early phase of viral infection. *J. Biol. Chem.* **284**, 807–817 (2009).
86. H. Oshiumi, M. Miyashita, M. Matsumoto, T. Seya, A distinct role of Riplet-mediated K63-Linked polyubiquitination of the RIG-I repressor domain in human antiviral innate immune responses. *PLoS Pathog.* **9**, e1003533 (2013).
87. M. U. Gack, *et al.*, TRIM25 RING-finger E3 ubiquitin ligase is essential for RIG-I-mediated antiviral activity. *Nature* **446**, 916–920 (2007).
88. K. Kuniyoshi, *et al.*, Pivotal role of RNA-binding E3 ubiquitin ligase MEX3C in RIG-I-mediated antiviral innate immunity. *Proc Natl Acad Sci U S A* **111**, 5646–5651 (2014).
89. J. Yan, Q. Li, A.-P. Mao, M.-M. Hu, H.-B. Shu, TRIM4 modulates type I interferon induction and cellular antiviral response by targeting RIG-I for K63-linked ubiquitination. *J Mol Cell Biol* **6**, 154–163 (2014).
90. S. Davidson, A. Steiner, C. R. Harapas, S. L. Masters, An Update on Autoinflammatory Diseases: Interferonopathies. *Curr Rheumatol Rep* **20**, 38 (2018).
91. K. Arimoto, *et al.*, Negative regulation of the RIG-I signaling by the ubiquitin ligase RNF125. *PNAS* **104**, 7500–7505 (2007).
92. K.-S. Inn, *et al.*, Linear ubiquitin assembly complex negatively regulates RIG-I- and TRIM25-mediated type I interferon induction. *Mol Cell* **41**, 354–365 (2011).
93. W. Chen, *et al.*, Induction of Siglec-G by RNA viruses inhibits the innate immune response by promoting RIG-I degradation. *Cell* **152**, 467–478 (2013).
94. W. Wang, *et al.*, RNF122 suppresses antiviral type I interferon production by targeting RIG-I CARDS to mediate RIG-I degradation. *PNAS* **113**, 9581–9586 (2016).
95. M. E. Davis, M. U. Gack, Ubiquitination in the antiviral immune response. *Virology* **479–480**, 52–65 (2015).

96. Y. K. Chan, M. U. Gack, Viral evasion of intracellular DNA and RNA sensing. *Nat Rev Microbiol* **14**, 360–373 (2016).
97. A. K. Overby, V. L. Popov, M. Niedrig, F. Weber, Tick-borne encephalitis virus delays interferon induction and hides its double-stranded RNA in intracellular membrane vesicles. *J Virol* **84**, 8470–8483 (2010).
98. L. Uchida, *et al.*, The dengue virus conceals double-stranded RNA in the intracellular membrane to escape from an interferon response. *Sci Rep* **4**, 7395 (2014).
99. C. J. Neufeldt, *et al.*, The Hepatitis C Virus-Induced Membranous Web and Associated Nuclear Transport Machinery Limit Access of Pattern Recognition Receptors to Viral Replication Sites. *PLOS Pathogens* **12**, e1005428 (2016).
100. T. Yoshizumi, *et al.*, Influenza A virus protein PB1-F2 translocates into mitochondria via Tom40 channels and impairs innate immunity. *Nat Commun* **5**, 4713 (2014).
101. M. U. Gack, *et al.*, Influenza A virus NS1 targets the ubiquitin ligase TRIM25 to evade recognition by RIG-I. *Cell Host Microbe* **5**, 439–449 (2009).
102. R. Rajsbaum, *et al.*, Species-specific inhibition of RIG-I ubiquitination and IFN induction by the influenza A virus NS1 protein. *PLoS Pathog* **8**, e1003059 (2012).
103. M. A. Clementz, *et al.*, Deubiquitinating and interferon antagonism activities of coronavirus papain-like proteases. *J Virol* **84**, 4619–4629 (2010).
104. M. E. Davis, *et al.*, Antagonism of the phosphatase PP1 by the measles virus V protein is required for innate immune escape of MDA5. *Cell Host Microbe* **16**, 19–30 (2014).
105. O. Kerscher, R. Felberbaum, M. Hochstrasser, Modification of Proteins by Ubiquitin and Ubiquitin-Like Proteins. *Annual Review of Cell and Developmental Biology* **22**, 159–180 (2006).
106. K. N. Swatek, D. Komander, Ubiquitin modifications. *Cell Research* **26**, 399–422 (2016).
107. P. Cohen, The origins of protein phosphorylation. *Nat Cell Biol* **4**, E127–E130 (2002).
108. E. Verdin, M. Ott, 50 years of protein acetylation: from gene regulation to epigenetics, metabolism and beyond. *Nat Rev Mol Cell Biol* **16**, 258–264 (2015).
109. I. L. Goldknopf, M. F. French, R. Musso, H. Busch, Presence of protein A24 in rat liver nucleosomes. *Proc Natl Acad Sci U S A* **74**, 5492–5495 (1977).

110. A. Hershko, A. Ciechanover, The ubiquitin system. *Annu Rev Biochem* **67**, 425–479 (1998).
111. Z. J. Chen, L. J. Sun, Nonproteolytic functions of ubiquitin in cell signaling. *Mol Cell* **33**, 275–286 (2009).
112. A. Calistri, D. Munegato, I. Carli, C. Parolin, G. Palù, The Ubiquitin-Conjugating System: Multiple Roles in Viral Replication and Infection. *Cells* **3**, 386–417 (2014).
113. C. M. Pickart, Mechanisms underlying ubiquitination. *Annu Rev Biochem* **70**, 503–533 (2001).
114. B. A. Schulman, J. W. Harper, Ubiquitin-like protein activation by E1 enzymes: the apex for downstream signalling pathways. *Nat. Rev. Mol. Cell Biol.* **10**, 319–331 (2009).
115. Y. Ye, M. Rape, Building ubiquitin chains: E2 enzymes at work. *Nat Rev Mol Cell Biol* **10**, 755–764 (2009).
116. R. J. Deshaies, C. A. P. Joazeiro, RING domain E3 ubiquitin ligases. *Annu Rev Biochem* **78**, 399–434 (2009).
117. J. J. Smit, T. K. Sixma, RBR E3-ligases at work. *EMBO Rep* **15**, 142–154 (2014).
118. D. Rotin, S. Kumar, Physiological functions of the HECT family of ubiquitin ligases. *Nat Rev Mol Cell Biol* **10**, 398–409 (2009).
119. M. J. Clague, *et al.*, Deubiquitylases from genes to organism. *Physiol Rev* **93**, 1289–1315 (2013).
120. D. Komander, M. J. Clague, S. Urbé, Breaking the chains: structure and function of the deubiquitinases. *Nat Rev Mol Cell Biol* **10**, 550–563 (2009).
121. M. J. Clague, C. Heride, S. Urbé, The demographics of the ubiquitin system. *Trends Cell Biol* **25**, 417–426 (2015).
122. M. Hrdinka, M. Gyrd-Hansen, The Met1-Linked Ubiquitin Machinery: Emerging Themes of (De)regulation. *Mol Cell* **68**, 265–280 (2017).
123. C. E. Berndsen, C. Wolberger, New insights into ubiquitin E3 ligase mechanism. *Nat Struct Mol Biol* **21**, 301–307 (2014).
124. F. Mattioli, T. K. Sixma, Lysine-targeting specificity in ubiquitin and ubiquitin-like modification pathways. *Nat Struct Mol Biol* **21**, 308–316 (2014).
125. V. Nagy, I. Dikic, Ubiquitin ligase complexes: from substrate selectivity to conjugational specificity. *Biol Chem* **391**, 163–169 (2010).

126. M. Koegl, *et al.*, A novel ubiquitination factor, E4, is involved in multiubiquitin chain assembly. *Cell* **96**, 635–644 (1999).
127. D. E. Spratt, H. Walden, G. S. Shaw, RBR E3 ubiquitin ligases: new structures, new insights, new questions. *Biochem J* **458**, 421–437 (2014).
128. S. A. Wagner, *et al.*, A proteome-wide, quantitative survey of in vivo ubiquitylation sites reveals widespread regulatory roles. *Mol Cell Proteomics* **10**, M111.013284 (2011).
129. W. Kim, *et al.*, Systematic and Quantitative Assessment of the Ubiquitin-Modified Proteome. *Molecular Cell* **44**, 325–340 (2011).
130. Y. Kravtsova-Ivantsiv, A. Ciechanover, Non-canonical ubiquitin-based signals for proteasomal degradation. *Journal of Cell Science* **125**, 539–548 (2012).
131. M. L. Matsumoto, *et al.*, K11-Linked Polyubiquitination in Cell Cycle Control Revealed by a K11 Linkage-Specific Antibody. *Molecular Cell* **39**, 477–484 (2010).
132. H. Huang, *et al.*, K33-Linked Polyubiquitination of T Cell Receptor- ζ Regulates Proteolysis-Independent T Cell Signaling. *Immunity* **33**, 60–70 (2010).
133. A. K. Al-Hakim, *et al.*, Control of AMPK-related kinases by USP9X and atypical Lys(29)/Lys(33)-linked polyubiquitin chains. *Biochem J* **411**, 249–260 (2008).
134. M. Lin, *et al.*, USP38 Inhibits Type I Interferon Signaling by Editing TBK1 Ubiquitination through NLRP4 Signalosome. *Molecular Cell* **64**, 267–281 (2016).
135. M. Karim, *et al.*, Nonproteolytic K29-Linked Ubiquitination of the PB2 Replication Protein of Influenza A Viruses by Proviral Cullin 4-Based E3 Ligases. *mBio* **11** (2020).
136. T. Kirisako, *et al.*, A ubiquitin ligase complex assembles linear polyubiquitin chains. *EMBO J* **25**, 4877–4887 (2006).
137. F. Ikeda, *et al.*, SHARPIN forms a linear ubiquitin ligase complex regulating NF- κ B activity and apoptosis. *Nature* **471**, 637–641 (2011).
138. B. Gerlach, *et al.*, Linear ubiquitination prevents inflammation and regulates immune signalling. *Nature* **471**, 591–596 (2011).
139. B. K. Fiil, M. Gyrd-Hansen, The Met1-linked ubiquitin machinery in inflammation and infection. *Cell Death Differ* **28**, 557–569 (2021).
140. C. S. Friedman, *et al.*, The tumour suppressor CYLD is a negative regulator of RIG-I-mediated antiviral response. *EMBO Rep* **9**, 930–936 (2008).

141. D. Tu, *et al.*, Structure and Ubiquitination-Dependent Activation of TANK-Binding Kinase 1. *Cell Reports* **3**, 747–758 (2013).
142. J. Hou, *et al.*, USP18 positively regulates innate antiviral immunity by promoting K63-linked polyubiquitination of MAVS. *Nat Commun* **12**, 2970 (2021).
143. S. Paz, *et al.*, Ubiquitin-regulated recruitment of I κ B kinase epsilon to the MAVS interferon signaling adapter. *Mol Cell Biol* **29**, 3401–3412 (2009).
144. F. You, *et al.*, PCBP2 mediates degradation of the adaptor MAVS via the HECT ubiquitin ligase AIP4. *Nat Immunol* **10**, 1300–1308 (2009).
145. M. Hochstrasser, Origin and function of ubiquitin-like proteins. *Nature* **458**, 422–429 (2009).
146. G. R. Bylebyl, I. Belichenko, E. S. Johnson, The SUMO isopeptidase Ulp2 prevents accumulation of SUMO chains in yeast. *J Biol Chem* **278**, 44113–44120 (2003).
147. Y. Fan, *et al.*, SUMOylation in Viral Replication and Antiviral Defense. *Adv Sci (Weinh)*, e2104126 (2022).
148. R. Geiss-Friedlander, F. Melchior, Concepts in sumoylation: a decade on. *Nat Rev Mol Cell Biol* **8**, 947–956 (2007).
149. T. Kubota, *et al.*, Virus Infection Triggers SUMOylation of IRF3 and IRF7, Leading to the Negative Regulation of Type I Interferon Gene Expression. *J Biol Chem* **283**, 25660–25670 (2008).
150. R. I. Enchev, B. A. Schulman, M. Peter, Protein neddylation: beyond cullin-RING ligases. *Nat Rev Mol Cell Biol* **16**, 30–44 (2015).
151. H. Song, *et al.*, MLN4924, a First-in-Class NEDD8-Activating Enzyme Inhibitor, Attenuates IFN- β Production. *J.I.* **196**, 3117–3123 (2016).
152. G. Yu, *et al.*, Neddylation Facilitates the Antiviral Response in Zebrafish. *Front Immunol* **10**, 1432 (2019).
153. H. Sun, *et al.*, Inhibition of neddylation pathway represses influenza virus replication and pro-inflammatory responses. *Virology* **514**, 230–239 (2018).
154. N. T. H. Nguyen, H. Now, W.-J. Kim, N. Kim, J.-Y. Yoo, Ubiquitin-like modifier FAT10 attenuates RIG-I mediated antiviral signaling by segregating activated RIG-I from its signaling platform. *Sci Rep* **6**, 23377 (2016).
155. Y. Du, *et al.*, LRR25 inhibits type I IFN signaling by targeting ISG15-associated RIG-I for autophagic degradation. *EMBO J* **37**, 351–366 (2018).

156. H.-X. Shi, *et al.*, Positive Regulation of Interferon Regulatory Factor 3 Activation by Herc5 via ISG15 Modification. *Molecular and Cellular Biology* (2010) <https://doi.org/10.1128/MCB.01466-09> (February 27, 2022).
157. M. Ganesan, L. Y. Poluektova, D. J. Tuma, K. K. Kharbanda, N. A. Osna, Acetaldehyde Disrupts Interferon Alpha Signaling in Hepatitis C Virus-Infected Liver Cells by Up-Regulating USP18. *Alcoholism: Clinical and Experimental Research* **40**, 2329–2338 (2016).
158. G. Liu, *et al.*, ISG15-dependent activation of the sensor MDA5 is antagonized by the SARS-CoV-2 papain-like protease to evade host innate immunity. *Nat Microbiol* **6**, 467–478 (2021).
159. C. Zhao, *et al.*, Influenza B virus non-structural protein 1 counteracts ISG15 antiviral activity by sequestering ISGylated viral proteins. *Nat Commun* **7**, 12754 (2016).
160. L. A. Durfee, N. Lyon, K. Seo, J. M. Huibregtse, The ISG15 Conjugation System Broadly Targets Newly Synthesized Proteins: Implications for the Antiviral Function of ISG15. *Molecular Cell* **38**, 722–732 (2010).
161. A. Rahnefeld, *et al.*, Ubiquitin-Like Protein ISG15 (Interferon-Stimulated Gene of 15 kDa) in Host Defense Against Heart Failure in a Mouse Model of Virus-Induced Cardiomyopathy. *Circulation* **130**, 1589–1600 (2014).
162. Y. Tang, *et al.*, Herc5 Attenuates Influenza A Virus by Catalyzing ISGylation of Viral NS1 Protein. *J.I.* **184**, 5777–5790 (2010).
163. M. Komatsu, *et al.*, A novel protein-conjugating system for Ufm1, a ubiquitin-fold modifier. *EMBO J* **23**, 1977–1986 (2004).
164. S. H. Kang, *et al.*, Two novel ubiquitin-fold modifier 1 (Ufm1)-specific proteases, UfSP1 and UfSP2. *J. Biol. Chem.* **282**, 5256–5262 (2007).
165. H. M. Yoo, *et al.*, Modification of ASC1 by UFM1 is crucial for ER α transactivation and breast cancer development. *Mol. Cell* **56**, 261–274 (2014).
166. J. Kulsuptrakul, R. Wang, N. L. Meyers, M. Ott, A. S. Puschnik, A genome-wide CRISPR screen identifies UFMylation and TRAMP-like complexes as host factors required for hepatitis A virus infection. *Cell Reports* **34** (2021).
167. D. L. Snider, M. Park, K. A. Murphy, D. C. Beachboard, S. M. Horner, Signaling from the RNA sensor RIG-I is regulated by ufmylation. *Proceedings of the National Academy of Sciences* **119**, e2119531119 (2022).
168. D. Millrine, *et al.*, Human UFSP1 is an active protease that regulates UFM1 maturation and UFMylation. *bioRxiv*, 2022.02.28.482207 (2022).

169. K. Tatsumi, *et al.*, A novel type of E3 ligase for the Ufm1 conjugation system. *J. Biol. Chem.* **285**, 5417–5427 (2010).
170. J. J. Peter, *et al.*, Non canonical scaffold-type ligase complex mediates protein UFMylation. *bioRxiv*, 2022.01.31.478489 (2022).
171. Y. Wei, X. Xu, UFMylation: A Unique & Fashionable Modification for Life. *Genomics Proteomics Bioinformatics* **14**, 140–146 (2016).
172. S. Banerjee, M. Kumar, R. Wiener, Decrypting UFMylation: How Proteins Are Modified with UFM1. *Biomolecules* **10**, 1442 (2020).
173. J. Huber, *et al.*, An atypical LIR motif within UBA5 (ubiquitin like modifier activating enzyme 5) interacts with GABARAP proteins and mediates membrane localization of UBA5. *Autophagy* (2019) <https://doi.org/10.1080/15548627.2019.1606637>.
174. R. Duan, *et al.*, UBA5 Mutations Cause a New Form of Autosomal Recessive Cerebellar Ataxia. *PLOS ONE* **11**, e0149039 (2016).
175. M. Zheng, *et al.*, UBE1DC1, an ubiquitin-activating enzyme, activates two different ubiquitin-like proteins. *J Cell Biochem* **104**, 2324–2334 (2008).
176. C. P. Walczak, *et al.*, Ribosomal protein RPL26 is the principal target of UFMylation. *PNAS* **116**, 1299–1308 (2019).
177. J. Kwon, *et al.*, A novel LZAP-binding protein, NLBP, inhibits cell invasion. *J. Biol. Chem.* **285**, 12232–12240 (2010).
178. J. R. Liang, *et al.*, A Genome-wide ER-phagy Screen Highlights Key Roles of Mitochondrial Metabolism and ER-Resident UFMylation. *Cell* **0** (2020).
179. J. Wu, G. Lei, M. Mei, Y. Tang, H. Li, A novel C53/LZAP-interacting protein regulates stability of C53/LZAP and DDRGK domain-containing Protein 1 (DDRGK1) and modulates NF-kappaB signaling. *J. Biol. Chem.* **285**, 15126–15136 (2010).
180. B. Qin, *et al.*, UFL1 promotes histone H4 ufmylation and ATM activation. *Nat Commun* **10**, 1242 (2019).
181. Z. Wang, *et al.*, MRE11 UFMylation promotes ATM activation. *Nucleic Acids Research* **47**, 4124–4135 (2019).
182. D. Simsek, *et al.*, The Mammalian Ribo-interactome Reveals Ribosome Functional Diversity and Heterogeneity. *Cell* **169**, 1051-1065.e18 (2017).
183. L. Wang, *et al.*, UFMylation of RPL26 links translocation-associated quality control to endoplasmic reticulum protein homeostasis. *Cell Res*, 1–16 (2019).

184. L. Wang, *et al.*, UFMylation of RPL26 links translocation-associated quality control to endoplasmic reticulum protein homeostasis. *Cell Research* **30**, 5–20 (2020).
185. Y. Zhang, M. Zhang, J. Wu, G. Lei, H. Li, Transcriptional regulation of the Ufm1 conjugation system in response to disturbance of the endoplasmic reticulum homeostasis and inhibition of vesicle trafficking. *PLoS ONE* **7**, e48587 (2012).
186. D. Thoresen, *et al.*, The molecular mechanism of RIG-I activation and signaling. *Immunol Rev* (2021) <https://doi.org/10.1111/imr.13022>.
187. H. Oshiumi, Recent Advances and Contradictions in the Study of the Individual Roles of Ubiquitin Ligases That Regulate RIG-I-Like Receptor-Mediated Antiviral Innate Immune Responses. *Front Immunol* **11**, 1296 (2020).
188. D. C. Beachboard, *et al.*, The small GTPase RAB1B promotes antiviral innate immunity by interacting with TNF receptor–associated factor 3 (TRAF3). *J. Biol. Chem.*, jbc.RA119.007917 (2019).
189. J. Daniel, E. Liebau, The Ufm1 Cascade. *Cells* **3**, 627–638 (2014).
190. I. A. Gak, *et al.*, UFMylation regulates translational homeostasis and cell cycle progression. *bioRxiv*, 2020.02.03.931196 (2020).
191. R. DeJesus, *et al.*, Functional CRISPR screening identifies the ufmylation pathway as a regulator of SQSTM1/p62. *eLife* **5**, e17290 (2016).
192. Y. Cai, N. Singh, H. Li, Essential role of Ufm1 conjugation in the hematopoietic system. *Exp. Hematol.* **44**, 442–446 (2016).
193. D. R. Balce, *et al.*, UFMylation inhibits the proinflammatory capacity of interferon- γ -activated macrophages. *PNAS* **118** (2021).
194. Y.-M. Loo, *et al.*, Viral and therapeutic control of IFN- β promoter stimulator 1 during hepatitis C virus infection. *PNAS* **103**, 6001–6006 (2006).
195. R. Sumpter, *et al.*, Regulating intracellular antiviral defense and permissiveness to hepatitis C virus RNA replication through a cellular RNA helicase, RIG-I. *J Virol* **79**, 2689–2699 (2005).
196. T. Saito, D. M. Owen, F. Jiang, J. Marcotrigiano, M. Gale, Innate immunity induced by composition-dependent RIG-I recognition of hepatitis C virus RNA. *Nature* **454**, 523–527 (2008).
197. M. J. McFadden, *et al.*, Post-transcriptional regulation of antiviral gene expression by N6-methyladenosine. *Cell Reports* **34**, 108798 (2021).
198. A. Mizutani, M. Fukuda, K. Ibata, Y. Shiraishi, K. Mikoshiba, SYNCRIP, a Cytoplasmic Counterpart of Heterogeneous Nuclear Ribonucleoprotein R,

- Interacts with Ubiquitous Synaptotagmin Isoforms*. *Journal of Biological Chemistry* **275**, 9823–9831 (2000).
199. E. Foy, *et al.*, Control of antiviral defenses through hepatitis C virus disruption of retinoic acid-inducible gene-I signaling. *Proc. Natl. Acad. Sci. U.S.A.* **102**, 2986–2991 (2005).
 200. E. Meylan, *et al.*, Cardif is an adaptor protein in the RIG-I antiviral pathway and is targeted by hepatitis C virus. *Nature* **437**, 1167–1172 (2005).
 201. X.-D. Li, L. Sun, R. B. Seth, G. Pineda, Z. J. Chen, Hepatitis C virus protease NS3/4A cleaves mitochondrial antiviral signaling protein off the mitochondria to evade innate immunity. *Proc Natl Acad Sci U S A* **102**, 17717–17722 (2005).
 202. R. Lin, *et al.*, Dissociation of a MAVS/IPS-1/VISA/Cardif-IKKeppilon molecular complex from the mitochondrial outer membrane by hepatitis C virus NS3-4A proteolytic cleavage. *J Virol* **80**, 6072–6083 (2006).
 203. K. Takahashi, *et al.*, Nonself RNA-Sensing Mechanism of RIG-I Helicase and Activation of Antiviral Immune Responses. *Molecular Cell* **29**, 428–440 (2008).
 204. N. Zamorano Cuervo, Q. Osseman, N. Grandvaux, Virus Infection Triggers MAVS Polymers of Distinct Molecular Weight. *Viruses* **10** (2018).
 205. C. Vazquez, C. Y. Tan, S. M. Horner, Hepatitis C Virus Infection Is Inhibited by a Noncanonical Antiviral Signaling Pathway Targeted by NS3-NS4A. *Journal of Virology* (2019) <https://doi.org/10.1128/JVI.00725-19> (February 8, 2022).
 206. B. Fredericksen, *et al.*, Activation of the Interferon- β Promoter During Hepatitis C Virus RNA Replication. *Viral Immunology* **15**, 29–40 (2002).
 207. F. A. Ran, *et al.*, Genome engineering using the CRISPR-Cas9 system. *Nat Protoc* **8**, 2281–2308 (2013).
 208. H. M. Liu, *et al.*, SYNCRIP (synaptotagmin-binding, cytoplasmic RNA-interacting protein) is a host factor involved in hepatitis C virus RNA replication. *Virology* **386**, 249–256 (2009).
 209. J. J. Chiang, M. E. Davis, M. U. Gack, Regulation of RIG-I-like receptor signaling by host and viral proteins. *Cytokine & Growth Factor Reviews* **25**, 491–505 (2014).
 210. C. Vazquez, C. Y. Tan, S. M. Horner, Hepatitis C Virus Infection Is Inhibited by a Noncanonical Antiviral Signaling Pathway Targeted by NS3-NS4A. *Journal of Virology* **93** (2019).

211. C. Miao, *et al.*, LXR α represses LPS-induced inflammatory responses by competing with IRF3 for GRIP1 in Kupffer cells. *International Immunopharmacology* **35**, 272–279 (2016).
212. M. M. Reily, C. Pantoja, X. Hu, Y. Chinenov, I. Rogatsky, The GRIP1:IRF3 interaction as a target for glucocorticoid receptor-mediated immunosuppression. *EMBO J* **25**, 108–117 (2006).
213. L. M. Stinton, S. Selak, M. J. Fritzler, Identification of GRASP-1 as a novel 97 kDa autoantigen localized to endosomes. *Clinical Immunology* **116**, 108–117 (2005).
214. M. Ascano, *et al.*, FMRP targets distinct mRNA sequence elements to regulate protein expression. *Nature* **492**, 382–386 (2012).
215. B. M. Edens, *et al.*, FMRP Modulates Neural Differentiation through m6A-Dependent mRNA Nuclear Export. *Cell Rep* **28**, 845-854.e5 (2019).
216. P. J. Hsu, *et al.*, The RNA-binding protein FMRP facilitates the nuclear export of N6-methyladenosine-containing mRNAs. *J Biol Chem* **294**, 19889–19895 (2019).
217. G.-W. Kim, H. Imam, A. Siddiqui, The RNA Binding Proteins YTHDC1 and FMRP Regulate the Nuclear Export of N6-Methyladenosine-Modified Hepatitis B Virus Transcripts and Affect the Viral Life Cycle. *Journal of Virology* **95**, e00097-21.
218. X. Wang, *et al.*, CCDC88A/GIV promotes HBV replication and progeny secretion via enhancing endosomal trafficking and blocking autophagic degradation. *Autophagy*, 1–18 (2021).
219. M. Garcia-Marcos, J. Ear, M. G. Farquhar, P. Ghosh, A GDI (AGS3) and a GEF (GIV) regulate autophagy by balancing G protein activity and growth factor signals. *Mol Biol Cell* **22**, 673–686 (2011).
220. Z. Han, *et al.*, Host Protein BAG3 is a Negative Regulator of Lassa VLP Egress. *Diseases* **6**, E64 (2018).
221. C. A. Kyratsous, S. J. Silverstein, BAG3, a host cochaperone, facilitates varicella-zoster virus replication. *J Virol* **81**, 7491–7503 (2007).
222. C. A. Kyratsous, S. J. Silverstein, The co-chaperone BAG3 regulates Herpes Simplex Virus replication. *Proc Natl Acad Sci U S A* **105**, 20912–20917 (2008).
223. M. Kabbage, M. B. Dickman, The BAG proteins: a ubiquitous family of chaperone regulators. *Cell Mol Life Sci* **65**, 1390–1402 (2008).
224. Y. Jia, *et al.*, Crystal structure of the INTS3/INTS6 complex reveals the functional importance of INTS3 dimerization in DSB repair. *Cell Discov* **7**, 66 (2021).

225. J. Li, *et al.*, Structural basis for multifunctional roles of human Ints3 C-terminal domain. *J Biol Chem* **296**, 100112 (2021).
226. J. R. Skaar, *et al.*, INTS3 controls the hSSB1-mediated DNA damage response. *J Cell Biol* **187**, 25–32 (2009).
227. K. L. Pennington, T. Y. Chan, M. P. Torres, J. L. Andersen, The dynamic and stress-adaptive signaling hub of 14-3-3: emerging mechanisms of regulation and context-dependent protein–protein interactions. *Oncogene* **37**, 5587–5604 (2018).
228. B. Foster, M. Attwood, I. Gibbs-Seymour, Tools for Decoding Ubiquitin Signaling in DNA Repair. *Front Cell Dev Biol* **9**, 760226 (2021).
229. Y. Aghazadeh, V. Papadopoulos, The role of the 14-3-3 protein family in health, disease, and drug development. *Drug Discovery Today* **21**, 278–287 (2016).
230. A. Aitken, Post-translational modification of 14-3-3 isoforms and regulation of cellular function. *Seminars in Cell & Developmental Biology* **22**, 673–680 (2011).
231. Z. Fang, Z. Pan, Essential Role of Ubiquitin-Fold Modifier 1 Conjugation in DNA Damage Response. *DNA and Cell Biology* **38**, 1030–1039 (2019).
232. Z. Wang, W.-G. Zhu, X. Xu, Ubiquitin-like modifications in the DNA damage response. *Mutation Research/Fundamental and Molecular Mechanisms of Mutagenesis* **803–805**, 56–75 (2017).
233. J. Liu, *et al.*, UFMylation maintains tumour suppressor p53 stability by antagonizing its ubiquitination. *Nat Cell Biol* **22**, 1056–1063 (2020).
234. M. D. Stewart, T. Ritterhoff, R. E. Klevit, P. S. Brzovic, E2 enzymes: more than just middle men. *Cell Res* **26**, 423–440 (2016).
235. J. Sluimer, B. Distel, Regulating the human HECT E3 ligases. *Cell Mol Life Sci* **75**, 3121–3141 (2018).
236. C. Kwak, *et al.*, Contact-ID, a tool for profiling organelle contact sites, reveals regulatory proteins of mitochondrial-associated membrane formation. *PNAS* **117**, 12109–12120 (2020).
237. Y. Merbl, P. Refour, H. Patel, M. Springer, M. W. Kirschner, Profiling of ubiquitin-like modifications reveals features of mitotic control. *Cell* **152**, 1160–1172 (2013).
238. L. Wang, *et al.*, UFMylation of RPL26 links translocation-associated quality control to endoplasmic reticulum protein homeostasis. *Cell Res*. **30**, 5–20 (2020).
239. B. Guo, G. Cheng, Modulation of the interferon antiviral response by the TBK1/IKKi adaptor protein TANK. *J. Biol. Chem.* **282**, 11817–11826 (2007).

240. D. J. Nevriy, *et al.*, Interaction of GRASP, a protein encoded by a novel retinoic acid-induced gene, with members of the cytohesin family of guanine nucleotide exchange factors. *J Biol Chem* **275**, 16827–16836 (2000).
241. B. Ye, *et al.*, GRASP-1: a neuronal RasGEF associated with the AMPA receptor/GRIP complex. *Neuron* **26**, 603–617 (2000).
242. B. Ye, W. Yu, G. M. Thomas, R. L. Huganir, GRASP-1 is a neuronal scaffold protein for the JNK signaling pathway. *FEBS Letters* **581**, 4403–4410 (2007).
243. C.-M. Miao, *et al.*, LXR α represses LPS-induced inflammatory responses by competing with IRF3 for GRIP1 in Kupffer cells. *Int Immunopharmacol* **35**, 272–279 (2016).
244. A. J. Verkerk, *et al.*, Identification of a gene (FMR-1) containing a CGG repeat coincident with a breakpoint cluster region exhibiting length variation in fragile X syndrome. *Cell* **65**, 905–914 (1991).
245. K. Garber, K. T. Smith, D. Reines, S. T. Warren, Transcription, translation and fragile X syndrome. *Curr Opin Genet Dev* **16**, 270–275 (2006).
246. P. Jin, *et al.*, Biochemical and genetic interaction between the fragile X mental retardation protein and the microRNA pathway. *Nat Neurosci* **7**, 113–117 (2004).
247. J. C. Darnell, *et al.*, FMRP stalls ribosomal translocation on mRNAs linked to synaptic function and autism. *Cell* **146**, 247–261 (2011).
248. Y. De Diego Otero, *et al.*, Transport of fragile X mental retardation protein via granules in neurites of PC12 cells. *Mol Cell Biol* **22**, 8332–8341 (2002).
249. D. E. Eberhart, H. E. Malter, Y. Feng, S. T. Warren, The fragile X mental retardation protein is a ribonucleoprotein containing both nuclear localization and nuclear export signals. *Hum Mol Genet* **5**, 1083–1091 (1996).
250. B. M. Edens, *et al.*, FMRP Modulates Neural Differentiation through m6A-Dependent mRNA Nuclear Export. *Cell Rep* **28**, 845-854.e5 (2019).
251. N. S. Gokhale, *et al.*, N6-Methyladenosine in Flaviviridae Viral RNA Genomes Regulates Infection. *Cell Host Microbe* **20**, 654–665 (2016).
252. G.-W. Kim, A. Siddiqui, N6-methyladenosine modification of HCV RNA genome regulates cap-independent IRES-mediated translation via YTHDC2 recognition. *Proc Natl Acad Sci USA* **118**, e2022024118 (2021).
253. N. S. Gokhale, S. M. Horner, RNA modifications go viral. *PLOS Pathogens* **13**, e1006188 (2017).

254. A. F. Durbin, C. Wang, J. Marcotrigiano, L. Gehrke, RNAs Containing Modified Nucleotides Fail To Trigger RIG-I Conformational Changes for Innate Immune Signaling. *mBio* **7** (2016).
255. J. Liang, *et al.*, Chaperone-Mediated Autophagy Protein BAG3 Negatively Regulates Ebola and Marburg VP40-Mediated Egress. *PLoS Pathog* **13**, e1006132 (2017).
256. L. Zhang, Z.-P. Zhang, X.-E. Zhang, F.-S. Lin, F. Ge, Quantitative proteomics analysis reveals BAG3 as a potential target to suppress severe acute respiratory syndrome coronavirus replication. *J Virol* **84**, 6050–6059 (2010).
257. C. Lyu, *et al.*, Host BAG3 Is Degraded by Pseudorabies Virus pUL56 C-Terminal 181L-185L and Plays a Negative Regulation Role during Viral Lytic Infection. *Int J Mol Sci* **21**, 3148 (2020).
258. A. Toffan, *et al.*, Viral nervous necrosis in gilthead sea bream (*Sparus aurata*) caused by reassortant betanodavirus RGNNV/SJNNV: an emerging threat for Mediterranean aquaculture. *Sci Rep* **7**, 46755 (2017).
259. Z. Liang, *et al.*, Functional characterization of BAG3 in orange-spotted grouper (*Epinephelus coioides*) during viral infection. *Fish Shellfish Immunol*, S1050-4648(22)00106–1 (2022).
260. G. Guo, *et al.*, Reciprocal regulation of RIG-I and XRCC4 connects DNA repair with RIG-I immune signaling. *Nat Commun* **12**, 2187 (2021).
261. E. L. Ryan, R. Hollingworth, R. J. Grand, Activation of the DNA Damage Response by RNA Viruses. *Biomolecules* **6**, 2 (2016).
262. N. G. Sampaio, *et al.*, The RNA sensor MDA5 detects SARS-CoV-2 infection. *Sci Rep* **11**, 13638 (2021).
263. G. Liu, *et al.*, ISG15-dependent activation of the sensor MDA5 is antagonized by the SARS-CoV-2 papain-like protease to evade host innate immunity. *Nature Microbiology*, 1–12 (2021).
264. L. Prescott, SARS-CoV-2 PLpro whole human proteome cleavage prediction and enrichment/depletion analysis. *bioRxiv*, 2021.10.04.462902 (2021).
265. J. R. St-Germain, *et al.*, A SARS-CoV-2 BioID-based virus-host membrane protein interactome and virus peptide compendium: new proteomics resources for COVID-19 research. *bioRxiv*, 2020.08.28.269175 (2020).
266. E. Helgason, Q. T. Phung, E. C. Dueber, Recent insights into the complexity of Tank-binding kinase 1 signaling networks: The emerging role of cellular localization in the activation and substrate specificity of TBK1. *FEBS Letters* **587**, 1230–1237 (2013).

267. A. K. Perry, E. K. Chow, J. B. Goodnough, W.-C. Yeh, G. Cheng, Differential requirement for TANK-binding kinase-1 in type I interferon responses to toll-like receptor activation and viral infection. *J. Exp. Med.* **199**, 1651–1658 (2004).
268. Y.-Y. Li, *et al.*, Ufm1 inhibits LPS-induced endothelial cell inflammatory responses through the NF- κ B signaling pathway. *International Journal of Molecular Medicine* **39**, 1119 (2017).
269. C. Chiang, G. Liu, M. U. Gack, Viral Evasion of RIG-I-Like Receptor-Mediated Immunity through Dysregulation of Ubiquitination and ISGylation. *Viruses* **13**, 182 (2021).
270. S. Gupta, P. Ylä-Anttila, T. Sandalova, A. Achour, M. G. Masucci, Interaction With 14-3-3 Correlates With Inactivation of the RIG-I Signalosome by Herpesvirus Ubiquitin Deconjugases. *Front. Immunol.* **11** (2020).

Biography

Daltry L. Snider received her Bachelor of Science degree in Biomedical Sciences (*cum laude*) with a concentration in chemistry from Tarleton State University in 2016. At Tarleton, Daltry worked with Dr. Dustin C. Edwards, studying the structure of retroviral human T-lymphotropic virus-1 (HTLV-1) protein, HBZ, for which she received both a competitive assistantship, and travel award based on her work. Concurrently, Daltry was awarded a Summer Mentoring and Research Training (SMART) program fellowship at Baylor College of Medicine where she worked in the lab of Dr. B. V. Venketar Prasad characterizing the structure and molecular mechanisms of monoclonal antibody targeting of the rotavirus spike protein.

Daltry began her PhD in August 2017 at Duke University through the Molecular Genetics and Microbiology (MGM) program and joined Dr. Stacy Horner's laboratory, where her thesis research has focused on characterizing novel regulators of RNA virus sensing by RIG-I, with an emphasis on the post-translational modification, ufmylation. A manuscript describing this work titled "Signaling from the RNA sensor RIG-I is regulated by Ufmylation" was published in 2022 in *Proceedings of the National Academy of Sciences (PNAS)*. Daltry has also contributed to several additional research studies on regulation of immune signaling, including publications titled "The small GTPase RAB1B promotes antiviral innate immunity by interacting with TNF receptor-associated factor 3 (TRAF3)" published in *Journal of Biological Chemistry* in 2019, and "The mRNA Cap 2'-O-Methyltransferase CMTR1 Regulates the Expression of Certain Interferon-Stimulated Genes" published in *mSphere* in 2020. She has also published a primer titled "RNA modification of an RNA modifier prevents self-RNA sensing" published in *PLOS Biology* in 2021.

Daltry has received several awards during her graduate studies. She was an NIH Viral Oncology Training Grant appointee in 2018, and awarded an honorable mention for her proposal entitled “Post-translational regulation of innate immune signaling through ufmylation” in the National Science Foundation Graduate Research Fellowship Program 2018-2019 cycle. Daltry has taken many opportunities to present her thesis work at Duke and has been awarded poster prizes at the MGM Departmental Retreat and the Duke University Innate Immunity Symposium. She was also privileged to earn an abstract award for her presentation entitled “Signaling from the RNA sensor RIG-I is regulated by Ufmylation” at the International Cytokine and Interferon Society Annual Meeting in 2021.

In addition to pursuing her thesis work, Daltry has been involved in multiple extracurricular community groups at Duke. She has been a member of the departmental Women in Science group since her start in MGM and served as the student leader from 2019-2021. She was also a founding member of the Diversity and Inclusion Committee from 2018-2021. Daltry has been an active mentor in her lab group, training four MGM rotation students and one undergraduate student through the National Summer Undergraduate Research Program (NSURP).

Publications to date:

- 1) **Snider DL**, Park M, Murphy KA, Beachboard DC, Horner SM. Signaling from the RNA sensor RIG-I is regulated by ufmylation. *Proceedings of the National Academy of Sciences*; 2022 Apr 8; e2119531119.
- 2) **Snider DL**, Horner SM. RNA modification of an RNA modifier prevents self-RNA sensing. *PLOS Biology*. Public Library of Science; 2021 Jul 30;19(7):e3001342.
- 3) Williams GD, Gokhale NS, **Snider DL**, Horner SM. The mRNA Cap 2'-O-Methyltransferase CMTR1 Regulates the Expression of Certain Interferon-Stimulated Genes. *mSphere*. American Society for Microbiology; 2020 May 13;5(3):e00202-20.
- 4) Beachboard DC, Park M, Vijayan M, **Snider DL**, Fernando DJ, Williams GD, Stanley S, McFadden MJ, Horner SM. The small GTPase RAB1B promotes antiviral innate immunity by interacting with TNF receptor-associated factor 3 (TRAF3). *J Biol Chem*. American Society for Biochemistry and Molecular Biology; 2019 Sep 27;294(39):14231–14240. PMID: 31375559